Evaluation of Physical and Chemical Parameters Effects on Different Ozone Monitoring Technologies

Mahsa Ghasemi

A Thesis

in

The Department

of

The Building, Civil and Environment Engineering

Presented in Partial Fulfillment of the Requirements

for the Degree Master of Applied Science (Civil Engineering) at

Concordia University

Montreal, Quebec, Canada

April 2021

CONCORDIA UNIVERSITY

School of Graduate Studies

This is to certify that the thesis prepared

By: Mahsa Ghasemi

Entitled: Evaluation of Physical and Chemical Parameters Effects on Different Ozone Monitoring Technologies

and submitted in partial fulfillment of the requirements for the degree of

Master of Applied Science (Civil Engineering)

complies with the regulations of the University and meets the accepted standards with respect to originality and quality.

Signed by the final Examining Committee:

_____ Chair, Examiner
Dr. Catherine Mulligan

_____ Examiner
Dr. Zhi Chen

_____ Thesis Supervisor
Dr. Fariborz Haghighat

_____ Thesis Supervisor
Dr. Chang-Seo Lee

Approved by _____ Chair of Department of Graduate Program Director
Dr. Ashutosh Bagchi

April 1st, 2021 _____ Dean of Faculty
Dr. Mourad Debbabi

ABSTRACT

Evaluation of Physical and Chemical Parameters Effects on Different Ozone Monitoring Technologies

Mahsa Ghasemi

Since most people spend about 90 percent of their time indoors, having good indoor air quality plays a significant role in human health. Based on EPA studies, indoor air pollution is among the top five environmental health risks. Ozone is considered as one of the typical indoor air contaminants. Air cleaners are one of the indoor sources of ozone production applied for the deodorization and disinfection of air and other indoor sources that release ozone, including printers and photocopiers. Therefore, reliable detection of ozone, especially in low concentrations using sensitive and accurate ozone monitoring technologies, is very noticeable and its market demand is on the rise. However, these detecting technologies suffer from positive or negative interferences from other chemical compounds which exist in the desired environment. Also, humidity and temperature changes can affect indoor ozone levels and ozone monitoring technologies performance.

In this research, different environmental physical parameters effects like air velocity, airflow direction, and humidity on the performance of ozone monitoring technologies were evaluated in a full duct and small-scale environmental chamber. Also, we examined the responses of these monitoring instruments in the presence of some interfering compounds, including Acetone, Toluene, and Ethanol, using a small-scale chamber at 50% RH and dry condition (0.01%).

The results demonstrated that different airflow rates and airflow directions had a negligible effect on the UV sensors response. While electrochemical and metal oxide sensors outputs were remarkably overestimated with increasing airflow rate. This increase was more evident for electrochemical and metal oxide sensors when placed perpendicular and parallel to the airflow, respectively. Furthermore, the responses of 211-2B, Teledyne, POM and BW experienced a positive interference with rapid humidity variations from 30% to about 80% and a negative bias from 80% to 30% RH. In contrast, BW Solo behaved oppositely. It was difficult to follow the metal oxide changing trend with humidity variations because of the instrument time interval (minimum 10 min). In the absence of ozone, Ethanol caused a slight negative interference to the 211-2B sensor in humid (50%) and dry air (0.01%) and a significant negative bias to Teledyne at 50% RH. 211-2B sensor did not respond to acetone at 50% RH, but it experienced a positive bias in dry air. A considerable positive interference was observed in Teledyne reading at 50% RH. Toluene led to a slight positive interference in 211-2B response in humid and dry conditions. BW Solo and ECO Sensor in the presence of these VOC compounds were consistently showing zero concentration.

ACKNOWLEDMENTS

I would like to express my deep gratitude to my supervisors Dr. Fariborz Haghighat and Dr. Chang-Seo Lee for all support, research guidance, and inspiration throughout my study. I am grateful for the opportunity they gave me for realizing the project.

I would like thank Mr. Luc Demers and Ms. Hong Guan, the experienced technicians of the Department of Building, Civil and Environmental Engineering for all their technical help to build and develop the setups. Many thanks to the Institut de recherche Robert-Sauve en sante et en securite du travail (IRSST) for supporting this project.

I am also very grateful to my colleagues (Marzieh, Zahra, Mohammad, and Mojtaba) for sharing their knowledge and experience and providing a friendly environment. Last but not least, I am deeply thankful to my family for their continuous support and encouragement.

TABLE OF CONTENTS

LIST OF FIGURES

LIST OF TABLES

LIST OF ABBREVIATIONS

Abbreviation	Description
AC	Accuracy Criterion
ACGIH	American Conference of Governmental Industrial Hygienist
ACH	Air Changes per Hour
ASHRAE	American Society of Heating, Refrigerating, and Air-Conditioning Engineers
ASME	American Society of Mechanical Engineers
CI	Confidence Interval
DAS	Data Acquisition System
EPA	Environmental Protection Agency
HEPA	High Efficiency Particulate Air
HMOS	Heated Metal Oxide Semiconductor
HVAC	Heating, Ventilating, and Air-Conditioning
hv	Planck Equation ($E = hv$)
IAQ	Indoor Air Quality
IDLH	Immediately Dangerous to Life and Health
IR	Infrared Radiation
NIOSH	National Institute for Occupational Safety and Health
OSHA	Occupational Safety and Health Administration
ppb	Parts per Billion
ppm	Parts per Million
PTFE	Polytetrafluoroethylene
RE	Reference Electrode
RH	Relative Humidity
S	Selectivity Factor
SD	Standard Deviation
TVOC	Total Volatile Organic Compound
TWA	Time Weighted Average
UV	Ultraviolet
VOC	Volatile Organic Compound
WE	Working Electrode

LIST OF SYMBOLS

English Symbols	Description
ac/h	Air changes per hour
C_{O_3}	Concentration of ozone
cfm	Cubic Feet per Minute
g/Nm^3	Grams per normal cubic meter
g/h	Gram per hour
I	Light Intensity through sample
Io	Light Intensity through sample free of ozone
in	Inch
inchWG	Inch of Water
l	Path length between light source and detector
L	Liter
$L\text{-}min^{-1}$	Liter per minute
M	Molarity
mV	Millivolts
m^3	Cubic meter
m^3/s	Cubic meter per second
nm	Nanometer
ng/m^3	Nanogram per cubic meter
P	Pressure
psi	Pound per square inch
R^2	Coefficient of determination
R_g	Resistance of metal oxide sensor in the presence of ozone
R_a	Resistance of metal oxide sensor in the absence of ozone
T	Sample temperature

Greek Symbols	Description
α	Absorption coefficient of O_3 at 254 nm
σ	Absorbance cross section at 254 nm
λ	Wavelength

Chapter 1: Introduction

1.1- Background

Today, the emission of hazardous gases, including nitrogen oxide (NO_x), SO_x, HCl, CO_2, volatile organic compounds (VOCs) and fluorocarbons, into the atmosphere that arise from industry, automobiles, and homes has increased. To prevent and minimize the effects of these pollutants, we need monitoring and controlling systems such as gas sensors that can rapidly and accurately monitor and measure the exact concentrations of these pollutants [1-3]. Gas sensors are applied in different areas, including industrial production (e.g., methane detection in mines) [1, 2], automotive industry (e.g., detection of polluting gases from vehicles) [3, 4], medical applications (e.g., electronic noses simulating the human olfactory system)[4, 5], indoor air quality supervision (e.g., detection of carbon monoxide, ozone, VOCs)[6, 7], environmental studies (e.g., greenhouse gas monitoring) [9, 10].

One of the uses of gas sensors, as mentioned above, is in the area of indoor air quality (IAQ). According to Environmental Protection Agency (EPA), people spend up to 90 % of their time indoors in developed countries. While in developing countries, this statistic is 70 %. Also, the results of EPA studies indicated that indoor concentrations of some pollutants are two to five times higher than outdoor air pollutants. Although most sources of indoor pollutants are inside buildings, outdoor pollutants can enter buildings through open doors, open windows, ventilation systems, and cracks in structures [8-10].

Based on the EPA, temperature and humidity changes can affect IAQ so that pollutants concentrations increase with increasing these parameters. Symptoms like headaches, fatigue, trouble concentrating, eyes, nose, throat and lung irritation are the signs of poor indoor air quality. Moreover, the quality of indoor air inside workplaces (offices, schools...) plays a vital role in the comfort, health, well-being, and productivity of workers [10, 11]. The most common indoor air pollutants are ozone, CO, CO_2, SO_2, NO_2, particulate matter (PM), and TVOC, which in this research, we examine ozone and its monitoring technologies [12].

1.2- Properties and Utilization of Ozone

Ozone is one of the hazardous and toxic gases. It is colorless with a very pungent odor in the air. Ozone is not emitted directly into the air. It is formed by the chemical reaction between NO_x and volatile organic compounds (VOC) in the presence of heat and sunlight. Since ozone is a strong oxidizer, human exposure to the ozone should be minimized even at a very low concentration. However, it is widely used in various areas because of its strong oxidizing power and ease of post-use treatment.

High ozone concentration can be applied to clean silicon wafers and remove the photoresist layer by decomposing organic contaminants in semiconductor manufacturing. Also, it is used for disinfection and deodorization in the hospital and pharmaceutical industries, disinfection and deodorization of air and water in clean rooms, buildings, vehicles, and food and livestock

industries. Absorption of UV light in the sunlight by the stratospheric ozone layer protects living organisms from damage. It should be noted that ozone concentration near the ground level is typically very low [3, 13, 14].

In the national ambient air quality standards, the exposure limit of 70 ppb (0.070 ppm) for an 8-hour average has been set by The United States Environmental Protection Agency. According to the regulation passed by the State of California, all air purification equipment that generates ozone should not increase indoor ozone levels more than 50 ppb [15-17]. EPA considers indoor ozone concentration typically 20 to 80% of the measured outdoors [18, 19]. The exposure limit of ozone based on the Occupational Safety and Health Administration (OSHA) for an 8-hour average and the National Institute for Occupational Safety and Health (NIOSH) for a 10-hour average is 0.1 ppm. The ozone concentration of 5 ppm was considered as the Immediately Dangerous to Life and Health (IDLH) by NIOSH. In other words, the IDLH exposure level is the point at which a person without appropriate respiratory protection could be fatally injured or could suffer irreversible or incapacitating health effects [20].

It should be noted that if ozone concentration in the air exceeds about one ppm, in this case, it is very toxic to humans so that it damages the eyes, respiratory systems, and nervous systems[21, 22]. Exposure to 0.1 ppm ozone for two hours causes a 20% loss of breathing capacity and, if exposed to 1 ppm ozone for six hours, will lead to bronchitis. The results show that if a mouse is exposed to 10 ppm ozone, it will not survive [23].

The exposure limit of ozone in a workplace according to ACGIH for light, moderate, and heavy work over eight hours and the definition of these types of work are explained in Table 1.1.

Table 1. 1- Exposure limit of ozone in workplace [12]

Exposure level	**Exposure limit**
0.05 ppm	Maximum allowable concentration averaged over an eight-hour period for heavy work[1].
0.08ppm	Maximum allowable concentration average over an eight-hour period for moderate work[2].
0.1ppm	Maximum allowable concentration average over an eight-hour period for light work[3].
0.2ppm	Maximum (short-term) exposure limit for light, moderate or heavy work, for less than or equal to 2 hours.

[1] Pick and shovel work; laying railroad tracks.
[2] Walking around with moderate lifting or pushing; hammering nails, filing metal, planning wood, raking a garden, cleaning a floor
[3] Sitting or standing to control machines, performing light hand or arm work; writing, typing.

Indoor ozone concentration is a function of outdoor contributions and indoor sources. Moreover, ozone can be generated by static electricity eliminators, welding machines, electric motors, photocopiers, printers, copiers, etc. [3, 24]. Due to its relatively short half-life (minutes in confined spaces), it does not create a uniform concentration in air. Thus, ozone concentration should be measured continuously at multiple locations of a specific area by ozone monitors [23].

1.3- Ozone Monitoring Technologies

Many instruments have been developed for the measurement of ambient ozone based on different techniques included chemiluminescent, electrochemical, semiconductor, and UV photometry. The features of these techniques are summarized in Table 1.2. Currently, the development of low-cost sensors as well as portable ozone sensors has been considered to raise environmental awareness of the importance of air quality by making access to these affordable instruments.

Indoor concentrations of ozone typically vary between 20% and 80% of outdoor levels. This ozone concentration changes depends on factors such as whether windows are open or closed, air conditioning is applied, and indoor sources. Hence, the development of more sensitive and selective ozone monitors at low concentrations is another topic that needs further study. UV photometric technique is the most accepted method for the accurate measurement of ozone concentration and it is used almost exclusively by EPA. UV ozone monitors have a fast response, high precision and are much more selective than the other methods [2, 19, 25, 26].

Table 1. 2- Specification of different ozone monitoring technologies [3]

Gas sensor	Output signal from sensor element	Generation of output signal from sensor	Gas sensitivity
Semiconductor	Electrical conductivity of metal oxide semiconductor	Change in the amount of oxygen on metal oxide by the reaction of oxygen and gases	Medium
Electrochemical	Electric current in the electrochemical cell	Electrochemical reaction among gas, electrode, and electrolytic solution in the electrochemical cell	High
UV absorption	Transmitted light intensity in the gas cell	Absorption of UV light by gas molecule device with high resolution	High
Chemiluminescence	Intensity of generated light in the reaction cell	Reaction between reagents and sample in the reaction cell	High

Since each sensor has particular capabilities and limitations, choosing a suitable sensor is important. The following factors should be considered in selecting a suitable sensor for a given application [27].

- Identification of the background gases in the monitoring areas since their presence can affect the sensor performance [28].
- The temperature ranges in which the sensor operates. A wide temperature variation can result in moisture condensation, especially in a confined space due to poor air circulation. This matter is significant in sensor performance.

Moreover, the following indicators should be considered for the evaluation of gas sensors performance [1]:

- Sensitivity: The minimum concentration of target gases that can be detected,

- Selectivity: The ability of a gas sensor for identification of a specific gas among a gas mixture,
- Response time: The time when gas concentration reaches a specific amount so that the sensor generates a warning signal,
- Energy consumption,
- Reversibility: It means that after detection, the sensing materials can return to their original state or not, and
- Adsorptive capacity (affects sensitivity and selectivity).

Among the above indicators, sensitivity and selectivity are considered vital indicators in designing and applying sensors. Since the selectivity of gas sensors is mainly poor, they may respond to multiple analytes, which is called cross-sensitivity [1, 20].

The factors that can lead to gas sensor instability include: “design errors (should be avoided), structural changes (such as variations of grain size), phase shifts (such as segregation of additives doped with sensing materials), poisoning caused by chemical reactions, a variation of the surrounding environment.” The following methods can help solve these issues [1]:

- “Using materials with chemical and thermal stability
- Optimizing elemental composition and grain size of sensing materials
- Utilizing specific technology during surface pretreatment of sensors.”

Accurate measurement of ozone concentrations in workplaces, especially at low concentrations, is one of the essential factors that should be considered for the health and safety of workers. The presence of other compounds in the desired environment and changing the physical environmental parameters such as airflow rate and humidity can lead to overestimation or underestimation of ozone concentration by the sensor. To this end, more studies are needed to examine the impact of different parameters on ozone monitors performance.

1.4- Research Objectives

The main objectives of this study are:

1-To evaluate environmental physical parameters effects like air velocity, airflow direction, and humidity on the performance of ozone monitoring technologies in a full duct and small-scale environmental chamber.

2-To examine the effect of some interfering compounds on the response of ozone monitors.

1.5- Thesis Outline

Chapter 2 contains the fundamentals of different ozone monitoring techniques, investigation of interfering compounds and physical and chemical parameters effects on the performance of ozone monitors. Chapter 3 describes the details of experimental set-up and methodology. Moreover, the results of calibration and full duct pre-qualification tests are provided in this

chapter. Chapter 4 discusses the results of this study. The conclusions and recommendations for future work are summarized and addressed in Chapter 5.

Chapter 2: Literature Review

2.1- Introduction

In this chapter, the principle of operation of each ozone monitor technology and physical and chemical parameters affecting the performance of these monitoring technologies is explained in detail. Moreover, the results of different related studies in this regard are summarized in each section.

2.2- UV Absorption Technology

Absorption of UV light is one of the methods applied for the measurement of ozone with high precision and accuracy. The highest absorption of UV light by ozone occurs at 254 nm, which coincides with a low-pressure mercury lamp's emission wavelength [25, 29, 30].

2.2.1- Principles of Operation

The principle of this technology is based on the absorption of UV light by the ozone molecules and the use of photometry for measuring the light intensity reaching the detector at 254 nm. The reduction of light intensity depends on the length of absorption tube, the ozone concentration in the tube, and the wavelength of UV light [31, 32].

The concentration of ozone is measured in this technique based on the Beer-Lambert absorption law. This law explains the absorption of light at a specific wavelength, temperature, pressure and a certain distance by the gas molecules. The following equation presents the mathematical expression of the Beer-Lambert Law [18, 30, 33, 34]:

$$C_{O_3} = \frac{1}{\alpha_{O_3}} \ln\left(\frac{I_0}{I}\right) \cong \frac{1}{\sigma_{O_3} l} \frac{\Delta I}{I_0} \tag{2.1}$$

Io= Lamp intensity at the detector in the absence of ozone
I= Lamp intensity with ozone present
α= Absorption coefficient of O_3 at 254nm (litre $\mathrm{mol^{-1}cm^{-1}}$or $\mathrm{M^{-1}cm^{-1}}$)= 1.15× $10^{-17}\mathrm{cm^2molecule^{-1}}$ or 308 $\mathrm{atm^{-1}cm^{-1}}$)
l= Path length between light source and detector (cm)
C_{O_3}= Concentration of ozone as *ppb* at standard temperature and pressure (STP) ($\mathrm{mol\ litre^{-1}}$)

The ozone density can be influenced by temperature and pressure. By variation of density, the number of ozone molecules inside the absorption cell also changes. So, this affects the amount of light absorbed by the ozone molecules [35, 36].

$$C_{O_3} = -\frac{10^9}{\alpha \times l} \times \frac{T}{273°K} \times \frac{29.92\ inHg}{P} \times \ln\frac{I}{I_0} \tag{2.2}$$

T: sample temperature in Kelvin, P: pressure in inches of mercury.

The UV monitor includes an absorption cell. A source lamp that emits an Ultraviolet light (UV) at a wavelength of 254 nm, is located on one side of the absorption cell, and a photodiode (the simplest light detector) is located on the opposite side of it to measures the reduction in UV intensity caused by the presence of ozone (Figure 2.1). There is an air pump to draw the sample air through the absorption cell. Besides, Io and I can be measured using an ozone scrubber to remove ozone and a solenoid valve to switch the sample air between going through the ozone scrubber or bypassing it. By passing the sample air through the solenoid valve or bypass line, ozone molecules absorb or block some of the light from reaching the photodiode, and the light intensity (I) is measured. When the sample air passes through the scrubber, no light is blocked, so the light intensity (Io) is measured. Besides, pressure and temperature are measured within the absorption cell [25, 31].

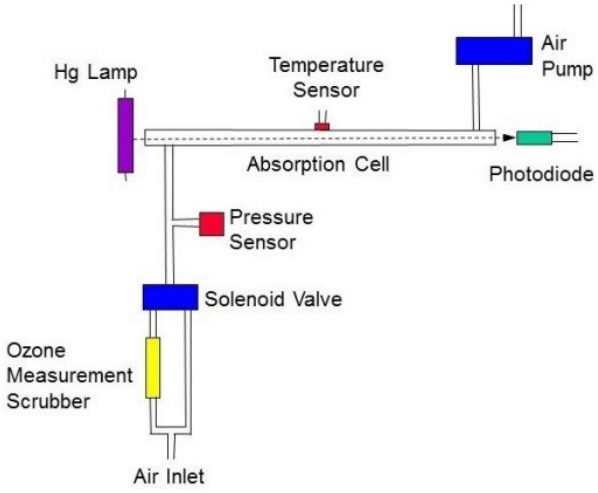

Figure 2. 1- UV absorption ozone sensor [37]

2.2.2- Interferences

The performance of UV ozone monitors can be affected in the presence of some gases, including sulfur dioxide (SO_2), nitric oxide (NO), nitrogen dioxide (NO_2), water vapor (H_2O), aromatic hydrocarbons (such as xylene, toluene, …), and mercury vapor [30, 33, 35]. Because of the high reactivity of ozone, significant care must be taken to retain the sample gas inlet, manifold and all tubing in a clean and dry condition [29, 32, 33, 38]. Modern ozone monitors use an ozone scrubber to remove only ozone from sample air. Nevertheless, some gases may be partially or temporarily absorbed or adsorbed by the scrubber. Generally, scrubbers applied in UV instruments contain MnO_2, Hopcalite (a mixture of Cu and Mn oxides) or heated silver wool (HSW). Manganese dioxide (MnO_2) scrubbers are commonly used for most UV ozone sensors [29, 31].

An ideal scrubber has two features: 1- it removes ozone from the sample air. 2- it does not remove other UV absorbing compounds at 254 nm or species which modify light transmission to the detector like water vapor. If the scrubber does not remove the other gases, their concentrations in the sample air and scrubbed air remain constant and then cancel in the Beer-

Lambert equation. Some factors, such as temperature or humidity variations, result in the release of the compound absorbed by the scrubber into the sample air. This situation leads to a negative bias in ozone measurement [18, 38, 39].

- **Water vapor**

Since water vapor does not absorb at 254 nm, no interference is expected for the ozone measurement. However, studies indicated that rapid humidity changes result in a false signal (positive or negative)[25, 40]. Based on the explanation of [40], rapid humidity variations lead to changes in the refractive index within the detection cell. In other words, the light emitted from the source in UV monitors reaches the detector through reflection from the cell wall. The presence of water layer on the cell interior surface can increase the amount of light lost, which in this case reflects less light and decrease the light intensity. These effects depend on the type of cell [40, 41].

In the case of high humidity, condensation may occur at various points in the system. Water vapor may be adsorbed by the scrubber and scratches in the cell can be a suitable place to form condensation. High humidity and condensation of sample air can affect the sensor performance so that other interfering compounds, such as aromatic hydrocarbons, may desorb from the scrubber. Condensation can reduce or prevent sample air from entering into the inlet lines and filters so that this condition can damage the cell [31]. In summary, the effect of humidity on the performance of UV sensors depends on scrubber surface area, absorption cell composition, and ozone scrubber material [40, 41].

- **Aromatic Compound**

Since aromatic hydrocarbons and their atmospheric oxidation products absorb 254nm UV light, they can interfere with ozone measurement. These aromatic compounds can be removed by ozone scrubber [29]. It should be noted that under humid conditions, these compounds may be desorbed from the scrubber. Therefore, it is better to use a UV sensor in an environment where it does not have a significant concentration of aromatic hydrocarbons [31].

According to different studies, aromatic compounds usually create a positive bias in UV ozone sensors. Generally, VOC compounds interfere with the ozone measurement in two different ways: 1- positive bias occurs when the scrubber adsorbs these compounds. 2- negative bias occurs when these compounds desorb from the scrubber due to eventual elution or variation in temperature or humidity. These two processes depend on environmental conditions (humidity and temperature), volatility, chemical properties of that compound, and reactivity and surface characteristic and area of the scrubber [18]. There is little information about the aromatic compounds in the atmosphere; thus, in this situation, the evaluation of interference caused by these compounds is difficult [29, 42, 43].

- **Mercury**

Since the atmospheric concentration of mercury is not usually very high, interference from mercury is not problematic. However, there may be high mercury concentration in the vicinity of the monitoring site [31]. Mercury strongly absorbs UV light 254 nm and creates a positive bias in the sensor [29].

The U.S. EPA (1999) reported that the presence of 0.04 ppb Hg (300 ng/m^3at room temperature) in 75 parts per billion (ppb) ozone causes a 12.8% increase at low humidity (RH= 20-30%) and 6.4% at high humidity (RH= 70-80%) in measured ozone concentration using a UV absorption ozone sensor. According to [44], one ppb of mercury provides a response equal to approximately 875 ppb of ozone in the same model of Thermo Electron Corporation photometric ozone monitor used in the case of low humidity of the EPA study. Furthermore, mercury can interfere with the ozone measurement when adsorb or desorb by the internal ozone scrubber. By increasing the scrubber temperature or humidity variations, mercury can be released from the scrubber into the gas stream [39].

2.3- Chemiluminescence Ozone Monitor

Luminescence is a phenomenon in which a matter emits light with a specific wavelength when the matter or molecule returns to the ground state from an excited state after absorbing external energy from an electromagnetic wave, heat, friction, electric field or chemical reaction [45]. If a chemical reaction is the source of energy absorbed, this phenomenon is called chemiluminescence. In other words, this phenomenon is the result of an oxidation or hydrolysis reaction in which chemical energy converts into the emission of visible light (luminescence). Chemiluminescent reactions can occur in the gas, liquid, and solid phase. For analytical applications, the liquid phase has the most potential, while chemiluminescent gas-phase reactions are applied to monitor and measure substantial components related to atmospheric chemistry [46, 47].

Many years ago, chemiluminescence sensors were widely utilized, but today, this sensor has been replaced by UV absorption sensors because the supply of ethylene used in chemiluminescence sensors is flammable and explosive [31].

2.3.1- Principles of Operation

Essential components of this technique include a reaction cell, a light-tight housing, a device for introducing and mixing reagent (ethylene) and sample (ozone), a light detector, and an acquisition and signal-processing system (Figure 2.2). A reaction cell is kept in the sample chamber and it must be sealed to minimize potential interferences. Besides, the cell should be able to transmit light in the visible range. The chamber is located close to the detector to maximize optical efficiency. The chemiluminescent reaction initiates after mixing the reagent and sample, then the intensity of emitted light is measured by a detector [46]. Two different configurations are usually applied for the detector: either to the side of the reaction cell (“side-on” configuration) or underneath the reaction cell (“end-on” configuration). The side-on model

is more economical and also needs less space. However, the end-on model has a large photocathode area and the light collection and the response is more uniform [45, 46, 48].

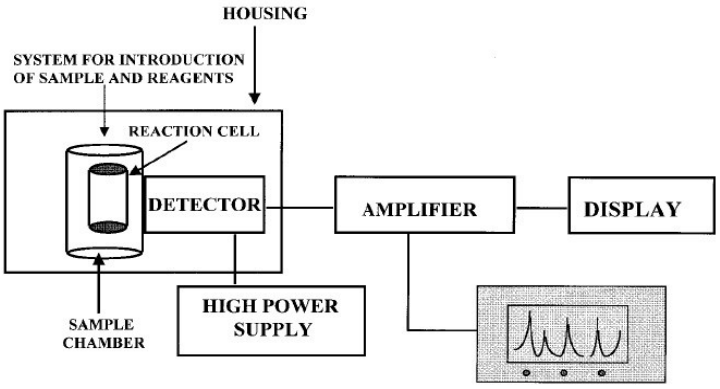

Figure 2. 2- Schematic of a basic luminometer [46]

2.3.2- Determination of Ozone in Gas Phase

Ozone, either in the gas phase or solutions, can be measured by chemiluminescence. According to studies, most chemiluminescent reactions done to detect ozone include gas-phase chemiluminescent reaction with ethylene, determination in solution or condensed phase chemiluminescence using rhodamine B or other dyes adsorbed on silica, and as well as chemiluminescent reaction with nitric oxide. Since the ozone measurement in gas phase chemiluminescent reactions is sensitive and should be controlled accurately, the determination of ozone in solution is considerable [47].

In the gas phase, ozone can be measured using chemiluminescence methods that is in contact either with ethylene or nitric oxide. Chemiluminescent reaction with ethylene is the most common method for measuring 3 ppbv to 30 ppmv of ozone, and this reaction has been indicated below [47, 49]:

$$2C_2H_4 + 2O_3 \rightarrow 4CH_2O + O_2 + hv \quad (\lambda_{max} = 440nm)$$

Since the products of this reaction are in the excited electronic state, chemiluminescence is generated by releasing light in the 300 to 600 nm region, with maximum intensity at 435 nm [46, 50].

It should be noted that by increasing relative humidity and temperature from 0 to 60% and 20°C to 25°C, a small positive signal can be produced, increasing ozone concentration by about 8% within the measurement. Besides, cooling the phototubes applied to detect emitted light or increase the ethylene flow rate can result in a tiny improvement in sensitivity [50].

According to the British standard, common air pollutants do not interfere with the ozone measurement in this reaction. However, if the particulate matter is not removed, it can cause measurable ozone destruction by accumulation in the sampling line. To remove particulate matters, an ozone-compatible filter such as fluorocarbon polymer can be used. The filter must

be changed regularly to prevent the loss of ozone from the sample air and pressure drop in the filter [51].

In chemiluminescent reactions with nitric oxide (NO), which are so sensitive, ozone can be measured by monitoring the light intensity ($\lambda > 600\ nm$) generated by the reaction. According to the following reaction, ozone and nitric oxide react together and create oxygen and nitrogen dioxide in the activated state. Moreover, when activated nitrogen dioxide returns to the ground state, light is emitted, then it breaks down to nitrogen dioxide and a photon [47, 52].

$$O_3 + NO \rightarrow O_2 + {NO_2}^*$$

$${NO_2}^* \rightarrow NO_2 + \text{light}\ (h\nu)$$

2.3.3- Interferences

Water vapor is one of the interfering compounds that can affect the performance of this sensor so that it causes a 3-4% positive bias in the ozone reading for each percent of water vapor in the air. In addition to water vapor, H_2S and CO_2 can interfere with the ethylene-chemiluminescence sensor. Interfering compounds that can affect the NO-chemiluminescence sensor include: H_2S, NO_2 and CO_2. Furthermore, the performance of this sensor is not affected in the presence of Hg vapor and aromatic compounds [29-31, 35, 38].

- **Previous Studies**

Investigation of UV and chemiluminescence ozone sensors cross-sensitivity has been carried out by a few studies, two of which are summarized in Table 2.1.

According to Table 2.1, the first study [29] investigated the effect of some potential interfering compounds, including water vapor, mercury, *o*-nitrophenol, naphthalene, p-tolualdehyde, on six ozone monitors response using an environmental chamber. Two monitors indicated by the suffix "N" include Nafion tubing. In other words, the Nafion tube is used to equilibrate humidity in the optical cell and minimize rapid humidity variations.

This study indicated that humidity changes had little effect on UV-MnO_2 and UV-HSW sensors in the absence of other interfering gases (Figure 2.3). In contrast, a positive interference was observed for the chem sensor during humidity variations so that the ozone concentration was overestimated by 3-10 ppb per 10,000 ppm water vapor over the 55 to 200 ppb O_3 range tested. It should be said that using a Nafion tube reduced the effect of humidity on the chem sensor to 1-2 ppb per 10,000 ppm over that range. A positive bias was observed for the UV-Hop sensor by increasing humidity, but the Nafion tube decreased this effect significantly.

Figure 2.4 illustrates that increasing humidity from 0 to 80% (23,600 ppm) at 100 ppb O_3 had the most effect on the response of the UV-Hop sensor. In comparison, the UV-Hop monitor equipped with the Nafion inlet tube did not show a strong increase with humidity variations.

Table 2. 1- Results of studies examined UV and chemiluminescence cross-sensitivities

Sensor Type	Scrubber	Interfering gases		Ozone generated	Flow & Pressure	Ref.
Bendix ethylene Chemiluminescence (Chem)	None required	**Water vapor:** Three tests were done at 55, 100, and 200 ppb O_3. RH: 0 – 80%		55, 100, and 200 ppb	**Flow:** 15 $L\text{-}min^{-1}$ **pressure drop** between the chamber and manifold: 1% or less	[29]
Bendix ethylene Chemiluminescence (Chem-N)	None required					
ThermoEnvironmental UV model 49 (UV-MnO_2)	MnO_2 unheated	**Hg: Test A** (78.7 ppt Hg) was performed under dry conditions (RH<3%). -**Test B** (6.8 ppt Hg) was done in humid air (RH~80%).				
Horiba UV APOA-370 (UV-HSW)	Heated silver wool	**Aromatic compounds**	**o-nitrophenol:** 7.6 ppb **Condition:** Low RH<3% & high RH~80%			
2B Tech UV model 202 (UV-Hop)	Hopcalite unheated		**Naphthalene:** 21.5 ppb **Condition:** Low RH<3% & high RH~80%			
2B Tech UV model 202 (UV-Hop-N)	Hopcalite unheated		**p-tolualdehyde:** 14 ppb **Condition:** Low RH<3% & high RH~80%			
Thermal Electron Model 49 UV photometer	MnO_2	**o-Cresol:** 25 ppb **Condition:** High RH		-**High RH:** 75.6 ppb	-	[32]
Horiba Model APOA-360 UV photometer	Heated silver wool	**o-Nitrotoluene**: 24 ppb **Condition:** High & Low RH		-**Low RH:** 75.9 ppb -**High RH:** 75.8 ppb		
Dasibi Model 1008-PC UV photometer	Heated metal	**Mercury:** 0.04 ppb **Condition:** High & Low RH		-**Low RH:** 75.9 ppb -**High RH:** 75.6 ppb		
Bendix Model 8002 chemiluminescent analyzer	None required					

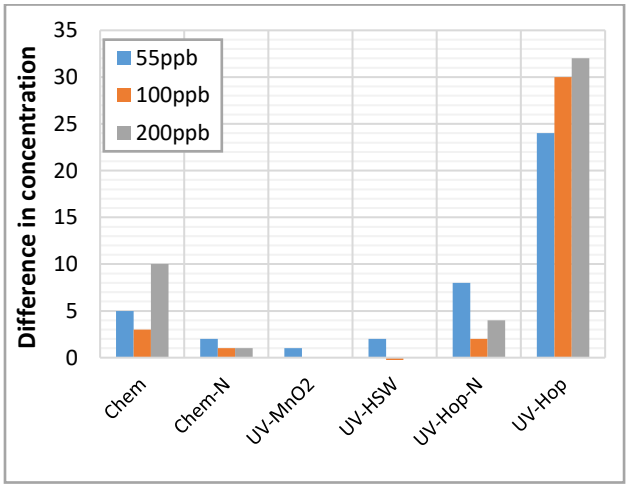

Figure 2. 3- Effect of humidity variations on ozone monitors response [29]

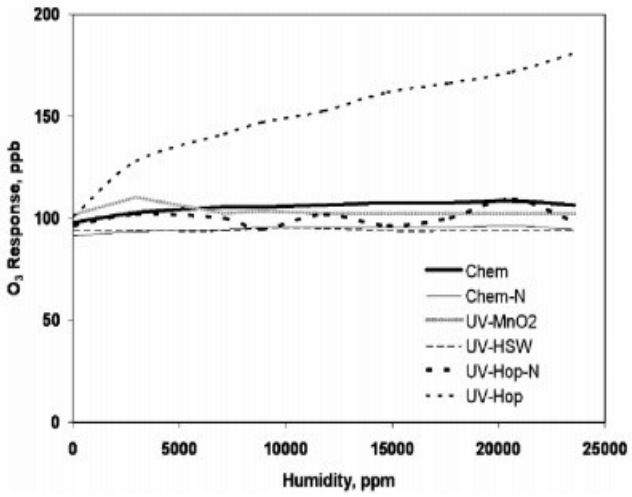

Figure 2. 4- Response of ozone monitors to increasing humidity at 100ppb [29]

According to Figure 2.5, Hg had no effect on chemiluminescence monitors, while a positive bias was observed to all of the UV monitors so that the interference at low levels of Hg for three UV monitors was about one ppb O_3 for every one ppt of Hg. Moreover, among these four UV monitors, UV-MnO_2 had better performance at low Hg concentration than the others. While at high Hg concentration, their performance was almost the same.

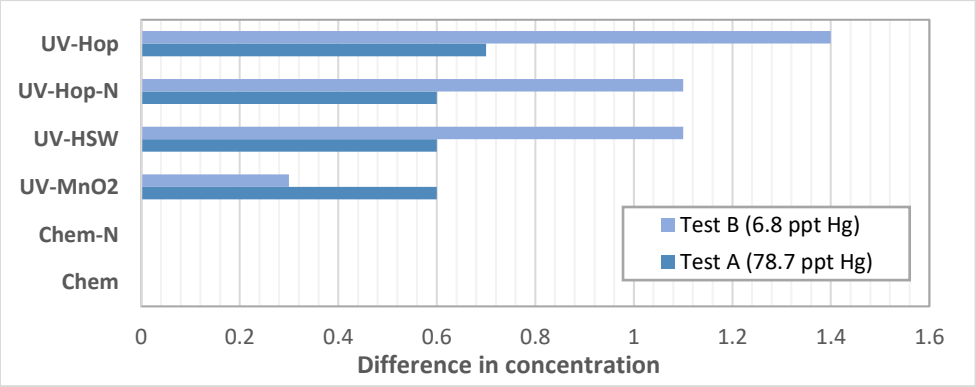

Figure 2. 5- Effect of Hg on ozone monitors response [29]

The results showed that aromatic compounds caused a positive bias to UV monitors, but they did not affect the chemiluminescence monitors response. As shown in Figure 2.6, among these four UV monitors, UV-HSW did not show a significant response in the presence of the three aromatic compounds. O-nitrophenol had a major effect on the response of the other three UV monitors, especially UV-MnO_2, at high and low RH. Nevertheless, its interference was eliminated in the UV-HOP-N at high RH because of the Nafion tube. The UV-MnO_2 monitor response was affected by the injection of naphthalene at low humidity, but no interference was observed in the performance of UV-MnO_2 monitor at high RH. The response of UV-HOP-N monitor was affected in the presence of p-tolualdehyde just at low humidity. While p-tolualdehyde at high humidity interfered with the performance of UV-HOP monitor, which was not equipped with the Nafion tube.

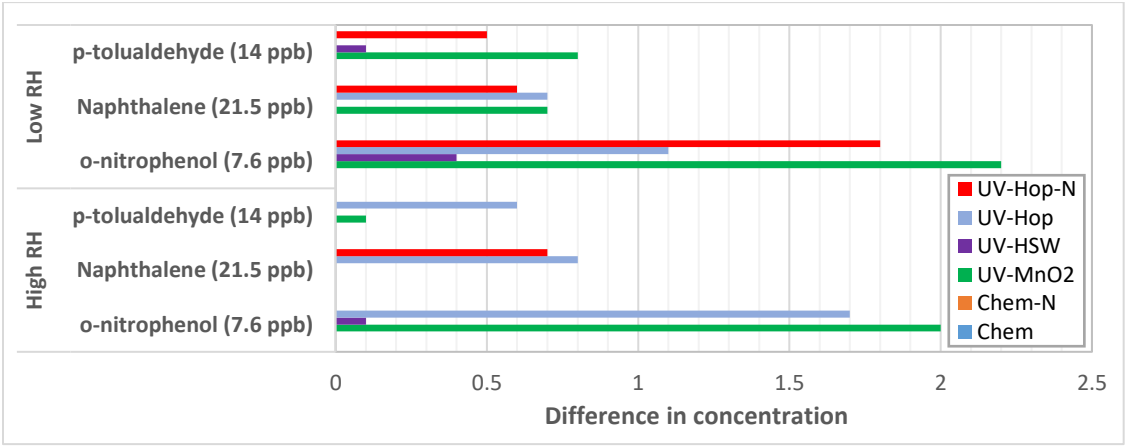

Figure 2. 6- Effect of aromatic compounds on ozone monitors response [29]

The other study examined the effect of three interfering compounds, including nitrotoluene, cresol, and mercury at low (20 to 30%) and high (70 to 80%) relative humidity on four ozone monitors [32]. The test lasted about 8 hours by introducing the interfering gases. After 8 hours, the experiment was continued for an additional 8 hours without these interfering compounds.

The results indicated that cresol had little effect on the performance of four ozone monitors. At low humidity, nitrotoluene significantly impacted the UV photometer with the standard scrubber and the heated metal scrubber. While, at high humidity, no major effect was observed in ozone measurements. Moreover, mercury had a major impact on the performance of three UV photometers at both low and high humidity. The highest effect was observed on the UV monitors with the heated metal and the silver wool scrubber.

2.4- Electrochemical Ozone Monitor

Electrochemical monitors are widely applied to detect common gas pollutants in many branches of industry, traffic, environmental, and medical monitoring [53, 54]. Electrochemical ozone monitors are inexpensive, lightweight, and portable; however, the monitor is not selective for ozone because it can produce a response for other oxidizing gases [25].

Electrochemical monitors operate by reacting with the target gas (ozone) and producing an electrical signal proportional to the ozone concentration. This ozone monitor consists of a gas permeable membrane, electrode, and electrolyte (Figure 2.8). The following briefly explains each part.

- **Gas Permeable Membrane (Hydrophobic Membrane)**

It is used to control the amount of gas molecules reaching the electrode surface. It is mainly made of thin, low-porosity Teflon membranes. Besides, it prevents the entry of unwanted particulates into the system. The membrane's pore size should be appropriate for transferring the suitable amount of ozone molecules and preventing liquid electrolyte from leaking out or drying out the sensor. In addition, the sensitivity and limiting current of the sensor are controlled by the rate of mass transfer through the membrane so that by increasing the thickness of the membrane, the sensor sensitivity decreases [27, 55].

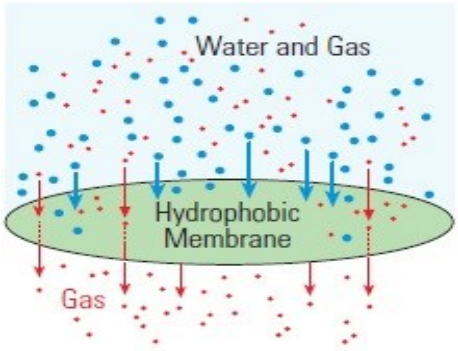

Figure 2. 7- Schematic of hydrophobic membrane [27]

It should be noted that membranes are mainly applied for the detection of ozone to achieve selectivity; however, sensor durability is decreased by using membranes. Also, thick membranes prevent ozone permeation, while ozone easily damages thin membranes. Thus, selecting a suitable membrane with an appropriate thickness is important [56].

- **Electrode**

Electrodes are typically made of a noble metal such as platinum or gold to have an adequate reaction with the target gas because they exhibit excellent stability in electrolyte solutions. The electrodes used in this sensor include a sensing electrode, counter electrode, and reference electrode. Each electrode can be made of different materials. It should be noted that, during the operation of the sensor, the counter electrode should be able to catalyze its half-cell reaction. The counter electrode used in electrochemical sensors is very often made from platinum [27, 55].

A few noble metals, including platinum, gold, and silver, can be applied as the sensing electrode materials for the detection of ozone because the oxidative properties of ozone are extremely high [56-58]. According to studies, the sensor has an optimal operation when the reference electrode forms a stable potential with the electrolyte and is not sensitive to temperature, pressure, and relative humidity or other contaminants in the sensor system[27, 55].

- **Electrolyte**

The electrolyte used for the sensor should be compatible with the sensor materials. It must also facilitate the cell reaction so that the ionic charges can be transferred easily within the electrolyte. Besides, the signal, sensitivity, and response time of the sensor can be affected by the rapid evaporation of the electrolyte. Aqueous electrolytes are useful for many electrochemical gas sensors [27, 55].

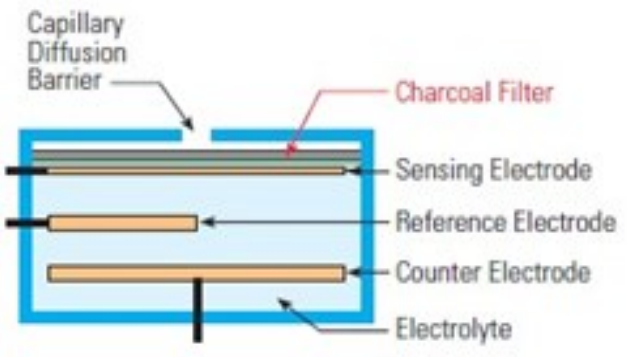

Figure 2. 8- schematic of electrochemical sensor [27]

Table 2.2 shows different types of sensing materials and operating temperature ranges used for electrochemical ozone sensors. Gold and platinum, because of high electrocatalytic activity and wide working range, are two precious metals used as sensing electrodes in ozone sensors [58].

Table 2. 2 Electrochemical ozone sensors and sensing materials used for their design[57]

Sensor type	Operation temperature	Sensing materials	Ref.
Electrochemical	RT	Iodine/iodide solution; Nafion, 0.5M H_2SO_4; bromide salt in alkaline electrolytes; Nafion, $HClO_4$; 0.005M H_2SO_4; Electrodes: Au; Pt; Ag; carbon	[15, 59]
Electrochemical (solid electrolytes)	200-300 ℃	$SmFeO_3$; $SmFe_{1-x}Co_xO_3$; porous $Si/Li_2Si_2O_5$ or Li_2SiO_3	[60, 61]

RT: Room Temperature

2.4.1- Principles of Operation

In this sensor, ozone passes through a small capillary-type opening and then diffuses through a hydrophobic barrier and eventually reaches the sensing electrode surface (sometimes called the working-electrode). Then, the ozone molecules are oxidized on the sensing electrode and generate an electric current. It should be noted that an external driving voltage is required for the sensor because the sensing electrode should be stable and have a constant potential. However, in reality, the continuous reactions are taken place on the electrode surface so that the sensing electrode potential does not remain constant; thus, the sensor performance can be affected. To this end, a reference electrode is placed within the electrolyte and near the sensing electrode to provide a stable constant potential for the sensing electrode.

Further, no current flows to or from the reference electrode. After the ozone reaction at the sensing electrode surface and generation of an electric current, the current flow between the sensing and counter electrode is measured. An amplifier connected to the sensor indicates the ozone concentration so that the generated current is related to the gas concentration [27, 62, 63]. A typical electrochemical sensor is shown in Figure 2.9.

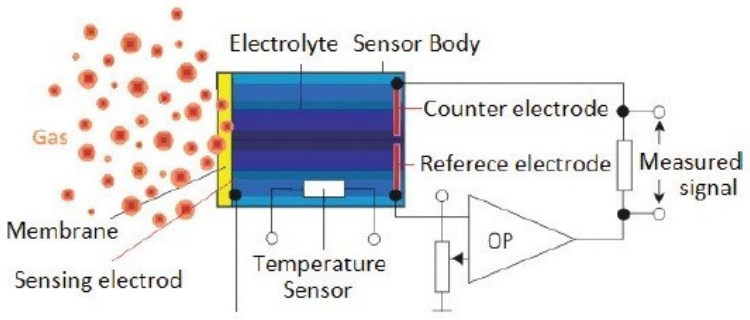

Figure 2. 9- Electrochemical sensor [64]

2.4.2- Interferences

Interfering compounds can poison electrodes of this sensor so that they create by-products that inhibit the electrode by absorption on the electrode surface or reaction with the electrode [63].

It should be noted that the selectivity of an electrochemical ozone sensor can be affected by cross interferences from gases, including SO_2, NO_2, NO, CO, NH_3 and humidity in the air [26, 35, 53, 58, 65]. Table 2.3 shows the results of studies that investigated this problem. These studies were conducted both in the laboratory and field. The values of interfering compounds, ozone concentration, relative humidity and other characteristics of each experiment are summarized in Table 2.3. Based on different studies, NO_2 has a significant effect on the response of electrochemical ozone sensors [66].

Table 2. 3- Results of studies examining electrochemical ozone sensors cross-sensitivities

Sensor specifications	**Concentration of non-target gas**	**Interfering gases**	**Humidity, pressure, temperature**	**Ozone concentration & Flow rate**	**Ref.**
Counter electrode: Gold & platinum wire. **Sensing electrode:** Gold-Nafion. **Electrolyte:** 0.5M H_2SO_4 or 0.5M NaOH	**-**NO= 1ppm **-**CO= 1ppm -SO_2= 1ppm -NO_2= 1ppm	-SO_2 -NO_2	-**RH=** 0-65%	**-Ozone concentration=** 0-20 ppm -**Flow rate=** 0-50 mL/min	[58]
(Model OX-B421) **Power Supply:** 5V direct current (VDC) **Total power consumption:** 5W	-NO_2 -NO -Humidity	-NO_2 -NO -Humidity	**-Temperature=** 12-26℃ **-Pressure=** 1.0003±0.0009 bar -**RH**= 40-90%	- **Flow rate=** 1 L/min -**Ozone concentration**= 10ppb-1000ppb	[26]
(O_X-B421) (Combined oxidant gases NO_2 and O_3).	-CO= 1 ppm -NO= 100 ppb -NO_2= 100 ppb -Humidity	-NO_2	-**The ambient air temperature=** 17 to 24℃ **-RH=** 54% to 95%	-**Sample air flow rate**= 1L/min **-Ozone concentration=** 100 ppb	[53]
(Alphasense Ltd., OX-B431)	-NO= 5 ppm -NO_2= 5ppm -SO_2= 10ppm -CO=500 ppb -CO_2= 10ppm	-Humidity -NO_2 (large interference) -CO and CO_2 (responds positively) -SO_2 and NO (responds negatively)	**-RH=** 15%, 30%, 45%, 60%, 75%, and 80% -**Inline gas temperature and sensor body temperature=** 20±1 ℃	**-The raw ozone mixing ratios=** 150 - 200 ppb -**Flow rate=** 1 L/min	[65]

According to the results of [58], SO_2 and NO_2 are the main potential interferents in ozone detection. In comparison, CO and NO had no effect on ozone measurement. As shown in Figure 2.10, SO_2 interference was negligible at potentials less than +50 mV (acid electrolyte- Figure 2.10.a) and -300 mV (base electrolyte- Figure 2.10.b). Also, the results showed that using a chemical filter (indigo filter) can reduce NO_2 interference. It should be noted that humidity variations had little effect on the sensor response.

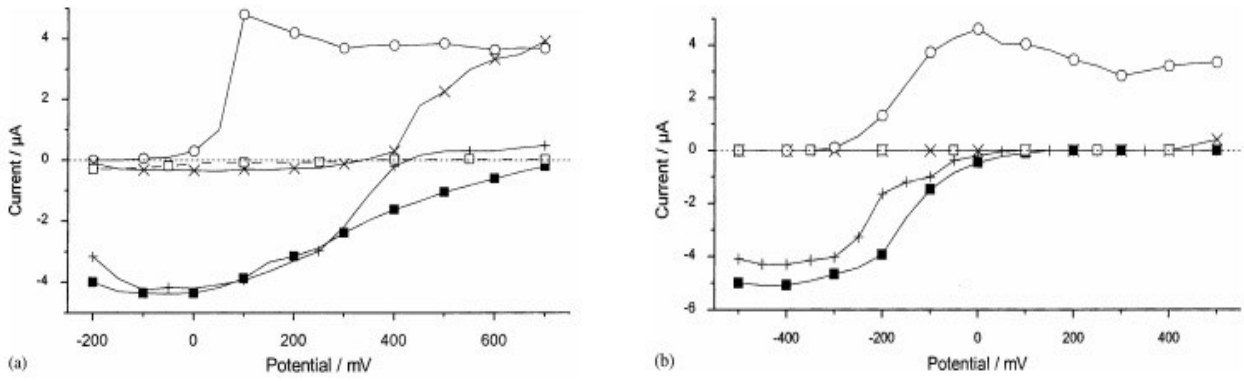

Figure 2. 10- Sensor response to ozone and possible interferants (each 1 ppm) by using gold-Nafion electrodes with (a) acidic and (b) basic electrolyte solution: (■)O3; (○)SO2; (×) NO; (+)NO2; (□) CO [58]

Based on tests performed by [26], NO, NO_2 , and relative humidity can affect the sensitivity and voltage outputs of working electrode or sensing electrode (WE) and reference electrode (RE) of electrochemical ozone sensors. As shown in Figure 2.11, by increasing RH, the voltage of WE and RE increased and subsequently stabilized at a higher amount. Furthermore, RH variations cause the WE voltage to increase dramatically at first, which can explain the overestimation of ozone concentration at the beginning of RH changes.

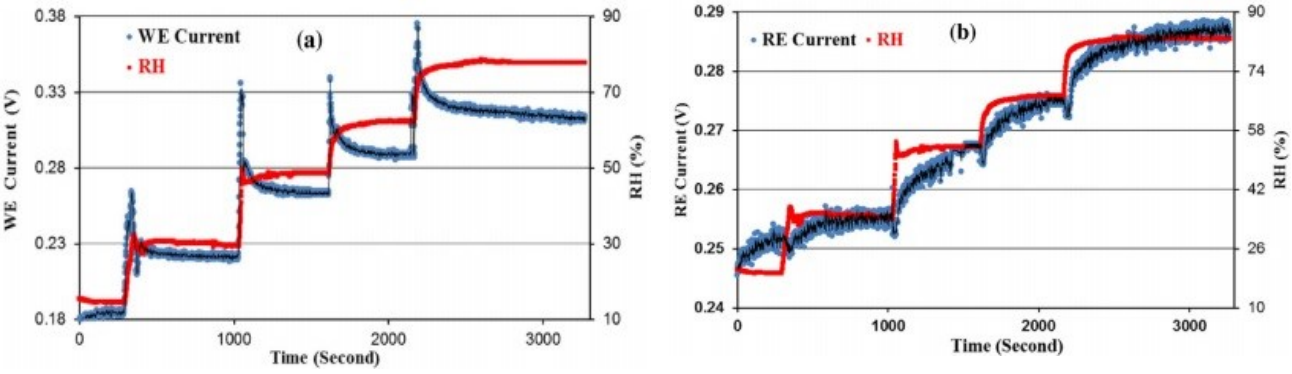

Figure 2. 11- Effects of RH on WE (a) and RE (b) voltage outputs of an electrochemical ozone sensor [26]

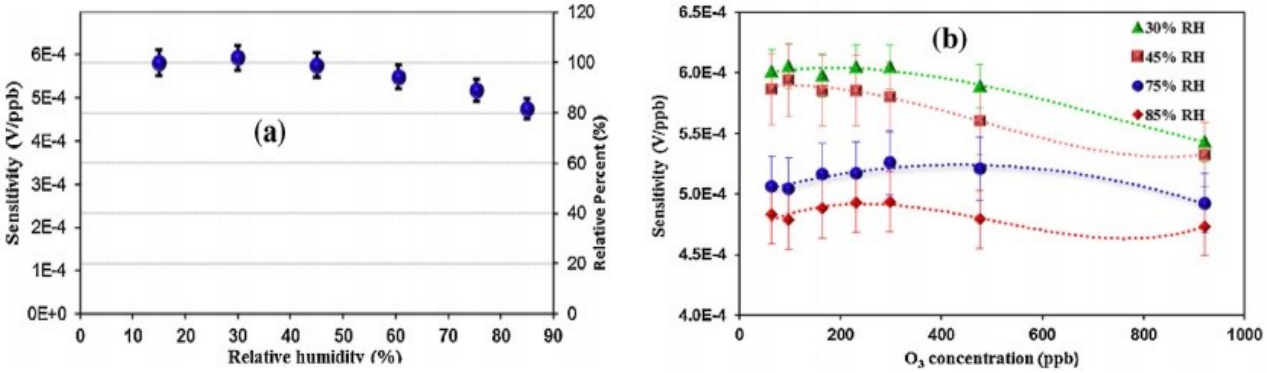

Figure 2. 12- Effects of RH on ozone sensor sensitivity (a) and variations of sensitivity with ozone concentration (b) [26]

These results demonstrated that the electrochemical ozone sensor sensitivities are almost constant between 15% and 60% RH and decrease gradually with increasing RH. As shown in the right-side Figure 2.12, at 30% and 45% humidity, the sensor sensitivities are stable in the range of 60 to 300 ppb and decrease by about 8% with increasing ozone concentration. However, at 75% and 85% humidity, the sensitivities are approximately stable over the whole concentration range.

2.4.3- Effect of Physical and Chemical Parameters on Sensor Performance

- **Pressure and Temperature**

The performance of this sensor can be affected by pressure and temperature changes. Since the sensor may be damaged by differential pressure, it is better to keep the entire sensor within the same pressure. Also, sudden variations in pressure can lead to variations in current. Due to the sensitivity of this sensor to temperature variations, it is important to keep the temperature stable. The sensor at a temperature of above 25℃ indicates a higher value, while below 25℃ shows a lower amount. The electrolyte can be dried out when the sensor operates continuously at high temperature (usually above 40ºC) [27, 63].

Depending on the type of electrolyte (liquid or solid) used for the sensor, we can apply this sensor in the temperature range of -30℃ to 1600℃. Electrochemical sensors with liquid electrolytes are mainly operated up to about 140℃, while sensors with solid electrolytes can be operated in the temperature range of greater than 500℃ [54].

- **Humidity**

The humidity does not directly affect the sensor performance, while the electrolyte content can be altered by continuous operation below 15% or above 90% relative humidity. This variation occurs slowly and also depends on the temperature, electrolyte, and vapor barrier. High humidity can increase the volume of the electrolyte and leads to its leakage from the cell, while low humidity can dry out the sensor. Moreover, sensors with less porous barriers designed to detect high gas concentrations are not affected by the humidity than sensors used to detect low concentrations (have more porous barriers) because it limits the amount of gas passing through the barrier. The electrolyte can be frozen more quickly at high humidity, but a dry condition can increase the acid content of the electrolyte so that it can cause crystallization or allow the acid to attack the seals [63].

- **Life Expectancy**

The life expectancy of sensor depends on the target gas and environmental conditions such as humidity, temperature, and exposure to interfering compounds. Generally, the average life expectancy of an electrochemical ozone sensor is between one and three years [63].

2.5- Metal Oxide Ozone Monitor

Metal oxide ozone monitors are considerable because of fast response time, low cost, and low weight [2]. This sensor is widely used to measure high ozone concentrations in industries [25]. One of the essential things that should be considered is that any sensor material may react with different gases beyond the target gas (ozone). In ideal conditions, these reactions are reversible; however, some irreversible reactions may occur to poison the sensor and lead to low sensitivity. The factors that can affect this reaction, including internal and external causes (such as natural features of base materials), microstructure of sensing layer, surface additives, temperature and humidity, etc. [20, 67].

In this sensor, gas adsorbs onto the sensor surface and alters the resistance of the sensor material. Then, after the gas disappears, the sensor returns to its original condition so that the sensor material is not consumed in this process. To this end, it has a long life expectancy. Figure 2.13 shows various types of interaction with the sensor. The left region is where the sensor is unpowered. The other areas explain different processes that coincide. Also, the sensor output is resistant to all sensor materials [67].

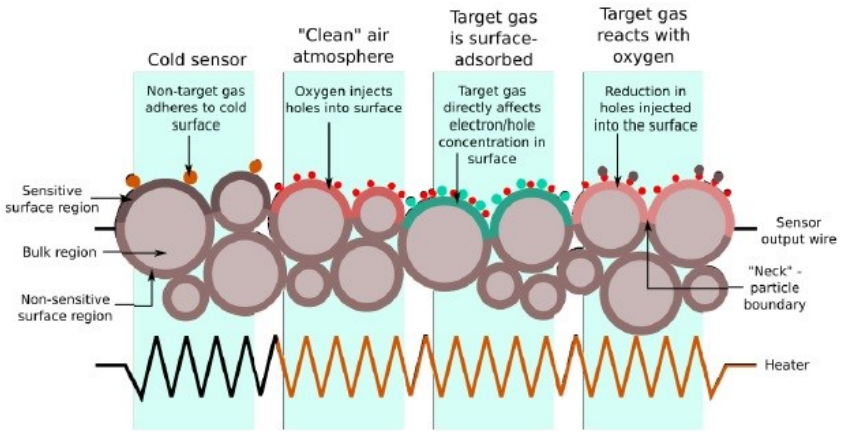

Figure 2. 13- Diagram of the various types of interaction between atmospheric gases and metal oxide semiconductor sensor surface [67]

- **Oxygen Requirements**

The presence of oxygen for having a proper operation is required in metal oxide sensors and depending on the type of the oxide and the amount of oxygen changes. It is also better to consult with the manufacturer when using these sensors in atmospheres with less or more than the normal concentration of oxygen in the air [63]. In metal oxide sensors used p-type semiconductor, oxygen atom reactions reduce the semiconductor resistance. In contrast, the opposite effect occurs for a p-type semiconductor in the presence of reducing gases. The reversal of all these is true for n-type semiconductors [67].

- **Types of Semiconductor**

Semiconductors are divided into two types: Intrinsic and extrinsic or doped. An intrinsic semiconductor is the pure form of semiconductor, while in an extrinsic semiconductor, impurities

are added intentionally to make it conductive. Extrinsic semiconductors are classified as n-type and p-type semiconductors. N-type semiconductors are the most commonly used sensing materials of metal oxide sensors [68].

Table 2. 4- Response of semiconductors to different types of gases *[69]*

Classification	Oxidizing gases	Reducing gases
n-type	*Resistance increase*	*Resistance decrease*
P-type	*Resistance decrease*	*Resistance increase*

2.5.1- Principles of Operation

One or more metal oxides used in this sensor belong to the transition metals, such as tin oxide and aluminum oxide. The metal oxide material should be heated to an optimal operating temperature range for the detection of ozone. This heating element can be a platinum or platinum alloy wire, a resistive metal oxide, or a thin layer of deposited platinum [27].

When ozone is in contact with the metal oxide, it dissociates into charged ions or complexes that lead to the transfer of electrons. To measure the change in the conductivity of metal oxide, a pair of biased electrodes should be embedded into the metal to measure this change as a signal. Typically, this sensor produces a powerful signal, especially at high gas concentrations [27]. The general chemical reaction steps occur during the sensor operation, including 1- pre-adsorption of oxygen on a semiconducting material surface. 2- Adsorption of the specific gas (ozone). 3- Reaction between oxygen and adsorbed gas. 4- Desorption of reacted gas on surface.

The basic reactions occur at the sensor surface, can be written as follows [2, 70]:

$$\frac{1}{2}mO_2 + \{\text{vacant site}\} + e^- \xrightarrow{k_1} \{O_m{}^-\}$$

$$X + \{XO_m{}^-\} \xrightarrow{k_2} \{XO_m\} + e^-$$

$$\{XO_m\} \rightarrow \text{further reaction}$$

where m is an integer, and X is a combustible species.

Different arrangements can be used for a metal oxide sensor. Two typical types of this sensor include: 1- Bead-type sensor, 2- Chip-type sensor.

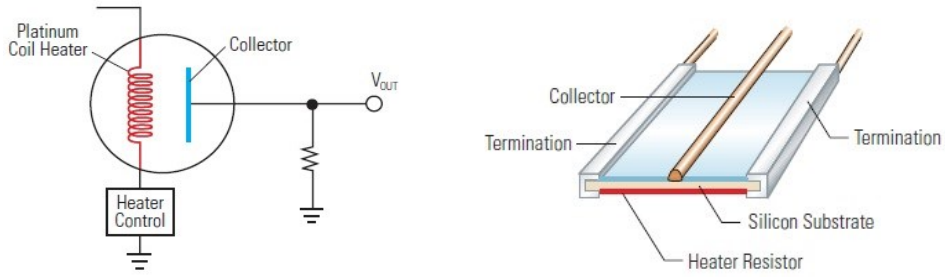

Figure 2. 14- Bead-type sensor (thick film sensor) and chip-type sensor (thin film sensor) [27]

Table 2.5 listed types of metal oxide applied for ozone detection [68].

Table 2. 5- Different sensing materials applied for semiconductor ozone sensors [68]

Sensing materials	Sensing gas	Operating temperature range (℃)	Range of detection limits	Sensing element form	Response time	Reference
In_2O_3	O_3	N.A.	-	-	-	[71, 72]
In_2O_3	O_3	Room temperature	-	Thin films	-	[71, 73]
In_2O_3	O_3	40 to 500	Up to 150 ppb	Thin film on silicon/alumina substrates	30 min to 2h	[74]
In_2O_3	O_3	N.A.	-	Thin films	-	[71, 75]
In_2O_3-MoO_3	O_3	150 to 350	400 to 800 ppb	Thin film on sapphire substrate	1 to 7 min	[76]
In_2O_3 with Fe_2O_3	O_3	300 to 550	10 to 330 ppb	Thick films on alumina substrate by screen printing	~2 min	[77]
Fe_2O_3 with In_2O_3	O_3	300 to 550	10 to 300 ppb	Thick films on alumina substrate by screen printing	~2 min	[77]
MoO_3	O_3	150 to 370	50 to 150 ppb	Thin films onto alumina	~2 min	[78]
SnO_2	O_3	200 to 700	800 ppm	Pressed powder disks	~30 s	[79]
SnO_2 (Bi_2O_3)	O_3	200 to 700	800 ppm	Pressed powder disks	~30 s	[79]
TiO_2, WO_3	O_3	150 to 370	50 to 150 ppb	Thin film onto alumina & sapphire substrate	~2 min	[78]
WO_3	O_3	200 to 400	0 to 175 ppb	Thin film on polished sapphire	2 to 5 min	[80]
WO_3	O_3	27 to 450	0 to 50 ppb	Thin films on to oxidized Si substrates	15 s	[81]
ZnO	O_3	200 to 400	800 ppm	Pressed powder disks	~30 s	[79]
ZnO & SnO_2-based materials	O_3	200 to 700	800 ppm	Pressed powder disks	~30 s	[79]
MoO_3-In_2O_3	O_3	150 to 350	400 to 800 ppb	Thin film on sapphire substrate	1 to 7 min	[76]

N.A. - Not Available

According to Utembe et al. [82], metal oxide sensors used WO_3 as the semiconductor can be considered a cost-effective sensor for detecting ozone than conventional ozone sensors. Studies show that a faster response is achieved by thin-film sensors [23, 57, 83, 84]. According to different studies, thick films are preferably suitable for reducing gases such as CO and CH_4, while thin films show a better response to oxidizing gases such as ozone and NO [85, 86]. At a thick enough film, ozone dissociation occurs at the surface of metal oxide without penetration into its deeper layers [87].

2.5.2- Interferences

Since various gases can affect ozone sensors performance, this problem should always be considered in experiments. However, only a few articles addressed this issue [60, 88-93]. According to studies, the appearance of interfering compounds such as H_2, CO, or vapors of volatile organic compounds (VOCs) in the desired environment, can affect the measurement of ozone concentration [87].

According to Table 2.6, the results of [87, 94] showed that the presence of SO_2, CO, and water vapor in the air does not have much effect on In_2O_3 sensors. Therefore, this type of sensor is suitable for ozone detection in a natural environment and has better selectivity than SnO_2 sensors.

Table 2. 6- Cross-sensitivity of metal oxide ozone sensor

Model or metal oxide material/gas	Concentration of Interfering Compounds	Cross-Sensitivities	Humidity, Pressure, Temperature	Ozone concentration	Ref.
-UnitecSens 3000 -SGX MICS oz-47 -SGX MICS 2610 -FIS-SP-61	-NO= 100 ppb -NO_2= 90 ppb -CO= 460ppb-8230 ppb -CO_2= 390 ppb -NH_3: 85 ppb	Little effect: NO, CO, NO_2, CO_2, NH_3	**-Humidity test:** 40%- 80% **-Temperature test:** 12- 32℃ **-Interfering test:** T: 22℃ RH: 60%	100 ppb	[66, 95]
In_2O_3; In_2O_3: MO	-NO_2= 0.2-2 ppm -SO_2=2-4ppm -CO=10-100ppm	NO_2	**-Humidity test:** 30-60%	0.1-3 ppm	[87, 94]
SnO_2L (Pd, Pt)		NO_2, SO_2, CO, humidity			

According to the results of [95] conducted in a laboratory exposure chamber, four metal oxide ozone sensors responses decreased by 0.7-3.86 ppb per 1 ℃ temperature increase. Humidity variations affected their response so that this change was 0.65 to 0.84 ppb ozone per 1% relative humidity increase. The results indicated that in the range of 0 to 110 ppb ozone, the difference between reference concentrations and measured concentrations was quite low for three sensors (2-4.2 ppb); however, the big difference was observed for the MICS-2610 sensor (13.3 ppb). Based on various studies [66], the response of metal oxide ozone sensors in the presence of CO

changed significantly (-6.8ppb to 20ppb). To this end, CO is one of the important interfering compounds for this sensor.

2.5.3- Effect of Physical and Chemical Parameters on Sensor Performance

- **Sensor Operating Temperature**

The operating temperature can affect sensor performance. Response time may be affected by the operating temperature of a sensor. The shape of a sensor signal response curve is a function of temperature and its changes depend on the type of oxide applied. Operating temperatures of p-type semiconductors are relatively lower than n-type ones. In addition, the high operating temperature of most metal oxide gas sensors is because of the reaction temperature of O^- [1, 20, 27]. Sensors use SnO_2 as semiconductor have an operating temperature from 25 ℃ to 500 ℃ so that this can cause potential selectivity problems for the sensor. In this case, a high deviation of temperature from optimal value may result in the reaction of other gas components with SnO_2, leading to poor selectivity [1, 96].

- **Humidity**

Humidity changes mainly affect all metal oxide sensors by showing zero and span variation during sensor operation. It should be noted that no electrons will be donated to sensing layers when water is absorbed on the metal oxide surface. The sensor resistance decreases due to the reaction of water molecules with the surface oxygen, leading to a decrease in sensitivity [20, 97, 98]. H_2S and H_2O are physically similar on the molecular level and are absorbed similarly on the metal oxide surface. Depending on the oxide used in the sensor, they act differently (either inhibit or enhance sensor response to toxic gas)[63].

- **Ambient Temperature**

Like operating temperature, ambient temperature can cause the same effects unless the sensor is operated at a constant temperature [63]. The variation of ambient temperature can lead to operating temperature fluctuations. This effect can change both the concentration of the charge carriers within the grains of the metal oxide semiconductor and the properties of the inter-grain contacts. Also, the kinetics of the gas-surface interaction strongly depends on temperature; thus, a small variation in temperature affects the sensor sensitivity and response time [99-101].

Longevity

The significant advantage of a metal oxide sensor is its long life expectancy so that in clean applications, it typically lasts 10 years or more. The presence of other compounds can interfere with the performance of the sensor. Thus, to minimize interferences, appropriate filtering materials should be applied to capture interfering compounds [27].

2.6- Comparison of Different Ozone Monitoring Technologies

Since each type of ozone sensor has certain specifications, advantages and disadvantages of all monitoring technologies have been mentioned in Table 2.7. Besides, almost all the interfering compounds based on different studies and information provided by some companies are listed in Table 2.8.

Table 2. 7- Comparison of different types of ozone monitoring technologies [3, 27, 51, 102, 103]

sensor	Advantages	Disadvantages
UV absorption	-High accuracy -High linearity at any ozone levels -High precision -Fast response	-Must absorbs light at a specific wavelength -Expensive
Electrochemical	-High sensitivity -Inexpensive -Low electricity consumption	-Frequent maintenance -Short lifetime in very dry and hot conditions
Semiconductor	-Good sensitivity -Inexpensive	-High electricity consumption for electric heating -Potential danger due to high temperature sensor element
Chemiluminescence	-Fast response time	-Supply of ethylene used in this sensor is flammable and explosive

Table 2. 8- Ozone monitors cross-sensitivities

Sensor Type	Potential interfering compounds
UV absorption	Water vapor, Hg, SO_2, NO, NO_2, Mercury, Aromatic hydrocarbon (Toluene, xylene, o-nitrophenol, Naphthalen, p-tolualdehyde, …), Benzene, m-Cresol, Benzaldehyde, Naphthalene, Methanol, Acetone, Formaldehyde, and Phenol
Electrochemical	SO_2, NO_2, NO, CO ,NH_3 , Humidity, H_2S ,H_2, C_2H_4 ,Cl_2, ClO_2 ,HCl, and CH_3SH
Semiconductor	SO_2, NO_2, CO , Humidity, NH_3 ,Butane ,Cl_2, Ethanol, Ethyl acetate, Heptane, H_2S , Isopropanol, Propane, and Toluene
Chemiluminescence	**-Ethylene-Chemiluminescence monitor:** water vapor, H_2S,and CO_2 -**NO-Chemiluminescence monitor:** H_2S ,NO_2, and CO_2

Chapter 3: Experimental Set-Up and Methodology

3.1- Introduction

In this part, the applied ozone monitors, the experimental set-up, environmental conditions, generation system, and test procedure are discussed. It should be noted that investigating the impacts of relative humidity variations, air velocity, and airflow direction on ozone monitors response was conducted in a full duct. A small-scale environmental chamber to study the effects of interfering compounds and humidity changes in the absence of ozone was used.

3.2- Selection of Interfering Compounds

Inadequate ventilation, high or low temperature and humidity, recent remodeling, other activities inside or near a building, and building materials and furnishings are factors that can affect indoor air quality. According to Health Canada, indoor relative humidity below 20% can cause dry eyes, mucous membranes, and skin. Moreover, it can cause static electricity build-up and affect office equipment operations such as printers and computers. High humidity (above 70%) can result in condensation on surfaces and within the interior of equipment and building structures. Indoor relative humidity in the range of 30% to 60 % is recommended by the ASHRAE and EPA.

The main indoor pollutants are particulate matter, nitrogen dioxide (NO_2), carbon monoxide (CO), volatile organic compounds (VOCs), tobacco smoke, and biological allergens. Among these, VOCs are the major pollutants in indoor environments because they easily evaporate at room temperature and are emitted from many products used indoors [104-106]. Indoor VOC emission sources include paint and associated supplies, cleaning and washing products, adhesives, organic solvents, building materials and appliances, pesticides, combustion materials, cosmetic products, office equipment (photocopiers and printers), permanent markers, and photographic solutions. The major health effects of VOC exposure include headache, nausea, fatigue, eye and throat irritation, allergic skin reaction, acute and chronic respiratory effects, neurological toxicity, and lung cancer [104, 106].

According to the study conducted by Shaw et al. [107], 45 VOC compounds were identified in office buildings. They measured the VOC concentrations emitted from office furniture in a full-scale chamber under conditions 23℃, 50% RH, and 5 ac/h supply air (0.5 ac/h ventilation rate).

Table 3. 1- VOCs emitted from the office workstation [107]

Aliphatic Hydrocarbons	Butane, Pentane, alpha-Pinene, Decane, Limonene, Branched C11, Undecane, Branched C12, Dodecane, Derivative of neoprene, Hexadecane.
Aromatic Hydrocarbons	Benzene, Toluene, Ethylbenzene, o-, m-, p-Xylene, Styrene, Propyl benzene, Trimethylbenzenes, 4-Phenylcyclohexene.
Aldehydes	Pentanal, Hexanal, Heptanal, Octanal, Nonanal, (E)-2-Nonenal, Decanal.
Ketones	Acetone, 2-Butanone, Acetophenone.
Chlorinated Hydrocarbons	Trichloromonofluoromethane, Methylene, Chloride, 1,4-dichlorobenzene.

Alcohol	Methanol, Ethanol, Isopropanol, 2-butoxy-ethanol, Undecanol.
others	Carbon disulfide, Acetic Acid, Propanoic acid, 3-ethoxy-, ethyl ester, Phenol, 2,6-t-Butylo, p-chinon, Butylated Hydroxytoluene.

They also took air samples from 24 Canadian workplaces so that 34 VOCs were found in the workplaces. The detected compounds are listed in Table 3.2.

Table 3. 2- VOC in Canadian Workplaces [107]

VOC compounds	Concentration ($\mathbf{mg/m^3}$)	mean
Benzene	0.001-0.021	0.008
Toluene	0.002-0.072	0.028
Xylene	0.003-0.071	0.020
C_3benzene	0.003-0.095	0.027
CCl_3CH_3	0.004-0.071	0.034
C_2Cl_4	0.001-0.026	0.011
Dichlorobenzene	0.001-0.085	0.020
Ethanol	0.019-0.387	0.119
Isopropanol	0.05-0.13	0.102
Propanone	0.001-0.447	0.074
TVOC	0.1-13.3	2.5
TVOC without copier	-	1.2

Based on the potential VOC compounds available in workplaces, we selected three compounds for this research: Acetone, Ethanol, and Toluene. Table 3.3 provides a list of test compounds specifications, possible sources, and their health effects.

Table 3. 3- Possible emission sources and health effects of selected interfering compounds

Chemical Class	Compound	Formula	Molecular weight (g/mol)	Density (g/mL)	Source	Health problem
Ketone	Acetone	C_3H_6O	58.08	0.784	Solvent, adhesives, paints, cleaner, coatings, lacquers, varnishes, removers.	Nose, throat, eyes, skin, and respiratory tract irritation. Central nervous system. Lung disease.
Alcohol	Ethanol	C_2H_5OH	46.07	0.789	Paint, adhesives, cleaners, cosmetics, aerosols.	Severe eye irritation, moderate skin irritation, disease of kidneys, heart, central nervous system, liver, respiratory tract.
Aromatic	Toluene	C_7H_8	92.14	0.87	Building materials (solvent and adhesives, paint, floor covering, chipboard), consumer and automotive products (cleaners, polishes, adhesive products, oils, greases, lubricants).	Disorders or diseases of the skin, eye, liver, kidney, nervous system, respiratory and/or pulmonary system.

3.3- Tested Ozone Monitors

Various ozone detectors, including four UV monitors, two electrochemical sensors, and one metal oxide instrument, were used for ozone measurement. Also, a Multi-Gas Photoacoustic Detector to monitor the interfering compounds was applied.

3.3.1- 2B Technologies Model 211

Scrubberless Ozone Monitor Model 211 (2B technologies) is one of the UV monitors that we applied to measure the ozone concentration. This monitor was selected as the reference instrument based on the EPA list [108]. The sensor uses a gas-phase scrubber to only remove ozone from the airflow. In the reference measurement step, by introducing a small concentration of NO (approximately 5 ppm) periodically into the sample air, it reacts with ozone and leads to removing ozone from the sample. The reaction is orders of magnitude faster than with any other ambient gas, which only leads to the removal of ozone.

$$NO + O_3 \rightarrow NO_2 + O_2$$

There are two approaches for supplying the NO gas scrubber:

1-Direct: Using NO gas cylinder.

2-Indirect: Using N_2O gas photolysis. This method was used to supply NO gas scrubber because N_2O is an inexpensive, non-corrosive, and low toxicity gas. In this method, NO is produced by photolysis of nitrous oxide (N_2O) via the internal NO generator, which uses a low-pressure mercury lamp.

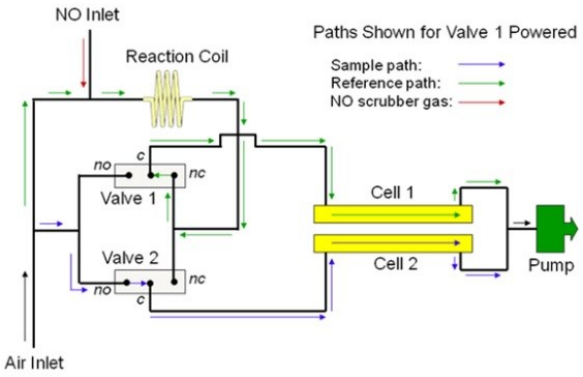

Figure 3. 1- Schematic diagram of the Model 211 Scrubberless ozone monitor [109]

As shown in Figure 3.1, this model uses the double beam spectrophotometer method (has two light paths, one passing through a reference solution and the other passing through the sample). This monitor includes an air pump to draw the sample into the system at an airflow rate of about 2 L/min. The flow is divided into two parts. Nitric oxide is added to one part and then passes through the reaction coil. A pair of solenoid valves in unison send scrubbed air and sample air through the absorption cells. On one side of these cells, a low-pressure mercury lamp and on the other side, photodiode are located. The light intensity of scrubbed air (I_0) is measured in cell 1,

while the intensity of sample air (I) is measured in cell 2. Then, ozone concentration is calculated by the Beer-Lambert Law in the range of 0-2 ppm. The monitored concentrations are stored by the instrument every 10 seconds.

3.3.2- Teledyne API Model 465L

The other UV photometric monitor selected for this study is the Multi-Channel Industrial Hygiene Ozone Monitor Model 465L (Teledyne Technologies). This six-channel ozone monitor measures the concentration based on the absorption of UV light emitted by a mercury lamp at 254 nm wavelength. The intensity of light inside the quartz tube (absorption cell) is measured by a light detector as the sample gas and scrubbed gas pass through it. Then, using the Beer-Lambert equation, the ozone concentration in the sample is calculated.

The Teledyne M465L operates at the airflow rate of 0.8 L/min with a low detection limit of less than 0.003 ppm, and records data every 5 seconds. Besides, it is suitable for measuring at low concentrations. It takes about six minutes for the monitor to complete a measurement cycle. Each channel takes about one minute, which includes a 30 second purge out and 30 second reading.

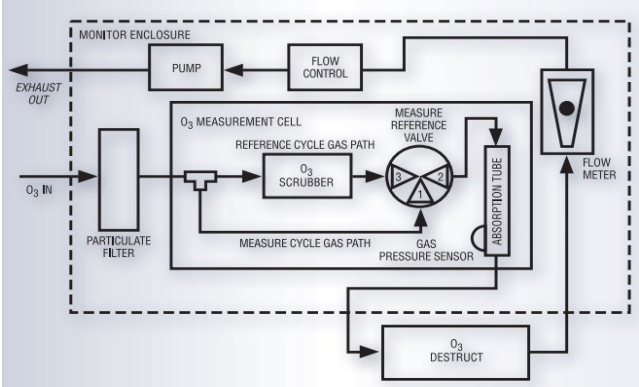

Figure 3. 2- Schematic diagram of Teledyne ozone monitor Model 465L [110]

3.3.3- 2B Technologies Model 202

This single-beam ozone monitor was designed based on the absorption of ultraviolet light at 254 nm. As shown in Figure 3.3, sample air is drawn into the instrument by an air pump at a flow rate of about 1 L/min. The light intensity inside the absorption cell when the sample air and scrubbed air pass through it (by switching the solenoid valve) is measured by a photodiode. The instrument measures the ozone concentration based on the Beer-Lambert equation. 202 model includes a Nafion Tube so that minimize the effect of humidity variations on the instrument reading.

This ozone monitor measures the concentration ranging from a low detection limit of 3 ppb to an upper limit of 250 ppm. The device records ozone concentrations every ten seconds. Hopcalite scrubber is applied for this device and the warm-up time is about 20 minutes.

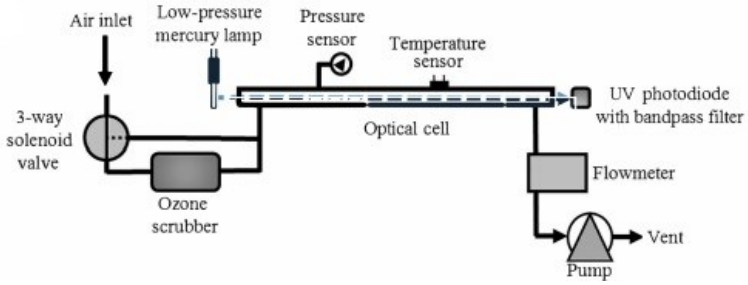

Figure 3. 3- Schematic diagram of the Model 202 single-beam ozone monitor [18]

3.3.4- 2B Technologies Personal Ozone Monitor (POM)

Similar to other UV ozone monitors, this instrument measures the ozone concentration based on the absorption of UV light at the wavelength of 254 nm. The difference between this monitor and the others is that it uses a U-shaped absorption cell, making this device smaller and lighter. As shown in Figure 3.4, the light emitted by the low-pressure mercury lamp is transmitted to the detector by two mirrors mounted at the cell corners. Also, the light intensity inside the absorption cell is measured by a photodiode when sample air and scrubbed air pass through the cell by switching the solenoid valve. The Dew Line installed after the solenoid valve reduces the impact of humidity changes on the response of monitor.

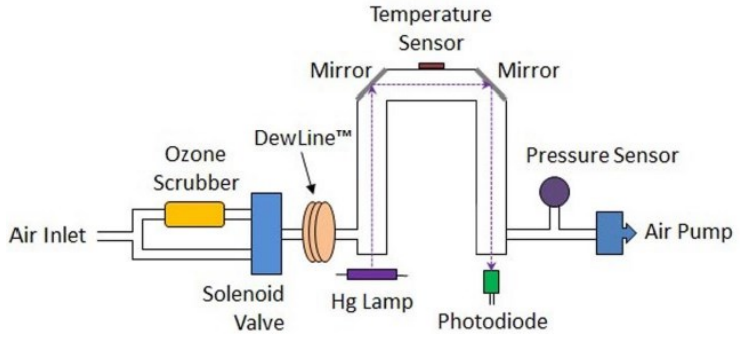

Figure 3. 4- Schematic diagram of the personal ozone monitor [111]

The sample air is drawn into the instrument by an air pump at a flow rate of about 0.8 L/min. The range at which this monitor can measure the ozone concentration starts from a low detection limit of 3 ppb to an upper limit of 10 ppm. The type of scrubber used for this monitor is hopcalite. It was set to store data every 10 seconds and it takes about 20 minutes to warm up.

3.3.5- ECO Sensors INC. Model C-30ZX

C-30ZX is the heated metal oxide semiconductor (HMOs) monitor. It can measure the concentration of ozone in the range of 0-0.14 ppm. In the case of using external data readout, the range of 0.02 to 0.30 ppm can be measured. In this sensor, oxygen and ozone are adsorbed on the surface of metal oxide. Ozone is broken down into charged ions by reaction with oxygen and contact with metal oxide. Then the change in metal oxide conductivity is measured as a signal

by biased electrodes. Its LED display consists of four green bars (0-0.04 ppm), three yellow bars (0.05-0.08 ppm), and three red bars (0.10-0.14 ppm).

The instrument needs about five minutes to warm up if it has been used recently, but it is a good precaution to warm-up the sensor overnight to burn off any absorbed chemicals that affect the calibration. The sensor operational temperature and humidity ranges are 15-27 ℃ and 0-85% RH. We applied an external datalogger (Wireless Monitoring & Data-logging Kit) to transfer data to the PC. The wireless analog sensor connected to the detector via USB first transmits the monitored gas concentrations to the gateway, then it sends data to the online portal.

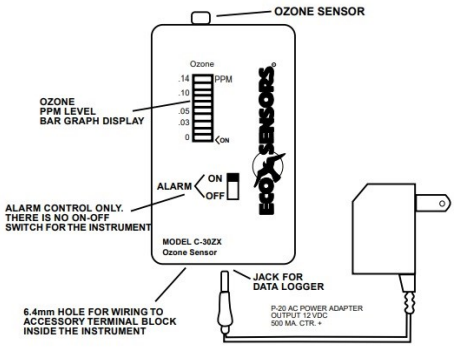

Figure 3. 5- ECO sensor Model C-30ZX [112]

3.3.6- Honeywell BW Solo

One of the electrochemical ozone monitors used in the study is BW solo. This monitor can measure ozone concentration in the range of zero to 1 ppm. In this sensor, the sample air enters the sensor through a capillary diffusion barrier and then passes through a filter to prevent unwanted gases from the system. Then, ozone molecules are immediately oxidized on the sensing electrode and generate an electric current. An amplifier measures the electric current generated between sensing and counter electrodes.

It can work at relative humidity in the range of 5% to 95% and operating temperature in the range of -30 to 50℃. One of the wireless Honeywell BW Solo features is that it can send the measurements to Honeywell desktop software by Honeywell mobile app paired with the monitor via Bluetooth.

3.3.7- Honeywell GasAlert Extreme BW Technologies

GasAlert Extreme is a small and lightweight electrochemical sensor. The range in which it can measure ozone concentration is from 0 to 1 ppm. The operating temperature and humidity at which it can operate are in the range of -20℃ to 50℃ and 15% to 90% RH, respectively. An external datalogger (IR DataLink) was used to transfer data from the detector to the PC.

3.3.8- Multi-Gas Photoacoustic Detector (INNOVA AirTech Instrument 1312)

A multi-gas photoacoustic detector was applied to measure the concentration of VOC compounds selected as potential interfering compounds. This equipment measures the gas concentration by irradiation of infrared radiation (IR) to gas molecules so that the IR is absorbed by the gas being monitored. Then, the absorbed light results in an increase and decrease in temperature and pressure of gas molecules and generate an acoustic signal detected by two microphones (Figure 3.6). This detector can selectively measure the concentration of up to five compounds and water vapor by using suitable optical filters installed in the filter carousel. The device was set to continuously analyze the concentration of TVOC (toluene), formaldehyde, CO_2, CO, and H_2O. The maximum flow rate of this device is 30 Cm^3/s (1.8 L/min).

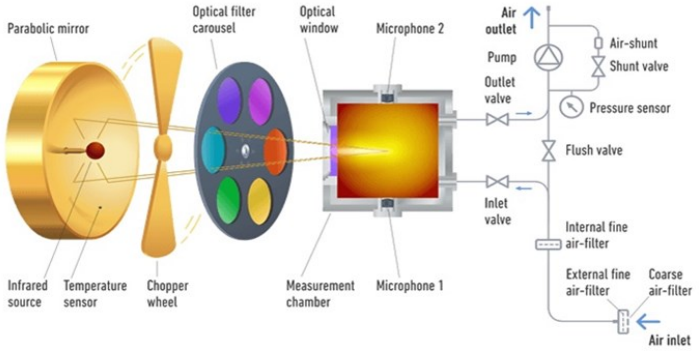

Figure 3. 6- Photoacoustic Spectroscopy

3.3.9- Multi-Channel Auto-Sampler

An automatic multi-channel sampler (CAI Intelligent Sampling System MK3) was connected to the photoacoustic detector to measure the selected VOC compounds concentrations at the chamber upstream and downstream simultaneously.

3.4- Duct Test Rig Specification

This stainless steel full-duct with 61cm×61cm cross-sectional area, 11.5 m length (the full length is 23 m) and 10 m^3 volume, was designed based on the ASHRAE Standard 145.2 [113]. Figure 3.7 shows the schematic diagram of this full duct. To minimize the adsorption of contaminant on the interior surface area, a smooth interior finish was considered for the system. As shown in Figure 3.7, a radial fan (Rosenburg America, DKNB-355) was placed before the clean-up bed so that it can provide up to 1 m^3/s airflow rate at 2 KPa pressure drop. A clean-up bed and a HEPA filter were installed downstream of the fan respectively to filter the carrier air.

This apparatus can perform in once-through (open-loop) or any percentage of recirculation modes. It should be said that the laboratory air is introduced to the system using the inlet damper. Also, the exhaust of the system vented directly to the exhaust duct of the laboratory, is cleaned by a clean-up bed before sending out of the building. In this system, a humidifier (Vapac Humidifiers) and a cooling coil have been placed before the blower.

The injection port is located after the clean-up bed and HEPA filter. The uniform dispersion of the challenge gas in the system is achieved by mixing baffles (containing a 30 cm diameter orifice plate and a 15 cm diameter 40% perforated plate) located after the injection point and downstream of the bend in the duct. This combination provides the single point sampling procedure from upstream and downstream. Moreover, an ASME long-radius flow nozzle located downstream of the system determines the airflow rate in accordance with ASHRAE Standard 145.2.

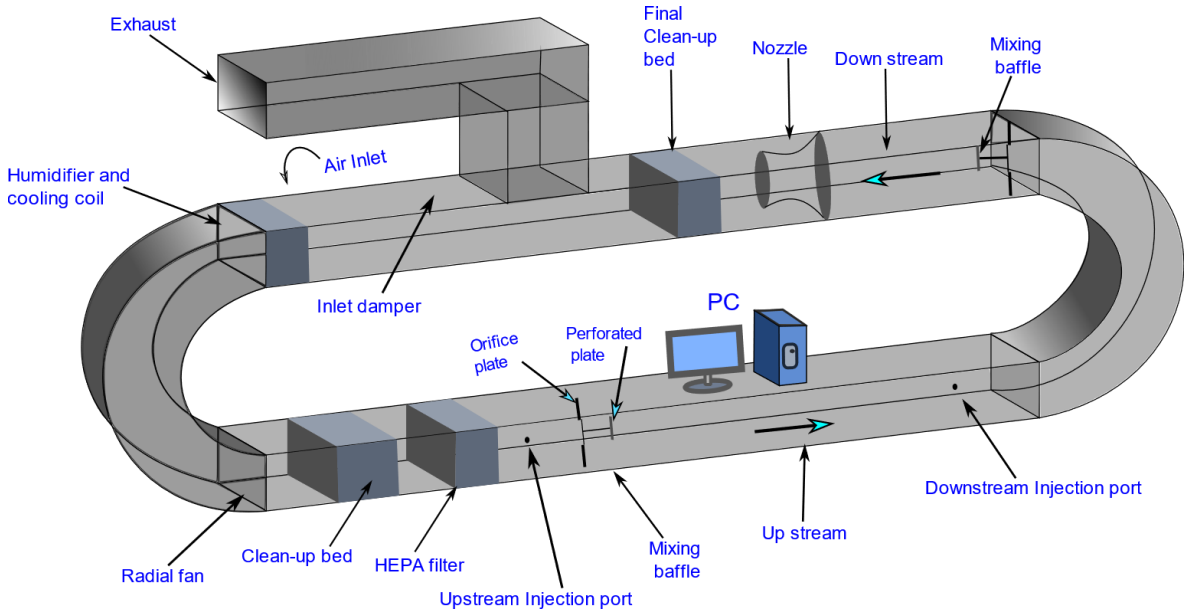

Figure 3. 7- Full-scale set-up schematic diagram

Some pre-qualification tests suggested by ASHRAE Standard 145.2 were carried out before starting the main tests to verify the validity of test procedure. The procedure and results of these tests are presented in Appendix A.

3.4.1- Environmental Condition

The temperature and relative humidity within upstream and downstream of the duct are monitored by temperature and humidity transmitters (Vaisala HUMICAP series HMT100) installed at the sampling port and before the nozzle. They were connected to a data acquisition system (DAS) (Agilent 34970A Data Acquisition/Switch Unit) to transfer data to the computer. The pressure drops created by the nozzle, is measured by a pressure difference transmitter (Cuba control pressure difference transmitter type-694) and two static taps mounted before and after the nozzle. The temperature is kept constant at 23 ± 2℃ within the experiments.

3.5- Test Chamber Characteristics

A stainless steel (316) chamber, according to the ASTM D 5116-90 guideline, with electropolished interior surfaces, was applied in this study. The volume, length, width, and height of the chamber

are 52.0 L (0.05202 m^3), 51.0 cm (20 in.), 40.0 cm (15.50 in.), and 25.5 cm (10 in.), respectively. A stainless steel (316) fan was mounted inside the chamber to ensure the uniformity of flow. Before initiating the tests, the chamber was cleaned with ethanol and deionized water and afterwards purged with compressed air. In this set-up, compressed air was considered as a carrier gas.

Figure 3.8 illustrates that the compressed air as a carrier gas with a specified pressure passed through the activated carbon filter (GAC) to remove possible interfering compounds in compressed air before entering the set-up. A portion of compressed air is then passed through the glass water bubbler (humidifier) controlled by flowmeter 2 (FM-1050 Series High Accuracy Flowmeter, Matheson). Flowmeter 3 shows the mixture of dry air and humidified air flowing into the Erlenmeyer Flask Vacuum, where the humidity sensor's probe was placed. The interfering compounds can be introduced into the flow at the T-connector using a syringe pump system. All the connections were made of Teflon tubing and stainless steel fittings to minimize gas losses. Within all experiments, the reference instrument (211-2B) was connected to the chamber outlet. Teledyne was connected to the upstream and output of the chamber. Furthermore, the concentrations of interfering compounds were continuously measured by Photoacoustic Detector connected to the upstream and outlet of chamber using Multi-channel Auto-Sampler.

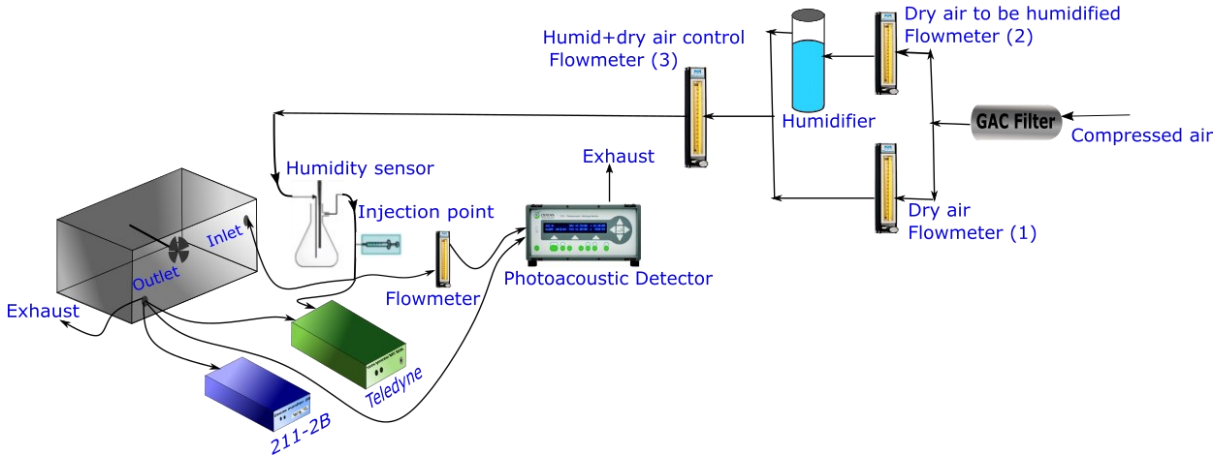

Figure 3. 8- Schematic diagram of small-scale chamber

3.5.1- Environmental Condition

The sample air temperature and relative humidity are measured using a humidity and temperature sensor included probe (Rotronic, HP32). Temperature and pressure were kept constant during each test to minimize their effects on sensors performance. The compressed air pressure was changed to 16 psi in all experiments because 10 psi (3.22 L/min- used for the INNOVA calibration) did not provide enough flow for the applied monitors in each test. At this pressure, the resulting flow rate was between 5.1 L/min and 5.2 L/min. Since one of the chamber inlets was covered with glass, increasing the pressure more than the set value may break the system. At this flow rate and by adjusting the dry air and inlet air to the humidifier, we could

reach the constant humidity levels from 20% to 70%. The system was not stable for RH more than 70%.

3.6- Instrument Calibration

All ozone detecting instruments were calibrated before use by their manufacturers. Besides, the monitors responses to stepwise increase and decrease in ozone concentration were evaluated. Due to the use of different VOC compounds, the photoacoustic detector had to be calibrated following the below procedure:

3.6.1- Ozone Monitor Response to Different Ozone Concentrations

This test was performed by connecting the selected sensors to an ozone calibrator (2B Technologies Model 306) under the fume hood. The calibrator was programmed at different concentrations and a specific time interval for each ozone monitor. The results of this experiment are stated in section 4.1.

3.6.2- Photoacoustic Detector Calibration

Since we selected different VOC compounds with different concentrations as potential interfering gases for the experiment, it is needed to calibrate the Photoacoustic Detector for each compound under the experimental conditions. The VOC compound was injected into the carrier gas with the flow rate of 3.22 L/min (pressure was set at 10 psi) and humidity 50% at four different concentrations using Hamilton syringes, see Figure 3.9. Then, the contaminated flow went to the detector controlled by the flowmeter (Dwyer Instruments Inc.).

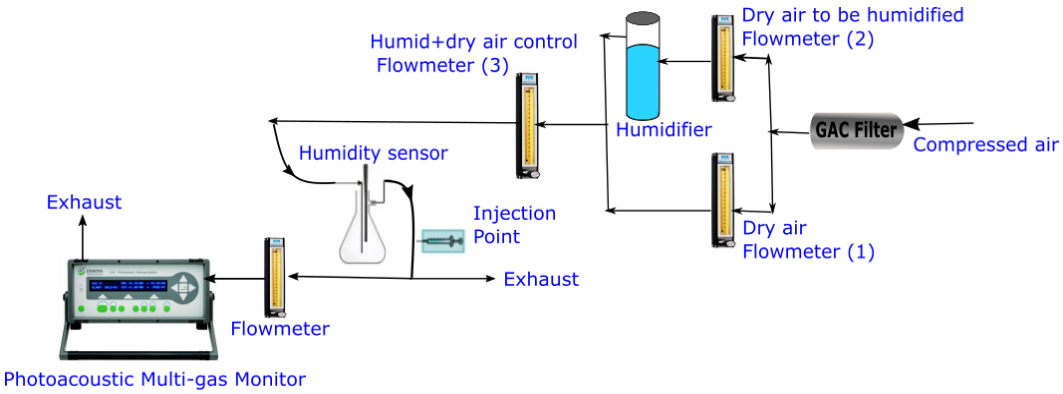

Figure 3. 9- Multi-gas photoacoustic detector calibration set-up

The photoacoustic detector was used to measure the concentration of TVOC, Formaldehyde, CO, CO_2, and water vapor. Since it was calibrated before with toluene as a standard equivalent compound for the total hydrocarbon (TVOC), the optical filter sensitivity and response factor are different for the selected VOC compounds. The calibration curves of all target compounds are represented in Appendix B.

3.7- Generation System

The selected ozone concentrations in this study include 50 ppb, 80 ppb, 100 ppb, 200 ppb, 500 ppb, and 1ppm. It should be said that concentrations of 500 ppb and 1 ppm have been selected in case of leakage in an industrial unit. The following described the applied ozone generations and injected VOC pump.

3.7.1- BMT 803N Ozone Generator

The BMT 803N ozone generator was used to inject ozone concentrations above 500 ppb. Since the ozone generator requires pure oxygen as the feed gas, an oxygen cylinder set at 10 psi was attached to a mass flow controller (Matheson Flow Controller Model 8270) to control the ozone generator inlet flow. The rate of ozone production at 100 g/Nm^3 and 20℃ is 8 g/h. It can operate at the flow rate of 0.1 to 4 L/min. It is also possible to adjust the output value from 15 to 100 % with the regulator on the front of device.

3.7.2- 1KNT-24 Ozone Generator, Enaly

This generator was applied for ozone concentrations less than 500 ppb (50, 80, 100, and 200 ppb). Compressed air was used as the source of oxygen supply for this ozone generator. The compressed air pressure was set at 10 psi. The optimum flow rate of this generator is between 1.5 to 2.5 L/min. The rate of ozone production of this instrument included:

1-Oxygen input (25 ℃):

Oxygen Flow (L/min)	Ozone Output (mg/h)
0.5	990
1	1100
1.5	1250

2-Dry air input (25 ℃, with air dryer):

-Ozone output:300 mg/h, Air flow:0.1 L/min

The ozone output can be manually adjusted between 0 to 100% by the controller installed on the front of instrument.

3.7.3- Ozone Calibrator Model 306, 2B Technologies

To examine the effect of stepwise increase and decrease of concentration on the response of sensors, we directly connected the inlet of each ozone monitor to this ozone calibrator output. In this instrument, ozone is produced by the photolysis of oxygen via a low-pressure mercury lamp in the range of 0-1000 ppb. Before the air enters the photolysis chamber, it passes through a particle filter, mass flow meter, an ozone /NO_x scrubber to remove any ambient ozone and NO_x, and another particle filter, respectively. A photodiode measures the lamp intensity inside the chamber. Then, the air containing ozone exits the cell through an overflow tee. The excess flow is vented through an internal ozone scrubber. The total output flow rate of this device is 4 L/min. The calibrator can be programed up to 10 individual steps.

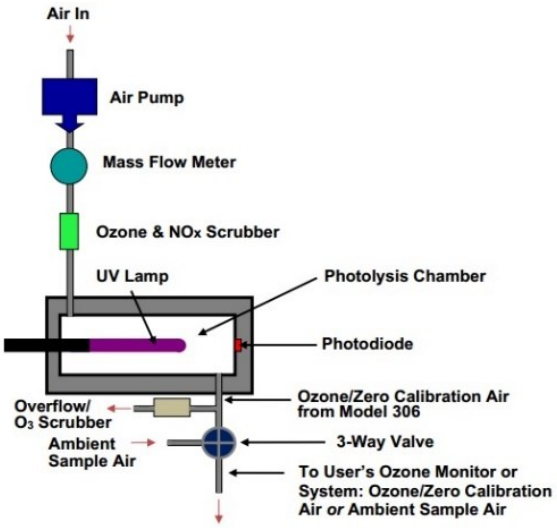

Figure 3. 10- Schematic diagram of the ozone calibrator Model 306 [114]

3.7.4- Syringe Pump System

Selected VOC compounds were injected into the chamber upstream using a syringe pumping device (KDScientific, KDS-210) and Hamilton gas-tight syringes. These compounds are liquid at room pressure and temperature. According to the TWA specified in ACGIH for these compounds, four concentrations of each test compound containing 10% TWA, 50% TWA, TWA, and twice of TWA were chosen for injection. The injection rates were controlled by adjusting the airflow rate in the chamber with rotameters 1 & 2.

3.8- Experimental Methodology and Procedure

3.8.1- Full Duct Tests

Six ozone monitors including 2B Technologies Model 211, Teledyne API Model 465L, 2B Technologies Personal Ozone Monitor (POM), ECO Sensors INC. Model C-30ZX, Honeywell BW Solo, and Honeywell GasAlert Extreme BW Technologies were used in this study to evaluate the impact of humidity variations, air velocity, and airflow direction in the presence of ozone.

Full-scale tests were conducted at three airflow rates of 500, 1000, and 2000 cfm and 50% RH. Also, ozone was injected into the duct using an ozone generator (Figure 3.11). Due to the maximum detection limit of ECO Sensor and BW solo, the injected ozone concentrations in the tests related to these two sensors included 50 ppb, 80 ppb, and 100 ppb.
Sensors were turned on at least 15 min before starting each experiment, allowing them to stabilize except for Teledyne, which required a long time to be stabilized. Before injection, we measured the background concentration as well. Because of the limited time interval of ECO Sensor (minimum 10 min), the tests related to this monitor ran for 1.5 hours to ensure having adequate data. Thirty minutes for other tests was considered after the stabilization of injected concentrations.

As shown in Figure 3.12, four ozone monitors (ECO Sensor, BW solo, POM, and BW) were mounted inside the duct at two different positions: perpendicular and parallel to the flow. Two monitors were placed in the duct upstream in each test due to having a uniform concentration distribution. Due to the location of the stainless-steel probe, the sensors holder was placed slightly away from that. The holder was located in a specific place during all experiments. In both directions, ozone monitors were located 7" and 5" from the duct wall and side holder. The stainless-steel probe direction was perpendicular to the flow and kept constant during all tests due to the connection to the reference sensor (2B Technologies 211). Teledyne was also connected to this probe using a cross fitting. It should be noted that Teledyne ozone monitor's channels, two by two, including 1&4, 2&5, 3&6, were connected to the upstream, before injection, and downstream of the duct using a wye (Y) connector, respectively.

Figure 3. 11- Part of full duct set-up (connected ozone generators)

According to the results of parallel and perpendicular experiments, the parallel position and the airflow rate of 500 cfm were selected to study the dynamic effect of humidity. In this experiment, we set the humidifier at a specific set point so that the humidity fluctuated between 30% and about 80%. Similar to the previous experiments, only two sensors were mounted into the system simultaneously in each study and 211-2B ozone monitor was also used as the reference sensor. The injected ozone concentrations in this study included 50 ppb, 80 ppb, 100 ppb, 200 ppb, and 500 ppb.

All the connections were made of Teflon tubing and stainless-steel connectors to avoid the decomposition of ozone. Also, the length of tubes was selected as short as possible to minimize ozone destruction. At the end of each experiment, the test rig was continued to flush out at the same airflow rate to prevent ozone residue in the system and give the monitors enough time to return to the background ozone concentration. All the output data logged by the sensors were downloaded to the PC using the manufacturers' proprietary software.

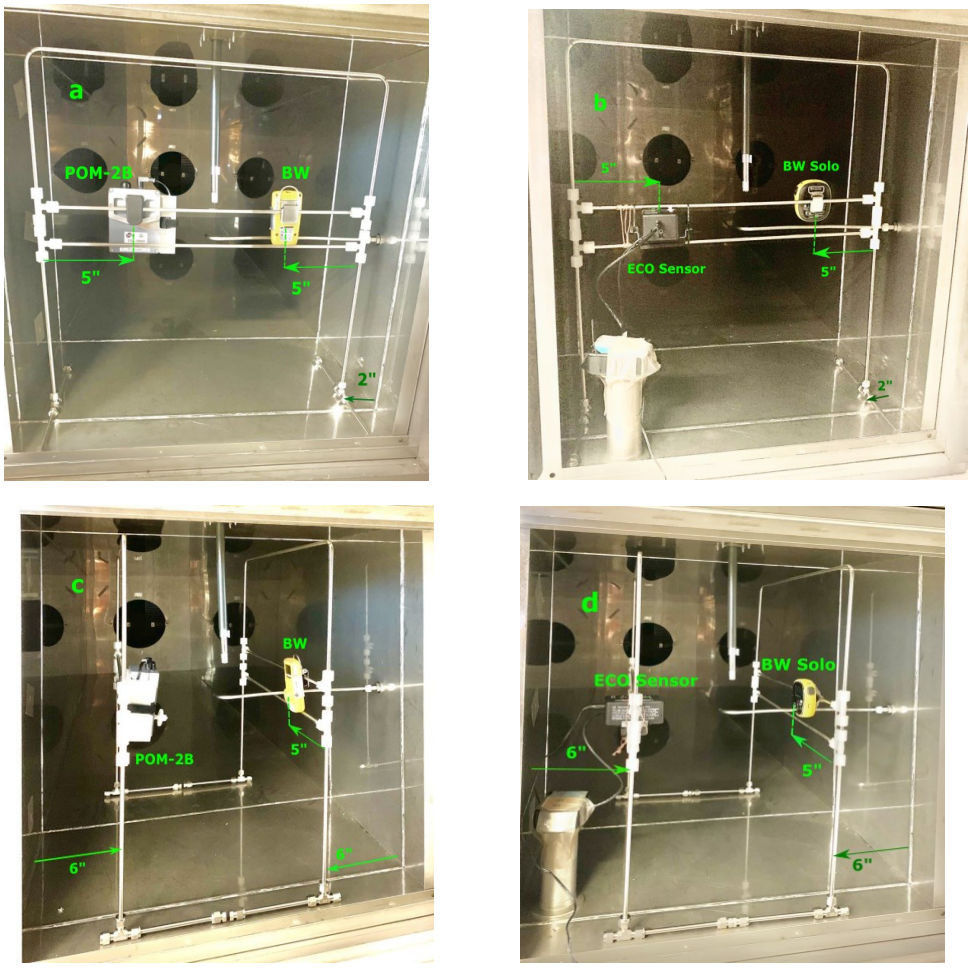

Figure 3. 12- Ozone Sensors location in the case of perpendicular and parallel to the flow, a and b: perpendicular direction. c and d: parallel orientation

3.8.1.1- Investigation of Concentration Uniformity in Perpendicular and Parallel Directions Experiments

The sensors were placed at the same location in each test to be exposed to the most identical conditions. Since there is a possibility of error in measuring locations, we evaluated the ozone concentration at points a few inches more and less than the desired place. This test was conducted at airflow rates of 500, 1000, and 2000 cfm. The injected ozone concentration into the full duct was 200 ppb. The ozone concentration was measured at different points by a PTFE probe connected to the 211-2B monitor. In the perpendicular direction, according to the width of each sensor, tubes with lengths 4.7” (ECO Sensor), 4” (BW and BW solo), and 2” (POM) were connected to the PTFE probe by a connector so that the sensor can measure the concentration in the exact place (Figures 3.13).

Based on Table 3.4, slight changes in the location of each sensor have a negligible effect on the response of sensor in both directions. Since this experiment was performed on two consecutive

days, small differences in the concentrations of two directions can be due to the different humidity of two days, ozone generator settings, and error in adjusting the direction of tube.

Figure 3. 13- PTFE tube positions in concentration uniformity test

Table 3. 4- Summary of concentration uniformity test

Direction	**Location**		**500 cfm** -dp-duct-lab air (inchWg): 0.260 -RH: 13% & 19%	**1000 cfm** -dp-duct-lab air (inchWg): 0.861 -RH: 13% &19%	**2000 cfm** -dp-duct-lab air (inchWg): 0.775 -RH: 13% & 19%
			Average	Average	Average
Parallel	**POM & ECO Sensor**	4”	202.35	203.13	201.70
		6”	202.02	203.03	201.40
		7”	201.16	204.99	203.68
	BW & BW solo	17”	207.22	216.57	223.69
		18”	206.80	218.17	224.79
		20”	207.9	218.86	227.29
Perpendicular	**POM**	6”	203.89	204.07	202.27
		7”	205.06	203.41	204.99
	ECO Sensor	6”	202.47	203.75	202.23
		7”	203.21	203.88	205.58
	BW & BW solo	17”	211.44	212.45	225.59
		18”	211.16	211.96	228.45

3.8.2- Small-Scale Environmental Chamber Tests

The influence of humidity and interfering compounds on the ozone monitors performance at different humidity levels (0.01%, 20%, 50%, and 70%) and by injection of three VOC compounds (Aceton, Ethanol, and Toluene) were investigated using the small-scale environmental test chamber. We selected six commercially available ozone monitors, including 2B Technologies Model 211, Teledyne API Model 465L, 2B Technologies Personal Ozone Monitor (POM), ECO Sensors INC. Model C-30ZX, Honeywell BW Solo, and Honeywell GasAlert Extreme BW Technologies for these two series of experiments. The airflow rate through the chamber and tubes was 5.1 L/min. The calculated air exchange (ACH) for the chamber with a volume of 52.02 L is 5.88 h^{-1}. The temperature was kept constant at 21.34 ± 0.5℃ within all experiments. Humidity was controlled by mixing the compressed air with the airflow that was passing through the glass bubbler. All sensors were turned on for at least 15 min prior to starting the main tests except for Teledyne, which needed more time.

To study the impact of humidity, four small ozone monitors (POM, BW, BW solo, and ECO Sensor) were housed inside the chamber (Figure 3.14). A stainless steel fan was installed inside the chamber and due to lack of sufficient space, only two small sensors could be placed inside at a time. 211 and Teledyne (channels 2,3,5,and6) were connected to the chamber outlet using Teflon tubing and a cross fitting. The remaining two channels of Teledyne were attached to the chamber upstream. The period of testing for each humidity set-point varied from one to one and a half hours.

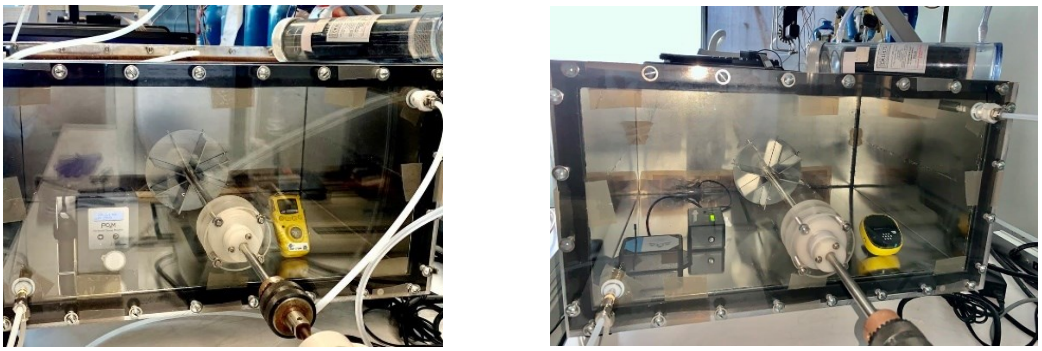

Figure 3. 14- Ozone sensors location inside the chamber

To evaluate the impact of interfering gases, different concentrations of selected VOC compounds were injected by syringes into the carrier gas. In this study, we used four ozone sensors (211-2B, Teledyne, BW solo, and ECO Sensor). BW solo and ECO Sensor were mounted into the chamber, and 211 and Teledyne were connected to the inlet and outlet of chember. Moreover, a Multi-Gas Photoacoustic Detector (INNOVA AirTech Instrument 1312) was applied to measure the VOC concentrations during this study. We examined the effect of these compounds at both dry (0.01% RH) and humid (50% RH) air. Each test was run for 15 to 30 min after the concentration inside the chamber reached equilibrium. At the end of each injection, the chamber was purged with clean air to return the sensors to the background reading.

3.9- Data Analysis

3.9.1- Calculation of Sensors Accuracy

Accuracy is defined as the ability of a monitor to measure the true concentration of the desired environment. According to the NIOSH accuracy criterion (AC), measurements of an acceptable monitor are within $\pm$25% of the true concentration of the analyte with 95% confidence interval (CI). In other words, in order an ozone monitor fulfills the AC, it should have a 95% confidence interval of mean error within -25 to +25% (lower limit of 95% CI $<$ mean error $<$ Upper limit of 95% CI) [115, 116].

All measured data were imported into MATLAB R2018b for data analysis. First, the percentage difference between the concentrations measured by the monitors and the reference instrument (211-2B) was calculated using the following equation [116]:

$$Error = \left(\frac{Ozone\ monitor_i - Reference\ instrument_i}{Reference\ instrument_i}\right) \times 100 \quad (3.1)$$

Then, the mean error was computed and since the distribution of the created error variables was not normal, we used the bias-corrected and accelerated (BCa) bootstrap method to calculate 95% CI using MATLAB [115, 116]. The calculation method is given in Appendix C. Figure 3.15 illustrates an example of the estimated 95% CI.

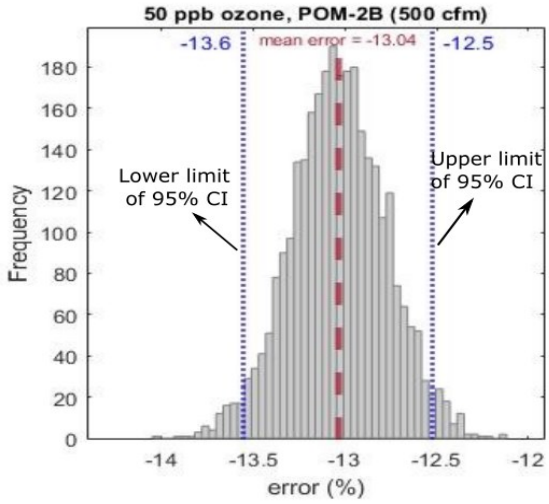

Figure 3. 15- 95% CI of mean error for POM instrument in perpendicular direction to the flow

3.9.2- Calculation of Sensors Precision

Precision refers to how close measurements of a monitor are to each other. In other words, it reflects the ability of a gas monitor to replicate measurement results [115]. Precision is calculated by dividing the measurements standard deviation by the measurement mean. The precision of 5% or less indicates that the performance of a sensor is satisfactory [26].

3.9.3- Maximum Level of Test Compounds Interference in UV Ozone Monitors

The degree of interference of any compound that absorbs UV light with a wavelength of 253.7 nm depends on these factors: The absorption cross-section of compound, Its ambient concentration, and Removal degree of that compound by the scrubber. The maximum interference of a given compound (with a known absorption spectrum) when using a UV ozone monitor can be estimated by the selectivity factor (S). The maximum interference occurs when the scrubber completely removes the desired compound [117].

$$S = \frac{\sigma_{O_3}}{\sigma_{Interferent}} = \frac{1.15\times10^{-17} cm^2 molec^{-1}}{\sigma_{Interferent}} \quad (3.2)$$

S= the relative response of ozone to the potential interferent
σ= Absorbance cross section at 253.7 nm

Table 3.5 provides a list of selected compounds with their absorption cross-sections and selectivity factors. For example, the selectivity factor of toluene is 29, which means that 29 ppb of toluene is required to produce a response equal to 1 ppb of ozone [117].

3.5- Theoretical selectivity factor of selected VOC compounds

Interferent	**σ** at 254 nm, $\mathbf{10^{-17} cm^2\ molecule^{-1}}$	Selectivity factor (S)
Acetone	0.003	290
Ethanol	-	-
Toluene	0.039	29

Chapter 4: Experimental Results and Discussion

In this chapter, the results of the experiments are discussed. In general, the experiments are divided into two categories. First, the effect of physical environmental parameters, including humidity, airflow rate, and airflow direction, is examined in a full duct and small chamber. The second part evaluates the sensors performance in the presence of some interfering gases (acetone, ethanol, and toluene) in a small-scale environmental chamber.

4.1- Ozone Monitors Response to Different Ozone Concentrations

4.1.1- UV Absorption Technology

The 211-2B sensor response was evaluated at ozone concentrations of 0, 50, 100, 200, 300, 500, 250, 100, 50, and 0 ppb in 10 consecutive steps, each of which lasted 15 min. At the start of each step, the sensor responded rapidly to concentration changes. The sensor outputs were nearly stable over the whole injected concentrations and continuous operation at different concentrations did not affect its performance. Figure 4.1 indicates that the sensor measurements were in good agreement with the ozone calibrator (R^2= 1). The slopes of regression lines are almost equal to unity, which implies the good performance of 211-2B. This monitor measured ozone concentration with a precision of 0.17%- 0.75%, which refers to precise measurement.

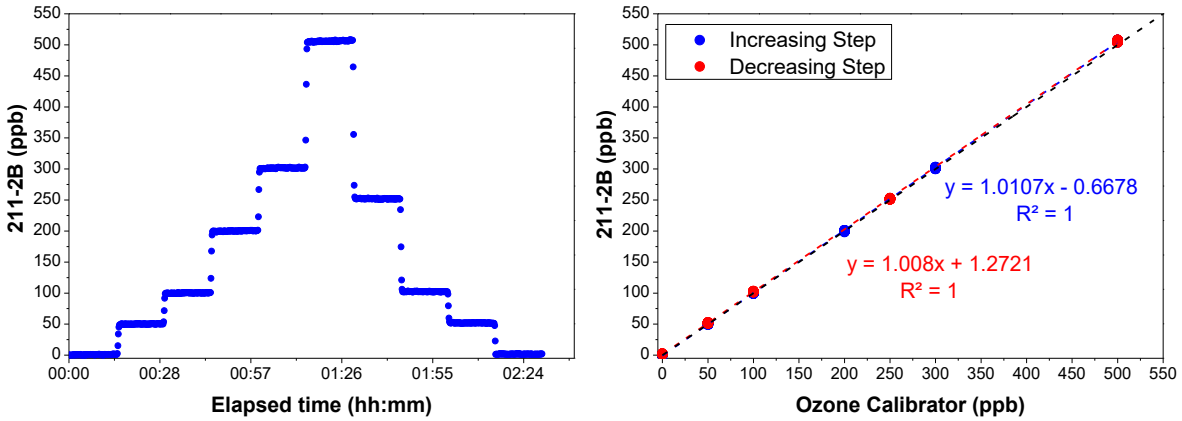

Concentration	0 ppb	50 ppb	100ppb	200 ppb	300 ppb	500 ppb	250 ppb	100 ppb	50 ppb	0 ppb
Average	0.60	50.16	100.11	200.05	301.41	505.9	251.91	102.31	51.82	1.62
SD	0.47	0.38	0.45	0.58	0.63	0.91	0.49	0.34	0.36	0.35
Precision (%)	78.33	0.75	0.44	0.28	0.20	0.17	0.19	0.33	0.69	21.60

Figure 4. 1- The 211-2B sensor response to stepwise increase and decrease of ozone

The ozone concentration was also measured continuously using POM at the same concentrations and timespan defined for 211-2B. The standard deviation (SD) values represent that the sensor reading was approximately stable within each injection. POM showed a quick response to changes in concentration, except in the transition from 300 ppb to 500 ppb, which took about two minutes to stabilize. As shown in Figure 4.2, the sensor outputs are linearly proportional to

the injected concentrations in increasing and decreasing steps (R^2= 0.99). The slopes of both regression lines, which are a little less than unity, refer to underestimating the ozone concentration in each step than the injected values. According to the results, continuous exposure to ozone resulted in a 2.88 ppb and 2.04 ppb increase at concentrations of 50 and 100 ppb in decreasing step. POM indicated good precision at different ozone concentrations.

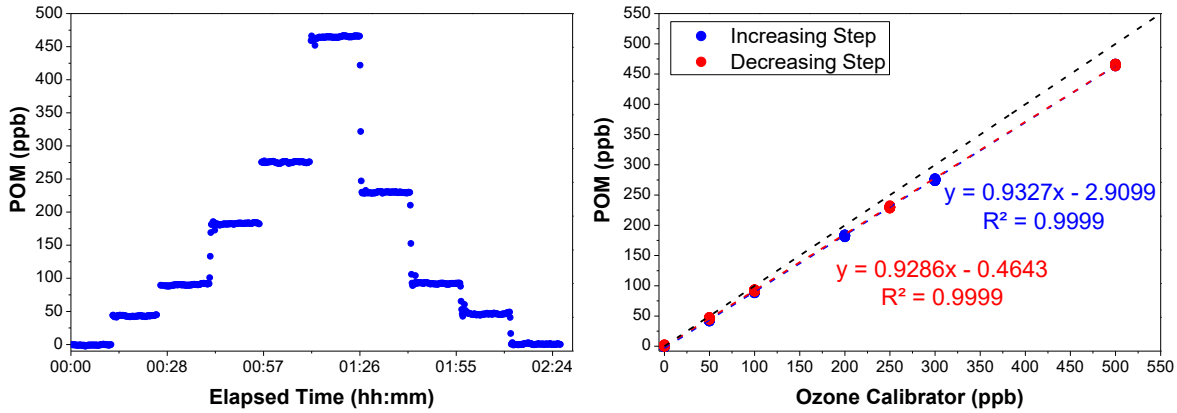

Concentration	0 ppb	50 ppb	100 ppb	200 ppb	300 ppb	500 ppb	250 ppb	100 ppb	50 ppb	0 ppb
Average	-0.84	43.15	90.17	182.60	275.40	464.93	229.79	92.21	46.03	0.56
SD	0.48	0.75	1.12	0.90	0.86	0.83	0.79	0.72	0.84	0.73
Precision (%)	57.14	1.73	1.24	0.49	0.31	0.17	0.34	0.78	1.82	130.3

Figure 4. 2- The POM sensor response to stepwise increase and decrease of ozone

A stepwise reduction from 500 ppb to zero ppb was considered for Teledyne. The sensor responded rapidly upon changing the concentration. This UV instrument outputs were nearly stable during the injection (SD ranged from 3.03 ppb to 0.73 ppb). As shown in Figure 4.3, the regression line is highly linear with R^2=0.999, and its slope is approximately near unity. The greatest difference between the injected and the measured average values was observed at 500 ppb and 50 ppb so that the ozone concentration was measured about 10 ppb less and 10 ppb more, respectively. It should be noted that at zero concentration, this sensor indicates the ozone concentration about 10 ppb to 15 ppb. Precise measurement of ozone is evident from the calculated precision values.

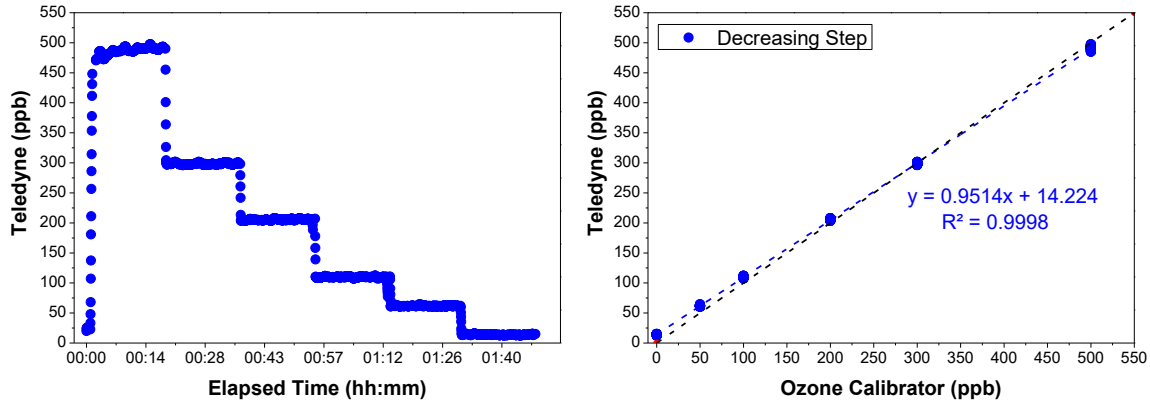

Concentration	500 ppb	300 ppb	200 ppb	100 ppb	50 ppb	0 ppb
Average	490.57	298.39	205.43	109.78	61.76	13.88
SD	3.03	1.44	1.08	1.005	0.76	0.73
Precision (%)	0.61	0.48	0.52	0.91	1.23	5.25

Figure 4. 3- The Teledyne sensor response to stepwise decrease of ozone

The 202-2B sensor was exposed to the same concentrations considered for the reference instrument (211-2B). The R^2 values of both regression equations (R^2> 0.99) are identical and indicate that the sensor outputs have a significant linear relationship with the defined ozone concentrations (Figure 4.4). In addition, the data scatter was almost the same throughout the experiments (SD=2.16-3). The sensor reading was immediately changed upon injection of a new concentration. Since this sensor underestimated the injected values, the slopes of regression lines are a little lower than unity. Continuous exposure to ozone slightly altered the sensor response at 50 and 100 ppb in decreasing step, leading to an increase of 2.54 ppb and 2.74 pp at these concentrations. This sensor showed good precision with increasing and decreasing the ozone concentration.

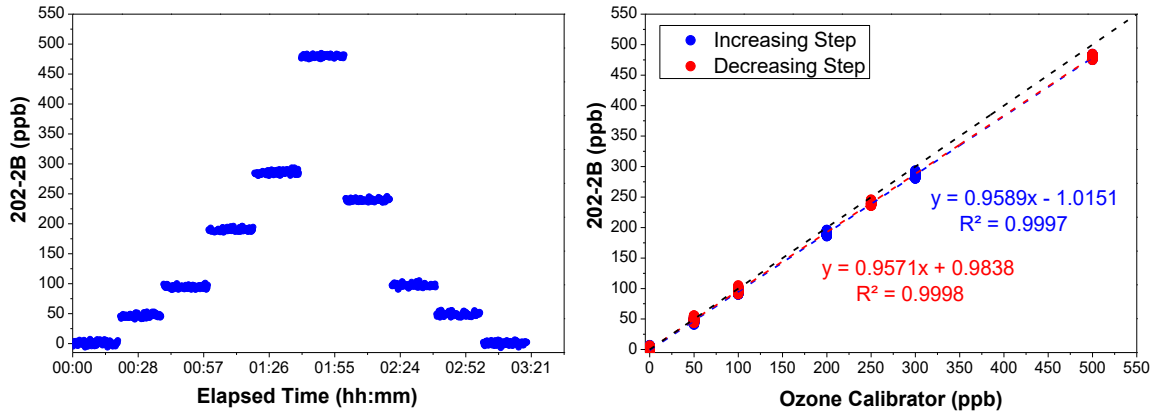

Concentration	0 ppb	50 ppb	100 ppb	200 ppb	300 ppb	500 ppb	250 ppb	100 ppb	50 ppb	0 ppb
Average	0.56	46.40	94.52	189.73	285.64	479.71	239.65	97.26	48.94	0.79
SD	2.99	2.81	2.38	2.42	3.004	2.16	2.29	2.72	2.92	2.67
Precision (%)	533.9	6.05	2.51	1.27	1.05	0.45	0.95	2.79	5.96	337.9

Figure 4. 4- The 202-2B sensor response to stepwise increase and decrease of ozone

4.1.2- Electrochemical Sensor Technology

The BW sensor response to stepwise increase and decrease of concentration was examined at concentrations of 0, 50, 100, 200, 300, 500, 250, 100, 50, and 0 ppb. Over time, the sensor measurements at each concentration stabilized so that the SD values became zero in the reduction step. Besides, this sensor immediately responded to the increasing or decreasing of concentration. A linear relationship with a coefficient of R^2> 0.96 can be observed between the sensor outputs and the ozone calibrator. Figure 4.5 shows that the slopes have a big deviation from unity, which means the sensor considerably underestimated the concentrations. This may

be related to the ambient humidity, which was lower than the sensor operation humidity (15%-90%). Precision values became zero as the ozone concentration and data scattering decreased.

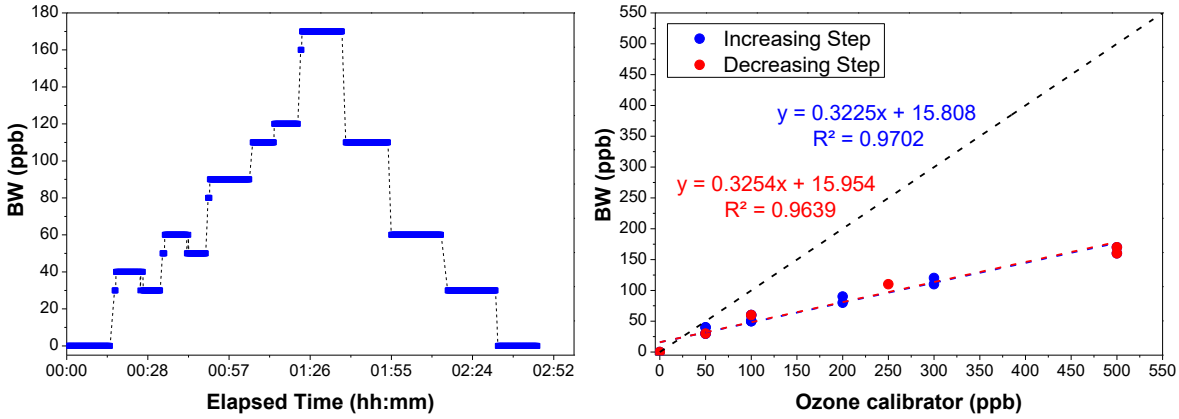

Concentration	0 ppb	50 ppb	100 ppb	200 ppb	300 ppb	500 ppb	250 ppb	100 ppb	50 ppb	0 ppb
Average	0	35.81	55.16	89.55	115.25	169.66	110	60	30	0
SD	0	4.95	5.02	2.08	5.01	1.81	0	0	0	0
Precision (%)	0	13.82	9.1	2.32	4.34	1.06	0	0	0	0

Figure 4. 5- The BW sensor response to stepwise increase and decrease of ozone

To investigate the BW solo sensor performance in the presence of ozone, we set the ozone calibrator at concentrations of 0, 50, 80, 100, 80, 50, and 0 ppb. The sensor reading was almost stable at each injected value (SD was between 0 and 5.88). It responded quickly to concentration changes. Although it exhibited a linear trend with increasing and decreasing of concentration (R^2= 0.99), the slopes of regression lines demonstrate that this sensor overestimated the ozone concentrations (Figure 4.6). BW Solo demonstrated good precision at all ozone levels.

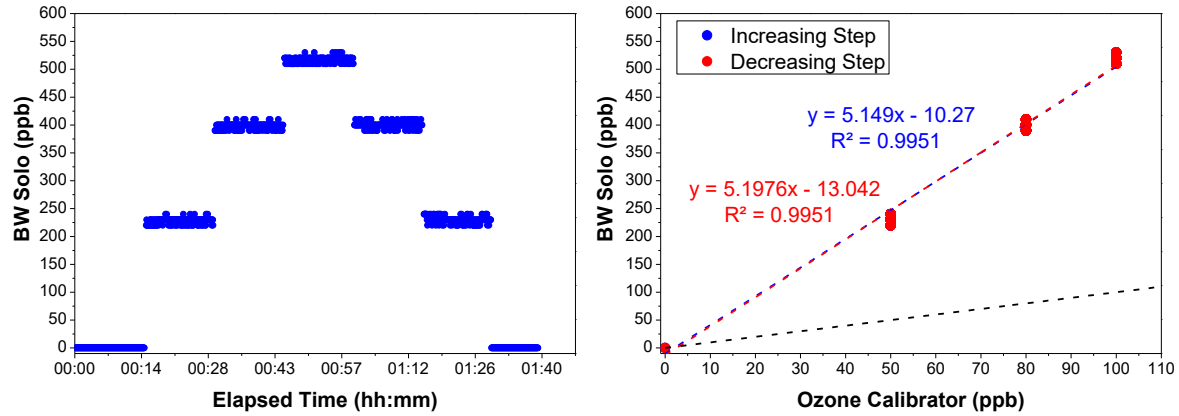

Concentration	0 ppb	50 ppb	80 ppb	100 ppb	80 ppb	50 ppb	0 ppb
Average	0	227.24	398.13	517.09	400.11	229.77	0
SD	0	5.30	5.04	5.34	5.23	5.88	0
Precision (%)	0	2.33	1.26	1.03	1.30	2.55	0

Figure 4. 6- The BW Solo sensor response to stepwise increase and decrease of ozone

4.1.3- Metal Oxide Semiconductor Sensor

According to the maximum detection limit of the ECO sensor, concentrations of 0, 50, 100, 140, 100, 50, and 0 ppb and a 60 minutes injection time were selected to check the sensor response. Continuous exposure to ozone led to a reduction in the SD value of 50 ppb, while 100 ppb ozone was associated with an 8.09 ppb increase. As it can be seen, in decreasing step, R^2 value is a little closer to unity. Figure 4.7 represents that the sensor was not constant at each concentration and its output was gradually increasing. Also, the ozone concentrations were overestimated by using this sensor. The slopes of both lines confirm this overestimation. This metal oxide sensor did not show good precision, especially at low concentrations.

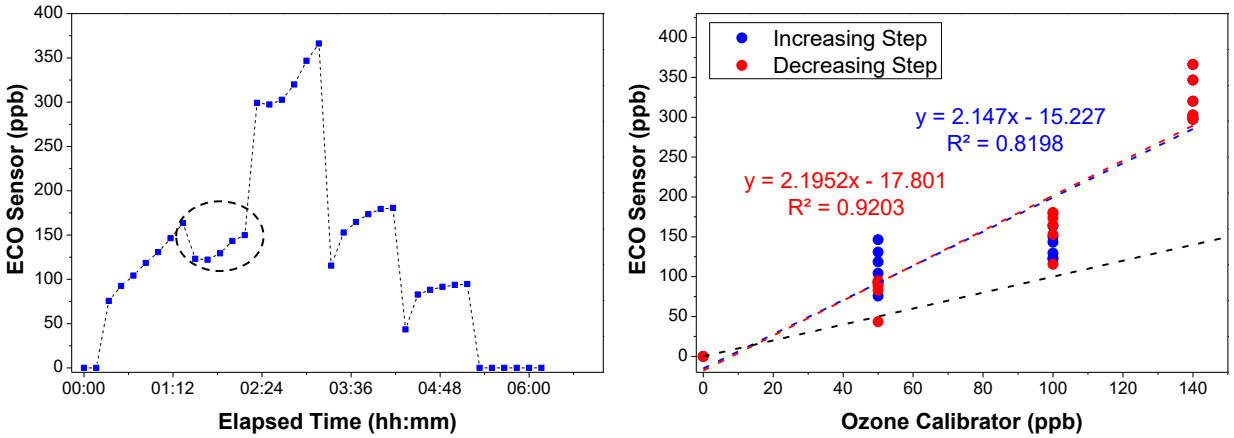

Concentration	0 ppb	50 ppb	100 ppb	140 ppb	100 ppb	50 ppb	0 ppb
Average	0	111.3	138.56	322.01	161.03	82.35	0
SD	0	25.83	16.54	28.53	24.63	19.56	0
Precision (%)	0	23.20	11.93	8.82	15.29	23.75	0

Figure 4. 7- The ECO Sensor response to stepwise increase and decrease of ozone

4.2- Effects of Physical Parameters on Ozone Sensors Performance

In the following, we explained and analyzed the influence of air velocity, airflow direction (perpendicular and parallel), and humidity variations on the response and accuracy of the sensors. Besides, the results were compared with the reference instrument, which is 211-2B.

4.2.1- Impact of Air Velocity and Airflow Direction

One of the essential environmental factors that can influence the response of ozone sensors is the airflow rate. Moreover, the orientation of sensors towards the airflow direction is another factor that can affect sensors performance. In this part, the impact of these two parameters on the performance of six ozone sensors (2B Technologies Model 211, Teledyne API Model 465L, 2B Technologies Personal Ozone Monitor (POM), ECO Sensors INC. Model C-30ZX, Honeywell BW Solo, and Honeywell GasAlert Extreme BW Technologies) was discussed.

The sensors were tested under three airflow rates, including 500, 1000, and 2000 cfm at a constant temperature of 24±1°C and 50±5% humidity. They were exposed to different ozone concentrations, including 0, 50, 80, 100, 200, 500 ppb, and one ppm. To investigate the effect of airflow directions, four small ozone sensors (ECO Sensor, BW solo, GasAlert Extreme (BW), and POM) were mounted inside the duct in two different positions: perpendicular and parallel to the flow. 211-2B and Teledyne sensors were connected to the stainless-steel probe, whose direction was kept constant and perpendicular to the flow. The results of these experiments are illustrated and reported in Figures 4.8 and 4.9 and Appendix D.

Figure 4.8 illustrates the sensors response in the perpendicular direction. According to the results, exposure to different airflow rates had little influence on UV ozone sensors performance. The mean concentrations and standard deviation (SD) values at concentrations below 200 ppb were almost identical (Appendix D). By increasing the airflow rate at 500 ppb ozone, the average of data at 1000 and 2000 cfm decreased by 4 ppb and 6 ppb for 211-2B, 6 ppb and 13 ppb for Teledyne, and 20 ppb and 22 ppb for POM compared to the mean concentration of 500 cfm. Also, at one ppm ozone, a minimal growth in 211-2B response and a slight decrease in the Teledyne and POM measurements were observed. According to the table in Appendix D, the SD decreased with increasing airflow rate, especially at 500 ppb and one ppm; this decrease is well evident. Accordingly, these UV sensors seem suitable for ozone measurement at different airflow rates.

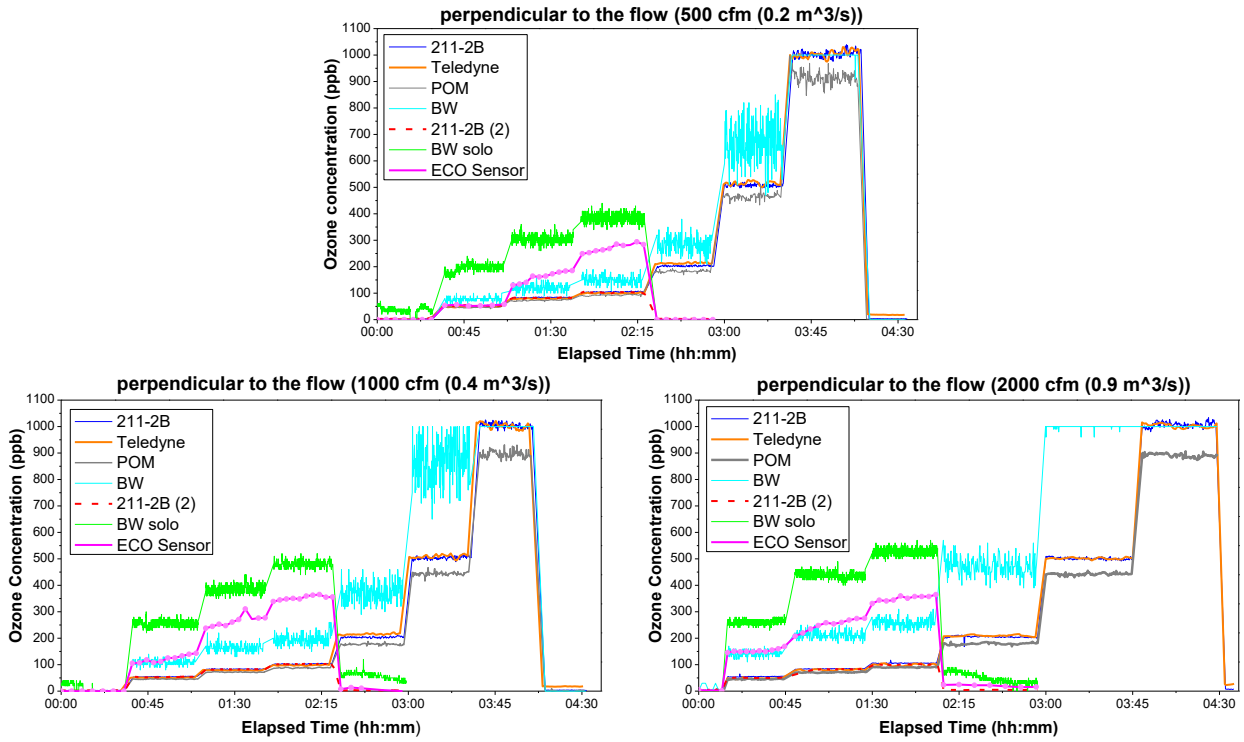

Figure 4. 8- The response of sensors in perpendicular direction toward the airflow

While two electrochemical sensors (BW and BW solo) responded significantly to the increase of airflow rate. The outputs of these monitors were overestimated by increasing the airflow. Also,

the difference between the average concentrations of 500 cfm and the other two flow rates considerably increased as the ozone concentration enhanced (Appendix D). BW indicated the most changes at 500 ppb so that sensor output was overestimated by 202.09 ppb at 1000 cfm and 330.77 ppb at 2000 cfm. This behavior was also observed for BW solo. It experienced the most changes at 100 ppb, indicating the ozone concentrations at 1000 cfm and 2000 cfm more than that of 500 cfm. The most BW data scattering occurred at concentrations of 200 ppb and 500 ppb. This dispersion was associated with an increase from 29 ppb to 37.12 ppb at 200 ppb ozone and a decrease from 80.4 ppb to 5.06 ppb at 500 ppb. However, the SD values at all concentrations were approximately the same for BW solo and slightly enhanced by increasing the ozone concentration.

ECO Sensor outputs went up remarkably with increasing airflow rate at each injected concentration, especially at 50 ppb (at 2000 cfm) and 80 ppb (at 1000 cfm), where the difference of average concentrations with the ozone concentration at 500 cfm was 98.49 ppb and 103.26 ppb, respectively. Also, this sensor experienced the highest data scatter at 80 ppb (Appendix D). According to the results, these electrochemical and metal oxide sensors are not as accurate and reliable as UV sensors.

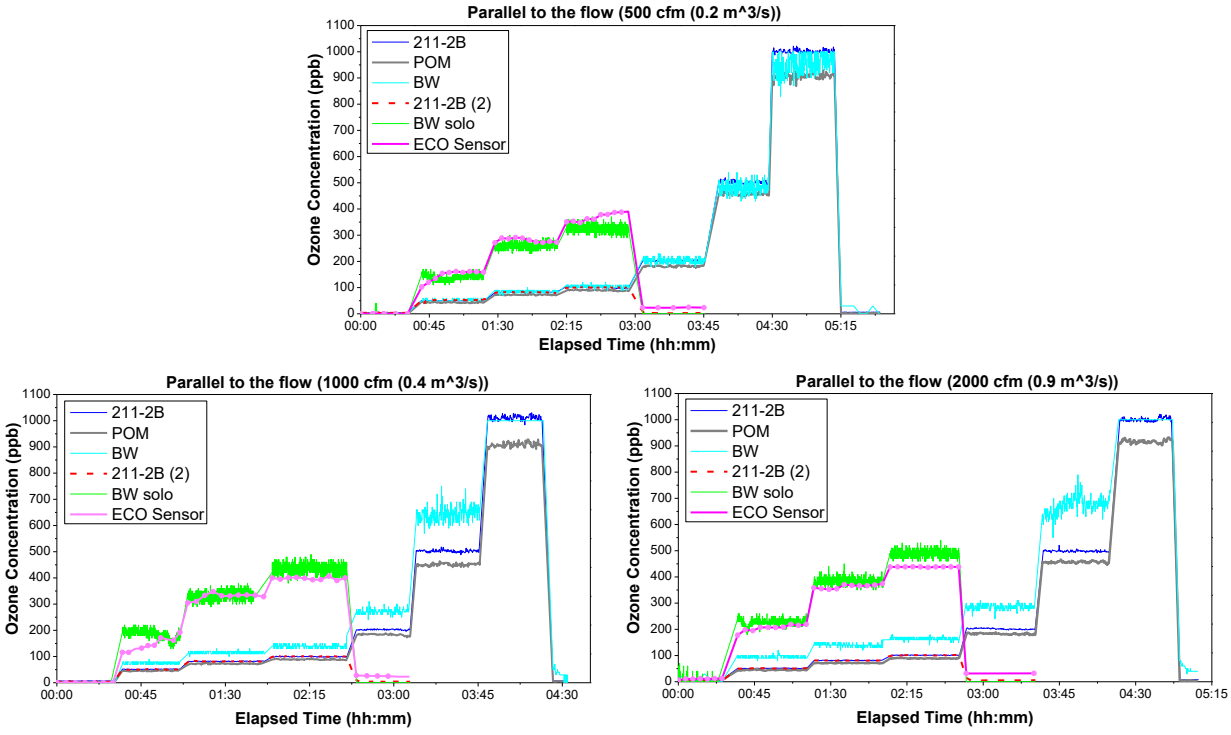

Figure 4. 9- The response of sensors in parallel direction toward the airflow

We examined the sensors performance in the parallel orientation as well. Results of this test at 50% RH are shown in Figure 4.9. The impact of increasing airflow rate and changing the airflow direction on the UV sensor (POM) was negligible. 211-2B outputs in this study were similar to the perpendicular direction test. POM response was identical at different airflow rates and

orientations. The highest SD values of POM were observed at 500 ppb and one ppm, with values decreasing from 5 to 3ppb and from 8 to 6ppb as the flow rate increased (Appendix D).

Both electrochemical sensors responded considerably to these changes. On average, the sensors reading was increased as the airflow rate and ozone concentration increased. The highest difference in mean concentrations of 1000 and 2000 cfm with the average concentrations of 500 cfm was observed during the injection of 500 ppb (163.96 and 193.48 ppb) and 100 ppb (111.01 and 164.54 ppb) for BW and BW solo, respectively. The greatest data scatter for these two sensors was also observed at these concentrations (500 ppb and 100 ppb). Increasing the airflow rate and ozone concentration led to an increase in the ECO Sensor measurements. The sensor had the worst performance at 2000 cfm. Also, the highest data scattering was observed with the injection of 50 ppb ozone. In comparison with 211-2B, it does not perform well at these airflow rates and airflow directions.

4.2.1.1- Comparison of The Sensors Measurements with The Reference Instrument Based on The Coefficient of Determination (R^2) Values

The performance of all sensors was compared with the reference instrument (211-2B) for both directions. As shown in Figures 4.10 and 4.11, the outputs of Teledyne and POM were linearly proportional to the reference measurements (R^2> 0.99) when ozone concentration and airflow rate varied in the range of 0-1 ppm and 500-2000 cfm. Teledyne indicated similar performance at different airflow rates. The slopes of regression lines, which are almost equal to unity, imply the similar performance of Teledyne to the reference monitor.

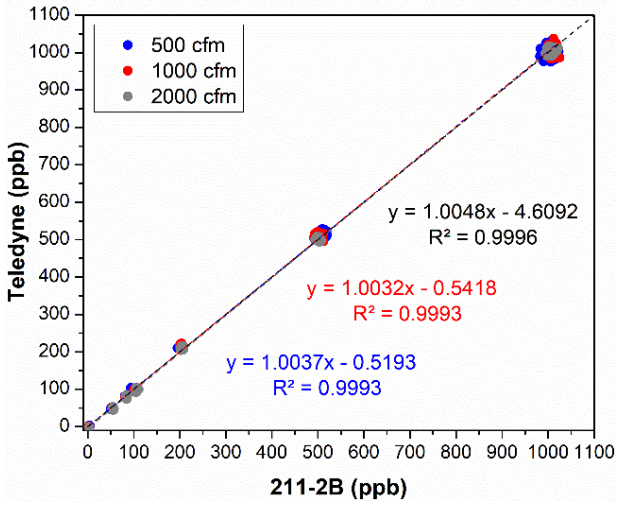

Figure 4. 10- The correlation between Teledyne outputs and reference instrument measurements at different flow rates

Figure 4.11 demonstrates that POM measured ozone concentrations consistently lower than the injected values. The results of section 4.1.1 experiment represent that POM response, even when tested outside the duct, was less than injected values, especially at high concentrations and was similar to the duct experiments. The most dispersion was observed at 500 cfm when POM was

placed perpendicular to the airflow direction (R^2=0.9988). The regression equations at 500 cfm (perpendicular) and 2000 cfm (parallel) with slopes approaching unity (0.9152 and 0.9195) exhibit that POM data are slightly closer to the reference instrument than the other tests. Totally, the sensor performed almost similarly in both orientations.

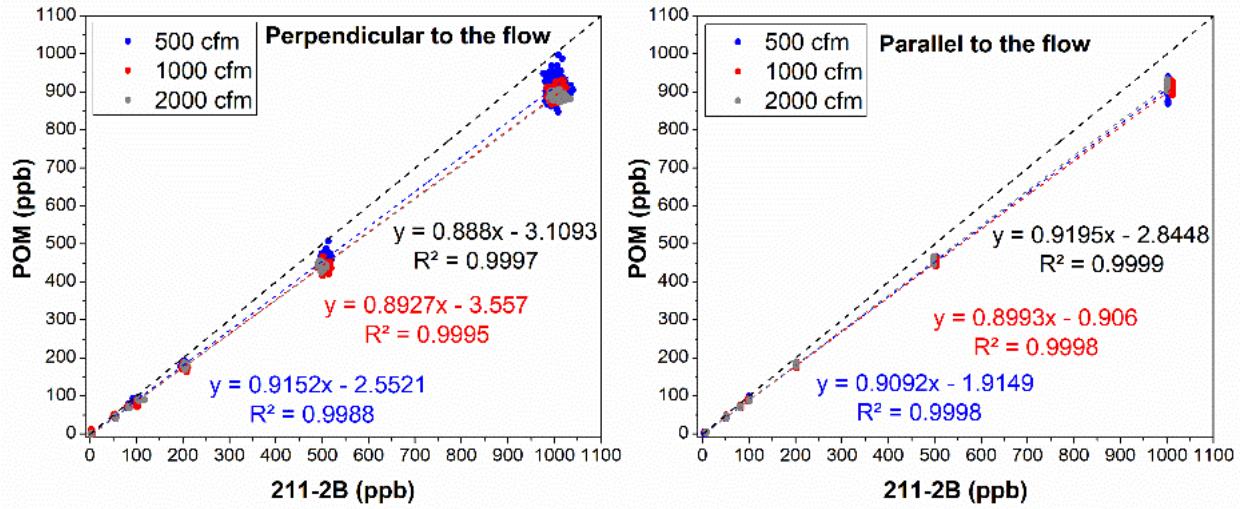

Figure 4. 11- The correlation between POM outputs and reference instrument measurements in parallel and perpendicular directions and different flow rates

BW sensor outputs exhibited a significant linearly growing trend at all parallel position airflow rates and 500 cfm perpendicular position (R^2> 0.96). A substantial increase in data scattering was observed in the perpendicular direction when the airflow rate and concentration were increased (R^2= 0.88 (1000 cfm) and 0.79 (2000 cfm)). While it experienced slight changes in R^2 values of parallel position as airflow rate and concentration were changing. Comparing the intercepts of regression lines in both positions, we find out that BW over-reported ozone concentrations in all perpendicular direction experiments and high airflow rates of parallel position (1000 and 2000 cfm). Since it had slight deviation from 211-2B (intercept=7.07, slop= 0.94) at 500 cfm (parallel), it represented more closer response to 211-2B at this airflow rate and direction. All BW solo plots were highly linear in both orientations with R^2> o.98. As shown in Figure 4.12, increasing the airflow rate resulted in more differences between the slopes of regression lines and unity. Unfortunately, this sensor overestimated ozone concentrations in all experiments and did not accurately operate at these airflow rates and directions.

A linear relationship with coefficient values of greater than 0.88 can be observed between the ECO Sensor outputs and 211-2B. It experienced the most data scatter in the perpendicular position at 500 cfm (R^2=0.88). The sensor performance deteriorated as the airflow rate went up (the difference between slopes and unity was growing). As shown in Figure 4.13, the least difference between the slope and unity was obtained in the perpendicular direction at the airflow rate of 500 cfm. It over-reported ozone concentrations at all airflow rates. Unlike the other

sensors, in the perpendicular position, the difference between the sensor reading and reference outputs was less than the parallel one. Overall, it is not a reliable sensor for measuring ozone.

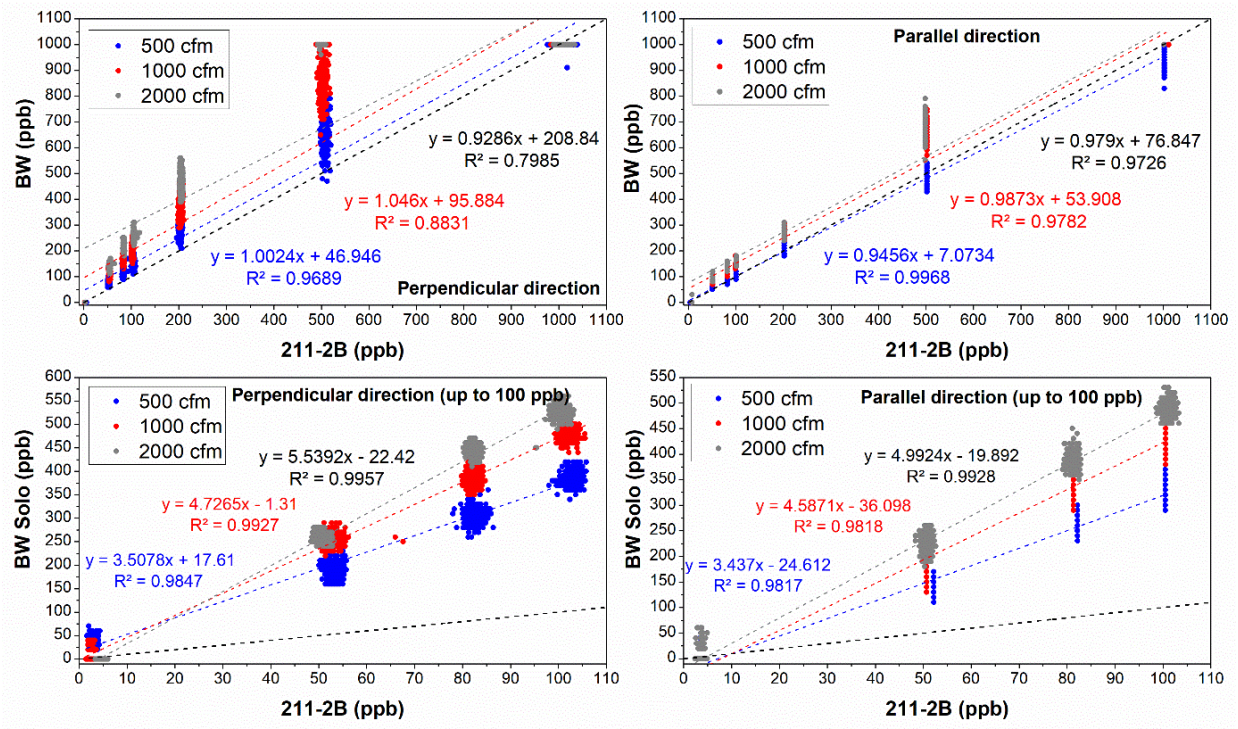

Figure 4. 12- The correlation between BW and BW Solo outputs and reference instrument measurements in parallel and perpendicular directions and different flow rates

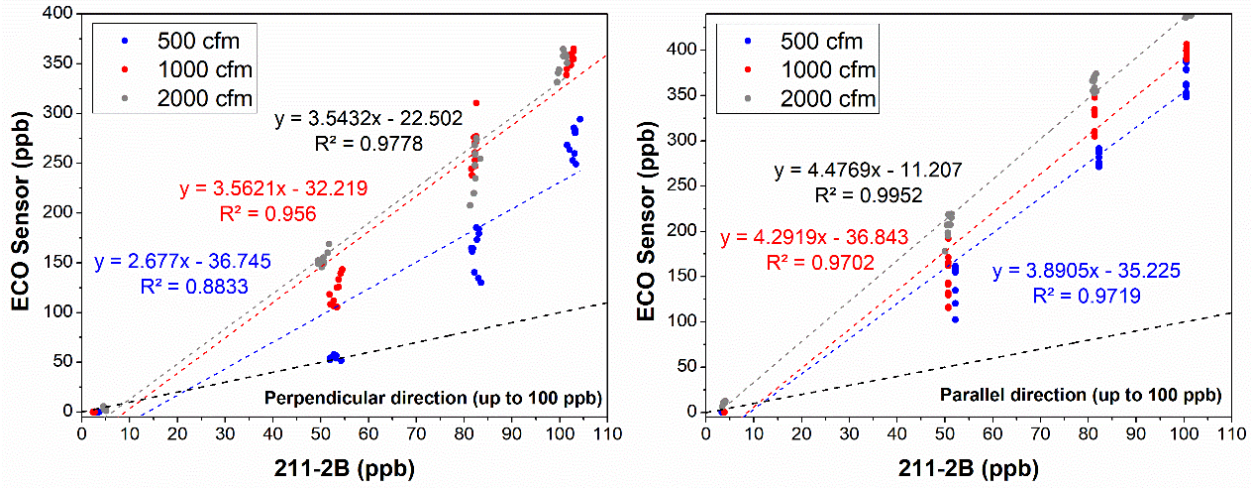

Figure 4. 13- The correlation between ECO Sensor outputs and reference instrument measurements in parallel and perpendicular directions and different flow rates

It can be concluded that the different airflow rates and orientations had a slight influence on the UV ozone sensors performance. It may be due to the fact that these sensors were equipped with an air pump that drawn the required amount of sample air into the instrument at a specific flow

rate in any situation. Therefore, placement in different directions and operation at different airflow rates do not affect their performance. Moreover, the results of concentration uniformity test done using reference instrument (section 3.8.1.1) indicated that 211 UV sensor measurements at points 4"-7" (location of POM) were almost identical in both directions and various airflow rates.

Since the electrochemical sensors work through gas diffusion, they rely on air movement and pressure to deliver the sample air to the sensing element. In the perpendicular position and by increasing the airflow rate, the airflow hits the sensor with more pressure and this pressure can result in more sample air reaching the working electrode (WE). In this case, more electrochemical reactions occur on the working electrode surface and increase the direct current (DC) flowing through the sensor, which indicates the level of ozone concentration. Maybe that's why the ozone concentrations in this position were overestimated than the parallel one. Thus, the rate of electrode reaction or diffusion of the reactant onto the electrode surface can affect the DC during exposure to the target gas. This increase in ozone concentrations was also observed with increasing the airflow rate in the uniformity test at this location (18"). Since this test was carried out by the UV sensor, changing the direction of tube did not affect its response.

According to the BW solo manual, zero calibration and bump tests are required after changing environmental conditions and prior to each day's use to have optimal performance. These items were checked at the beginning of each test, but the sensor consistently overestimated the ozone concentrations. Different studies showed that the increase of airflow rate had a negative influence on the sensor sensitivity. Since the main goal of this research is to examine the response of ozone monitors in different situations, we did not go deep into the detail of these changes in the structure of sensors. To this end, we cannot explain with certainty the reasons of these changes without evaluating parameters such as working electrode voltage and sensitivity.

ECO Sensor works through gas diffusion similar to the electrochemical sensors. The sensitivity of n-type semiconductor metal oxide sensor is defined as R_g/R_a for oxidizing gases (R_g= resistance of sensor in the presence of ozone, R_a= resistance in the absence of ozone). In comparison, a p-type semiconductor sensor has the opposite definition. Moreover, R_g and R_a have a significant relationship with the surface reactions. In the case of n-type semiconductors, the resistance increases when the sensor is in contact with oxidizing gases (such as ozone). However, the resistance of p-type semiconductors decreases in the presence of oxidizing gases [20, 118]. Information about the type of metal oxide utilized in ECO Sensor could not be found. The results represent that the ECO Sensor measurements were higher in the parallel direction than the perpendicular position. According to different studies, continuous exposure to the target gas leads to the reduction of sensor sensitivity. It should be noted that we first performed the perpendicular direction experiments, then the parallel direction. Loss of sensitivity with time may be due to this sequence. The other reason could be because of the continuous operation of the sensor in the presence of moisture (50% RH), which poisoned the sensor over time. Although the sensor was warmed up before the commencement of each test to burn off any absorbed

chemicals, it was consistently overestimating the concentrations. Since the sensor resistance measurement was not part of this study, it is difficult to discuss precisely the changes made in the sensor structure. Based on the uniformity experiment, the response of sensor at this location (6“) should not be changed with increasing airflow rate and changing the direction, but ECO sensor measurements were overestimated by increasing the airflow rate and affected by changing the direction.

4.2.1.2- Investigating the Ozone Sensors Accuracy and Precision

The accuracy and precision of sensors were examined to ensure that the sensors measurements are within the NIOSH accuracy criterion (95% CI within $\pm$ 25%) and evaluate their performance and precision. The calculated 95% CI and precision of sensors are listed in Appendix E.

As shown in Figure 4.14, The Teledyne met this accuracy criterion at all ozone concentrations and airflow rates. The accuracy of Teledyne at each concentration was almost the same and the sensor exhibited accurate results. Slightly underestimation of concentrations at 50 and 100 ppb ozone (2000 cfm) caused the mean error be around 7% and 5% less (mean error= -13.67% and -8.95%). The sensor exhibited precision ranging from 0.58% to 3.45%, which is less than 5%.

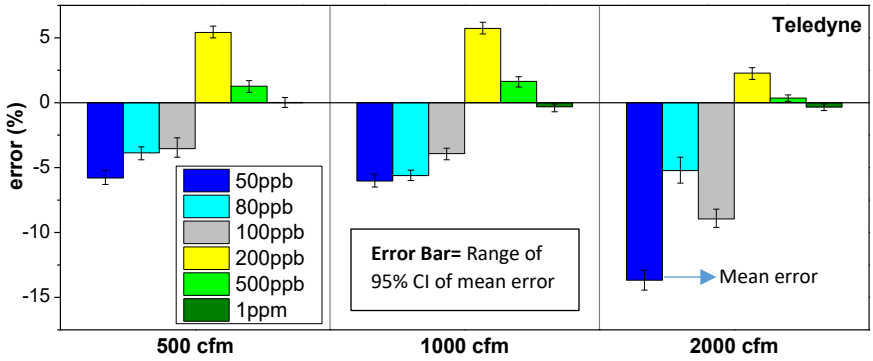

Figure 4. 14- 95% CI of mean error (Teledyne)

Moreover, POM accuracy was within the NIOSH criterion in both directions and different airflow rates (Figure 4.15). At each concentration, the mean error values of POM were identical at 500 cfm. At the airflow rate of 1000 cfm, the most difference between the mean error values was obtained at 100 and 200 ppb, which were 6.07% and 3. 58% less than the parallel position. This difference was also observed at 2000 cfm by injection of 50 and 80 ppb ozone. POM measured ozone concentrations with a precision of 0.77% - 2.72% in the perpendicular direction and 0.69% -3.21% in the parallel experiment, which refers to the precise measurement of concentrations.

The BW sensor exhibited the best performance at 500 cfm in the parallel direction so that it had a 95% CI of mean error within $\pm$ 25% (Figure 4.16). While during the other experiments, it exhibited low accuracy for ozone concentrations below 500 ppb, but it indicated a good accuracy at 1 ppm ozone. It should be noted that at 1000 and 2000 cfm by injection of 1 ppm ozone, this sensor was consistently showing the maximum detection limit (1 ppm) and because of the sensor

analog output limitation, it could not measure the values higher than 1 ppm. Thus, the calculated mean errors at these two airflow rates are not reliable. The results represent that the sensor accuracy deteriorated with increasing the airflow rate. Although the sensor outputs at 2000 cfm were higher than the other airflow rates, better precision was observed at 2000 cfm (0-7.36% (perpendicular), 0-6.15% (parallel)). The sensor precision was less than 5% at concentrations above 100 ppb in the parallel direction and 1 ppm in the perpendicular test.

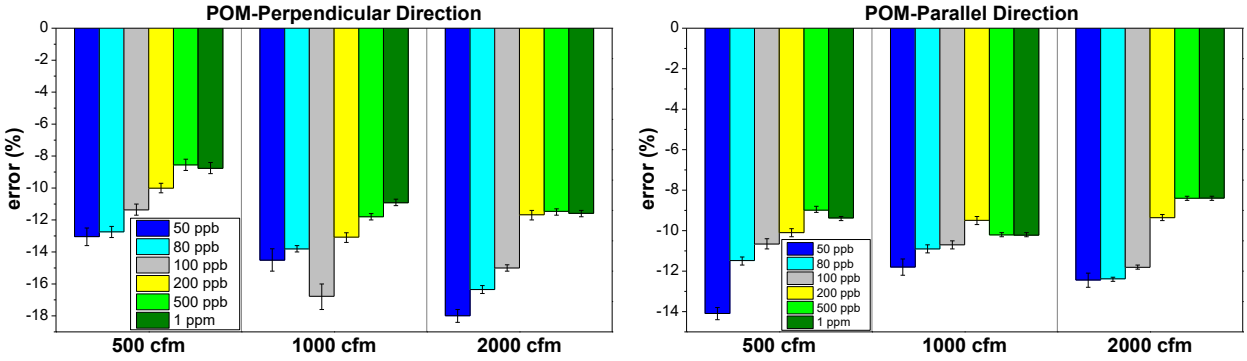

Figure 4. 15- 95% CI of mean error (POM)

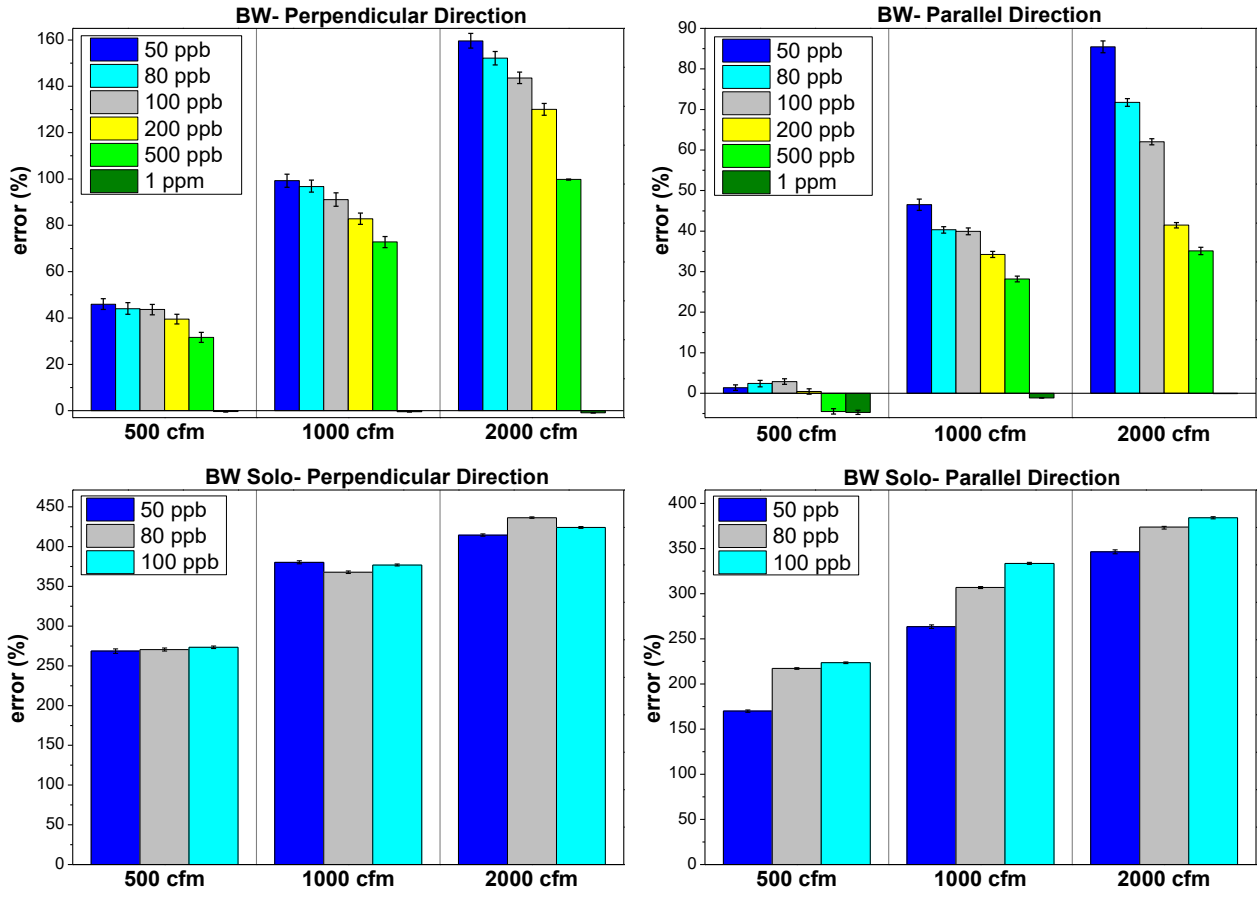

Figure 4. 16- 95% CI of mean error (BW and BW Solo)

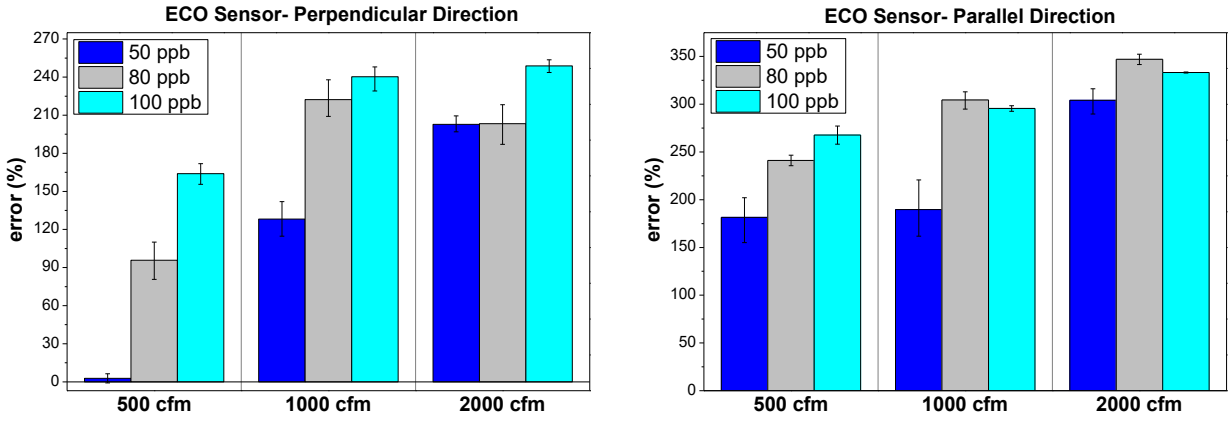

Figure 4. 17- 95% CI of mean error (ECO Sensor)

None of the experiments performed by the BW solo sensor had 95% CI within the NIOSH accuracy criterion range (figure 4.16). The sensor performed worse with increasing the airflow rate, especially in the perpendicular orientation. However, BW Solo precision was less than 5% in perpendicular and parallel (at 80 and 100 ppb) directions. Also, this electrochemical indicated better precision when placed perpendicular to the airflow (2.24%- 5%).

Conversely, the ECO Sensor indicated better performance in the perpendicular direction, but in this direction, it met the accuracy criterion only at the airflow rate of 500 cfm by injection of 50 ppb ozone (Figure 4.17). By increasing the airflow rate and ozone concentration, ECO Sensor represented better precision.

4.2.2- Impact of Humidity Variations on Sensors Measurements

Changing environmental factors such as relative humidity can significantly affect sensors performance. Sudden changes in humidity can occur during personal monitoring by moving the sensor into and out of buildings [40]. To this end, dynamic tests were conducted in two different set-ups, full duct and small-scale chamber, to investigate the effect of this physical parameter on the response of six ozone monitors, including 2B Technologies Model 211, Teledyne API Model 465L, 2B Technologies Personal Ozone Monitor (POM), ECO Sensors INC. Model C-30ZX, Honeywell BW Solo, and Honeywell GasAlert Extreme BW Technologies. In the following, the results of these experiments are reported and explained.

4.2.2.1- Chamber Experiments

The response of sensors was evaluated at four different humidity levels during the chamber experiments, including dry air (0.01%), 20%, 50%, and 70%, with an airflow rate of 5.1 L/min in the absence of ozone. This test was performed in two days because: 1- two small sensors (POM, BW, BW solo, and ECO Sensor) could be placed in the chamber simultaneously. 2- To supply the required flow of the sensors due to the low airflow rate. The 211-2B and Teledyne sensors were connected to the chamber outlet and inlet. Figure 4.18 indicates the sensors responses to

humidity changes when relative humidity increased from 0.01% to 70% and then returned to the dry air.

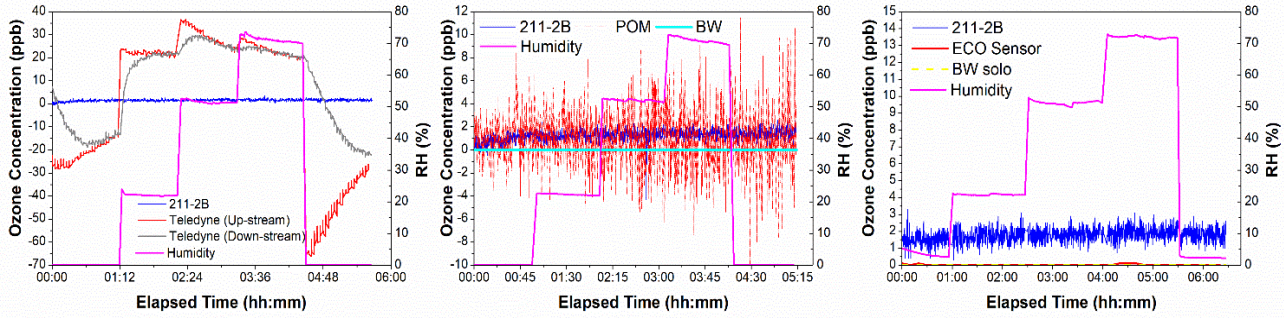

Figure 4. 18- Ozone sensors response to different levels of humidity

As shown in Figure 4.18, Teledyne response was stabilized in dry condition after 40 minutes at a concentration of about -14 ppb. Its reading increased to about 23, 36, and 29 ppb at the beginning of each step and then gradually dropped down to about 20 ppb after 20 min. In fact, in humid air, the scrubber absorbs the water vapor of the airflow passing through it and leads to an increase in light intensity (I_0) measured by the detector. Thus, according to the Beer-Lambert law, a positive interference occurs when I_0 is larger than I. Switching from 70% to dry condition (0.01%) resulted in a significant reduction in the sensor reading (-66 ppb) and then gradually recovered to its initial value (-14 ppb).

Table 4.1- Ozone sensors measurements in various humidity

Detector	Humidity	0.01% RH	20% RH	50% RH	70% RH	0.01% RH
211 (ppb)	Average	1.21	1.53	1.69	1.73	1.67
	SD	0.53	0.36	0.37	0.42	0.42
Teledyne (ppb)	Average	-14.08	22.20	29.11	23.28	-44.06
	SD	0.84	0.84	4.16	2.77	11.79
POM (ppb)	Average	1.14	0.83	1.08	0.84	1.23
	SD	1.58	1.90	2.69	2.73	3.03
BW (ppb)	Average	0	0	0	0	0
	SD	0	0	0	0	0
ECO Sensor (ppb)	Average	0.033	0	0	0.037	0
	SD	0.051	0	0	0.051	0
BW Solo (ppb)	Average	0	0	0	0	0
	SD	0	0	0	0	0

It should be said that the 211 and POM sensors are equipped with Nafion tube so that the use of this tube can eliminate or minimize the water vapor interference. The results demonstrate that increasing and decreasing of humidity had a negligible effect on the response of 211. While POM experienced many fluctuations within all different levels of moisture. BW was continuously indicating zero concentration during all experiments and did not respond to humidity changes. Although the BW Solo response was zero within the experiments, the sensor was constantly beeping because of negative concentrations. This electrochemical sensor cannot quantify

negative concentrations due to the analog output limitation and its minimum detection limit. Thus, it can be concluded that humidity negatively interferes with the sensor performance. The outputs of ECO Sensor were almost close to zero.

4.2.2.2- Full Duct Experiments

This study was carried out at the airflow rate of 500 cfm, constant temperature 23±2℃ and humidity range of 30% to 80% on two different days because only two small sensors could be mounted inside the duct at the same time. The sensors were tested under different ozone concentrations in this humidity range (0, 50, 80, 100, 200, 500 ppb ozone). Figures 4.19 and 4.20 represent the results of these experiments. Besides, the low humidity test was also conducted at temperature of 20±1℃, relative humidity of 7.5±0.3% and 15±2%, and the mentioned concentrations to compare the data (Figure 4.21). In this experiment, small sensors were placed parallel to the airflow direction.

Results demonstrate that all six sensors, more or less, responded to changes in humidity at all ozone levels tested. The calculated standard deviation (SD) of each test reported in Table 4.2 confirms the humidity interference-effect. 211-2B, Teledyne, POM, and BW sensors experienced a positive interference when switching from 30% to 80% RH and a negative interference upon changing from 80% to 30% RH. Also, 211-2B, ECO Sensor and POM indicated slight changes at zero ppb ozone. The humidity changes had no effect on the BW sensor in the absence of ozone. By comparing this test SD (54.9 ppb) with the low humidity condition (0.75 ppb) at zero ppb, we find out that Teledyne was subjected to interference from humidity fluctuations. In contrast, BW solo indicated opposite effects to the same humidity changes so that transition from 80% to 30% RH and 30% to 80% RH resulted in positive and negative bias. It should be noted that the BW solo sensor cannot quantify negative concentrations. Thus, it was beeping with increasing humidity from 30% to 80% in the absence of ozone due to negative concentrations. In the absence of ozone, the SD of this sensor increased from zero ppb measured in the low humidity test to 27.2 ppb evaluated within humidity variations.

As shown in Figures 4.19 and 4.20, the 211-2B sensor response was affected more by increasing ozone concentration so that sensor reading was overestimated with increasing humidity and reduced when the humidity dropped down. At concentrations below 100 ppb, the SD values are between 1 and 3, which are nearly similar to the SD values in the low humidity test (varied from 0.9 ppb to 1.8 ppb). Although the SD values of low humidity test at concentrations of 200 and 500 ppb were between 2 and 5 ppb, their values during the period of changing humidity ranged from 5-11 ppb, which means more effect of moisture at these concentrations.

According to Table 4.2 and Figure 4.19, Teledyne demonstrated almost similar changes (SD varied from 36 to 45 ppb) at all ozone concentrations coinciding with variations in humidity. The impact of these fluctuations on the sensor outputs is evident if we look at the range of SD changes in the low humidity test (between 1.43 ppb and 5.34 ppb). The humidity fluctuations had a substantial

effect at 500 ppb ozone (SD=43 ppb) on Teledyne so that a positive and negative interference on the order of 99.4 ppb and 76.2 ppb occurred for this sensor.

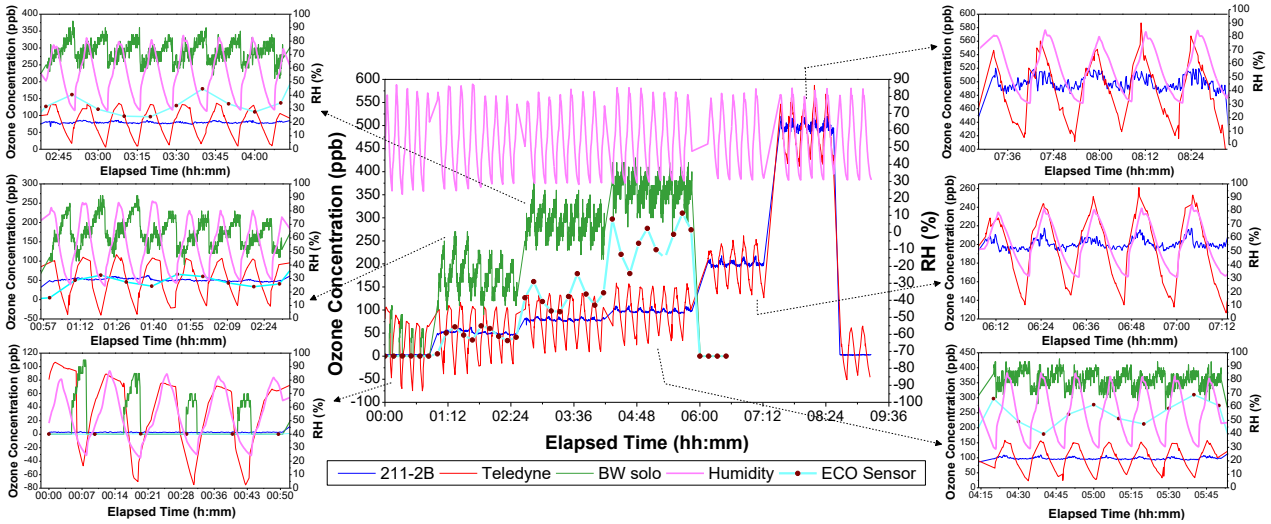

Figure 4. 19- Ozone sensors response to rapid humidity variations

Results indicate that at concentrations below 100 ppb, The POM and BW SD values had a slight difference from the values of the low humidity test; especially for POM, this difference was negligible (Table 4.2). POM and BW had the most fluctuations at 200 and 500 ppb. Compared to the low humidity test, the SD values at 200 and 500 ppb increased from 2.4 ppb to 6.8 ppb and 7.38 ppb to 14.6 ppb for POM and from 2.5 ppb to 15.2 ppb and 7.5 ppb to 33.8 ppb for BW, respectively. At these concentrations, an unusual positive bias of 19.47 ppb and 50.92 ppb to POM and 38 ppb and 90.68 ppb to BW was observed upon increasing humidity. In comparison, switching from 80% to 30% resulted in a negative bias of 16.52 ppb and 24.87 ppb to POM and 31.99 ppb and 69.31 ppb to BW.

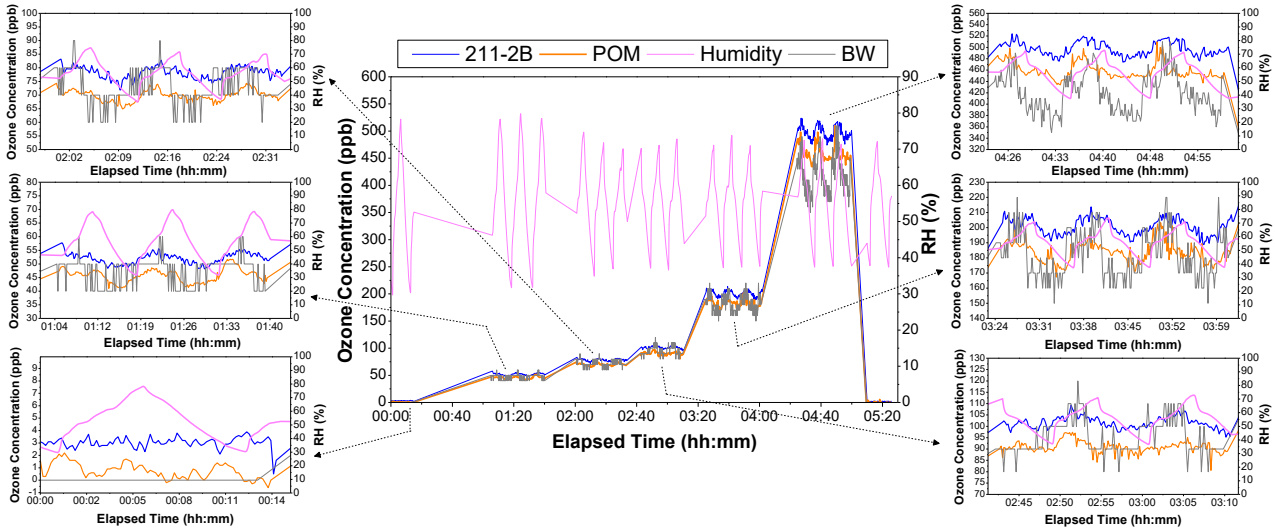

Figure 4. 20- Ozone sensors response to rapid humidity variations

Humidity fluctuations had the opposite impact on BW solo (Figure 4.19). According to Table 4.2, the SD values were approximately the same at all concentrations (between 26 and 35 ppb). In the low humidity experiment, these values were between 10 and 16 ppb, which this difference points out to the humidity effect on the sensor performance. Due to the fluctuations of sensor response with the humidity variations, the average data reduced slightly than the low humidity condition with increasing ozone concentration.

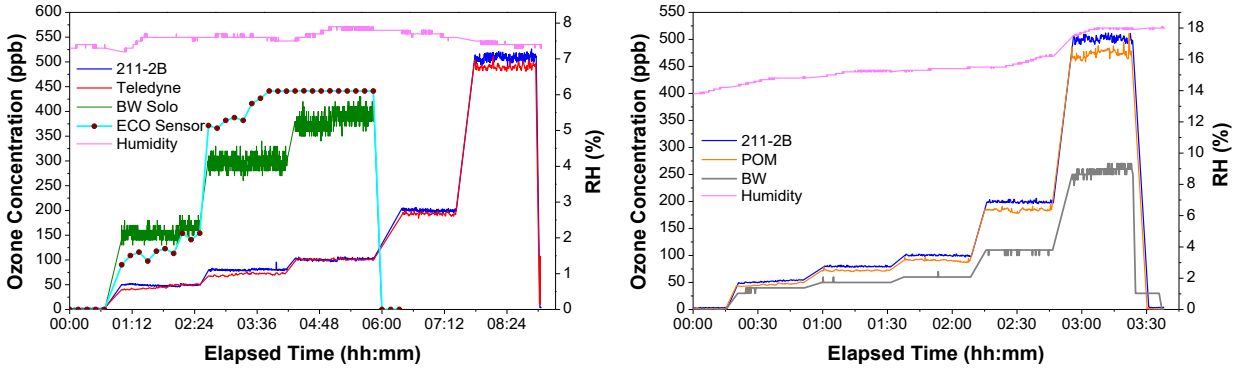

Figure 4. 21- Ozone sensors response to various concentrations at low humidity

As mentioned earlier, an external data logger was used to transfer the ECO Sensor data to the computer. Unfortunately, the minimum time interval specified in the software was 10 minutes. Based on the allotted time for each injection, ten data were obtained in each test. Figure 4.19 indicates that its increasing and decreasing process is not consistent with the others due to the long time interval. To this end, it is difficult to diagnose when it responded positively and when answered negatively. It should be said that in case of constant humidity, such as the low humidity test and the parallel direction of the previous test performed at a constant humidity of 50%, the sensor response gradually increased at a specific ozone concentration. Since humidity variations caused fluctuations in the response of this sensor, the averaged concentrations were remarkably lower than the low humidity test. The most data dispersion compared to the average, which was about 58.99 ppb increase and 71.81 ppb decrease, occurred at 100 ppb ozone for ECO Sensor. While in the low humidity test, the SD value was very small at this concentration because the sensor was continuously showing the sensor maximum detection limit, which was four times the amount injected. Due to the continuous increase of sensor response in the low humidity condition, the values of SD at 50 ppb and 80 ppb were 4.05 ppb and 4.56 ppb more than the humidity variations test. It should be noted that from the beginning, BW solo and ECO Sensor were indicating off concentrations.

According to different studies, the increase and decrease in the response of applied UV sensors (211-2B, POM, and Teledyne) may be due to physical interactions of humidity with the absorption cell surface. In other words, the light emitted from the source in these sensors reaches the detector through reflection from the cell wall. Thus, absorption (when humidity increases) and desorption (when humidity reduces) of water from the scrubber affect the measurements of light intensity by changing the reflectivity of the cell surface [18, 29, 40]. Furthermore, this difference

in the response of sensors to humidity may relate to the water absorptive capacity of scrubbers [29]. Among these three UV sensors, only Teledyne responded significantly to humidity fluctuations. Since the 211-2B sensor is equipped with the Nafion tube to minimize the humidity interference, humidity changes led to a slight positive and negative interference, especially at concentrations of 200 ppb and 500 ppb. The Nafion tube was also applied in POM, but at high concentrations (200 and 500 ppb), the sensor responded to humidity fluctuations.

Table 4.2- Summary of measurements in humidity variations and low humidity experiments

Detector	Condition (500 cfm)	Concentration	Background	50 ppb	80 ppb	100 ppb	200 ppb	500 ppb	Background
211-2B	Humidity Variation (30%-80%)	Ave. (ppb)	2.72	51.42	79.41	98.12	200.59	497.96	2.83
		SD (ppb)	0.37	3.50	2.65	3.51	5.19	9.16	0.40
		Precision (%)	13.60	6.80	3.33	3.57	2.58	1.83	14.13
	Low RH (7.5±0.3% and 15±2% RH)	Ave.	1.96	49.03	80.20	101.25	200.12	508.74	4.03
		SD	0.40	1.49	1.51	1.87	2.11	5.69	0.29
		Precision (%)	20.40	3.03	1.88	1.84	1.05	1.11	7.19
Teledyne	Humidity Variation	Ave.	33.28	49.86	78.77	98.67	196.98	487.83	9.88
		SD	54.97	45.08	40.10	39.23	36.46	43.12	35.22
		Precision (%)	165.17	90.41	50.90	39.75	18.50	8.83	356.47
	Low RH	Ave.	0.99	45.37	70.77	100.91	193.01	490.33	10.64
		SD	0.75	4.06	2.43	1.43	2.56	5.34	0.51
		Precision (%)	75.75	8.94	3.43	1.41	1.32	1.08	4.79
POM	Humidity Variation	Ave.	0.74	45.71	69.82	90.86	183.82	458.97	-0.50
		SD	0.62	2.47	2.06	2.56	6.83	14.62	1.56
		Precision (%)	83.78	5.40	2.95	2.81	3.71	3.18	312
	Low RH	Ave.	0.63	46.30	72.08	90.83	184.32	473.75	0.50
		SD	0.71	2.05	0.94	1.68	2.44	7.38	1.07
		Precision (%)	112.69	4.42	1.30	1.84	1.32	1.55	214
BW	Humidity Variation	Ave.	0	47.33	72.97	95.02	181.99	419.31	0
		SD	0	5.22	6.58	7.75	15.24	33.84	0
		Precision (%)	0	11.02	9.01	8.15	8.37	8.07	0
	Low RH	Ave.	0	38.33	50.10	60.05	109.30	255.96	25
		SD	0	3.73	1.01	0.73	2.55	7.52	11.67
		Precision (%)	0	9.73	2.01	1.21	2.33	2.93	46.68
BW Solo	Humidity Variation	Ave.	14.11	173.43	288.98	360.50	-	-	0
		SD	27.73	35.76	28.95	26.68	-	-	0
		Precision (%)	196.52	20.61	10.01	7.40	-	-	0
	Low RH	Ave.	0	156.29	297.43	382.92	-	-	0
		SD	0	10.49	11.84	16.46	-	-	0
		Precision (%)	0	6.71	3.98	4.29	-	-	0
ECO Sensor	Humidity Variation	Ave.	0.13	44.26	129.1	251.01	-	-	0
		SD	0.15	17.84	26.14	40.81	-	-	0
		Precision (%)	115.38	40.30	20.24	16.25	-	-	0
	Low RH	Ave.	0	121.46	405.36	441.23	-	-	0
		SD	0	21.89	30.70	0.13	-	-	0
		Precision (%)	0	18.02	7.57	0.02	-	-	0

As examined in different studies, humidity variations can cause changes in working and reference electrodes voltage of electrochemical sensors, which can justify the overestimation and underestimation of ozone concentration [26, 66]. The BW and BW solo sensors are specified to operate in the humidity range of 15%-90% and 5%-95%. Continuous operation in humid or dry conditions can increase the water vapor content of electrolyte or dry it out. Therefore, these changes in electrolyte viscosity can affect the migration rate of electrons within the electrolyte and the sensor output. Although the type of sensor applied in these two instruments is the same, BW solo responded in the opposite manner. Since the sensing electrode voltage and sensitivity were not measured, the reason of this difference in the performance of these two sensors cannot be explained precisely.

When water is absorbed on the metal oxide surface in semiconductor sensors, no electrons will be donated to sensing layers. The sensor resistance decreases due to the reaction of water molecules to the surface oxygen, leading to a decrease in sensitivity. In this case, sensor response and recovery time increase. Based on studies, heating the sensor to high temperatures (usually>400 ℃) can eliminate the humidity effect and leads to a full recovery of the signal [20, 97, 98]. There are several hypotheses about the sensor behavior in humid air. Firstly, the chemical adsorption of the oxygen species is reduced due to the adsorption of water molecules on the metal oxide surface. Secondly, competition is made between ozone and water molecules to react on the same adsorption sites [119]. Due to the sensor time interval, it is difficult to follow the sensor behavior with humidity fluctuations.

4.2.2.2.1- Comparison of The Sensors Measurements with the Reference Instrument

Figures 4.22 and 4.23 represent the comparisons between the ozone sensors outputs and reference instrument (211-2B) based on the coefficient of determination (R^2) and regression plot slope. As shown in Figure 4.22, Teledyne and POM sensors response linearly increased in humidity variations and low humidity tests (R^2> 0.90) as ozone concentration enhanced from zero to 500 ppb. In both sensors, the slopes were not significantly different from unity. The R^2 value of Teledyne in the humidity fluctuations test (0.91), which is less than that of the low humidity test (0.99), indicates more scatter in the data with humidity variations. However, the regression lines of the POM sensor in both tests are almost coincident with each other. According to Table 4.2, the average of measured concentrations by POM at low humidity is slightly higher than the humidity variations test so that its slope is 2% higher. Although the slope of the low humidity test for Teledyne is 1% greater than the humidity changes experiment, the average of measurements at 50, 80, and 200 ppb are slightly lower.

Also, two applied electrochemical sensors (BW and BW solo) are highly linear with R^2> 0.90. The results show that BW performance deteriorated under the low humidity condition with a 52% deviation from the slope of 1.0 (Figure 4.23). While the slope was 17% lower than unity within the humidity fluctuations test and also the average of measurements was remarkably higher than the low humidity test. Also, the data scattering was 1% more in the humidity variations test (R^2=0.98) than the low humidity experiment (R^2=0.99). BW solo performed poorly in both

experiments so that the slopes of regression lines were considerably greater than unity. Humidity fluctuations resulted in a 5% increase in the dispersion of this sensor data (R^2=0.93) compared to the low humidity condition (R^2=0.98). Between these two sensors, BW solo had the worst performance.

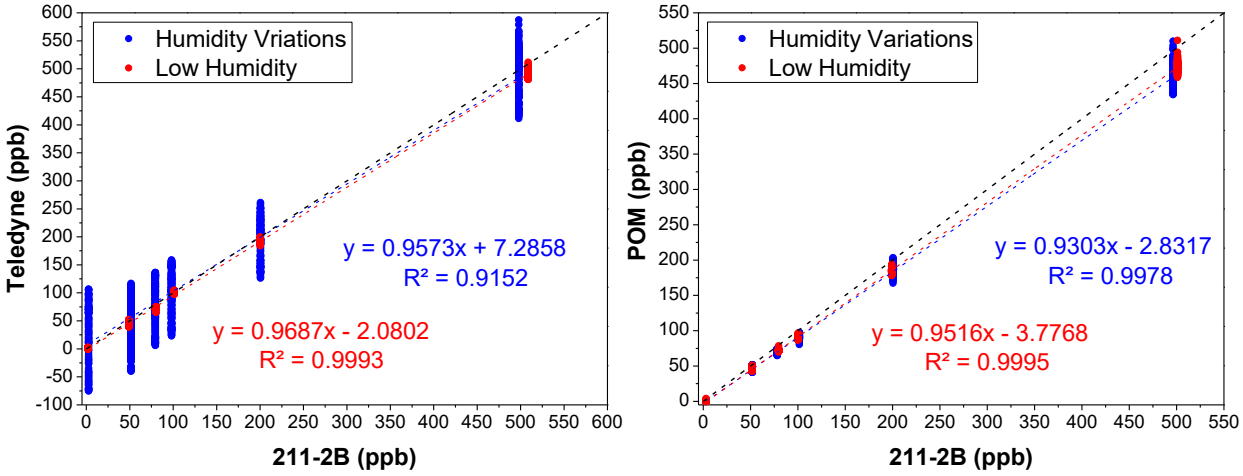

Figure 4. 22- Correlation between Teledyne and POM outputs and reference instrument measurements in the case of humidity changes

The ECO Sensor had linear behavior in the low humidity test (R^2= 0.90), but its R^2 value in the humidity fluctuations experiment was 14% less and the scatter in data was more (Figure 4.23). Based on the slopes, the average of sensor measurements had the most difference with the reference instrument in the low humidity test (slope= 5.05).

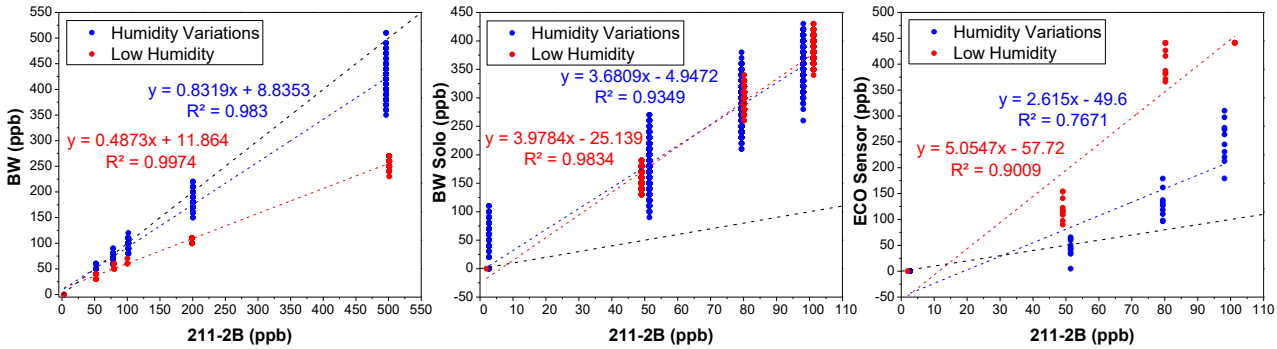

Figure 4. 23- Correlation between BW, BW Solo, and ECO Sensor outputs and reference instrument measurements in the case of humidity changes

4.2.2.2.2- Investigating the Ozone Sensors Accuracy and Precision

In this part, the sensors performance was examined by estimating accuracy and precision in order to see whether humidity variations affect the sensors performance. The calculated 95% CI and precision of sensors are listed in Appendix E.

As shown in Figure 4.24, Teledyne met the NIOSH accuracy criterion in both tests. The sensor mean error values in the low humidity study at concentrations of 50 and 80 ppb were estimated 4.38% and 10.95% lower than those of the humidity test. It is because of the ozone concentrations underestimation by the sensor at these values. Teledyne indicated better precision as the ozone concentration increased so that in humidity variations and low humidity tests ranged from 90.41% to 8.83% and 8.94% to 1.08%. POM had a good performance in all conducted experiments so that the mean error values were within the accuracy criterion range. Since the sensor showed a lower amount at 500 ppb during humidity changes, its mean error was 2.09% lower than the low humidity experiment. POM had a precision of less than 50% in both experiments.

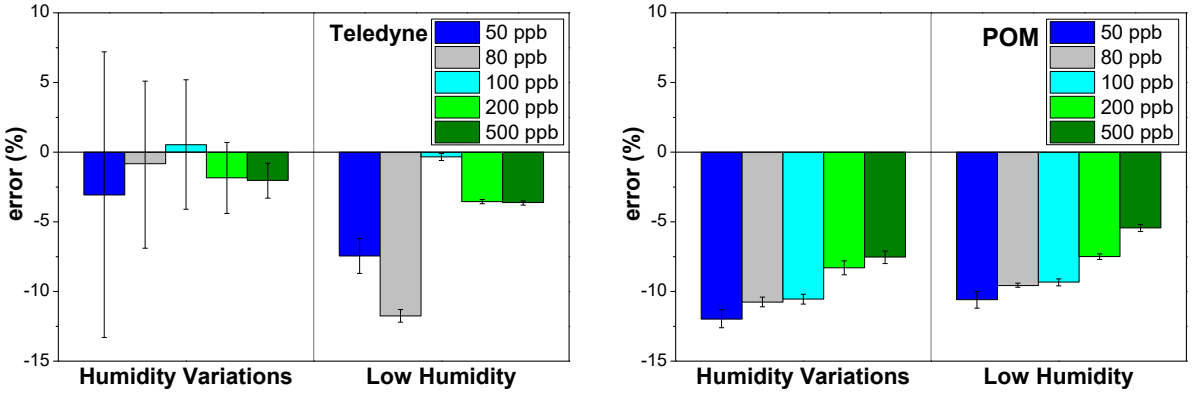

Figure 4. 24- 95% CI of mean error (Teledyne and POM)

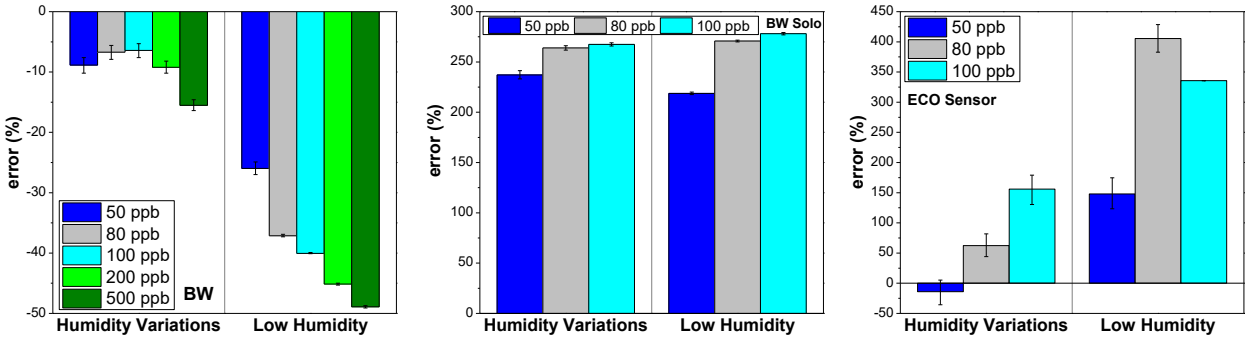

Figure 4. 25- 95% CI of mean error (BW, BW Solo, and ECO Sensor)

Based on the results, humidity fluctuations did not affect the BW accuracy and it was in the range (Figure 4.25). While the sensor accuracy did not comply with the NIOSH accuracy criterion in the low humidity study. It may be due to the low humidity level, which was slightly lower than the humidity recommended by the manufacturer (15%-90%). To this end, the sensor did not perform well in this experiment. Precision values calculated for BW with humidity fluctuations and at low humidity were from 11.02% to 8.07% and 9.73% to 2.93%, respectively. The BW solo sensor did not meet the accuracy criterion under any circumstances. This behavior was also observed for the ECO Sensor so that it performed worse in the low humidity experiment. BW Solo measured

ozone concentration with a precision of 20.61% to 7.40 in the humidity variations test and 6.71% to 4.29% when the humidity was low. Precision values for ECO Sensor were in the range of 40.30% to 16.25% (humidity fluctuations) and 18.02% to 0.029% (low humidity).

4.3- Effect of Chemical Parameters on Ozone Sensors Performance

The presence of VOC compounds in the desired environment has the potential to interfere with ozone measurements. This study examined VOC interferences in the absence of ozone using two UV instruments (2B Technologies Model 211, Teledyne API Model 465L), an electrochemical sensor (Honeywell BW Solo), and a metal oxide sensor (ECO Sensors INC. Model C-30ZX). Acetone, ethanol, and toluene were considered as interfering compounds in this experiment. VOC concentrations were also measured by a Multi-Gas Photoacoustic Detector (INNOVA AirTech Instrument 1312).

4.3.1- VOC Interferences in Dry and Humid (50% RH) Air

This study was carried out under dry (0.01% RH) and humid (50% RH) conditions in a small-scale chamber. Compressed air was used as the carrier gas, passing through the tubes and chamber with a flow rate of 5.1 L/min and a constant temperature of 21.34±0.5℃. Figures 4.26, 4.27, and 4.28 indicate the sensors response during this test. It should be noted that Teledyne could not complete the tests because its response was not similar to the previous experiments.

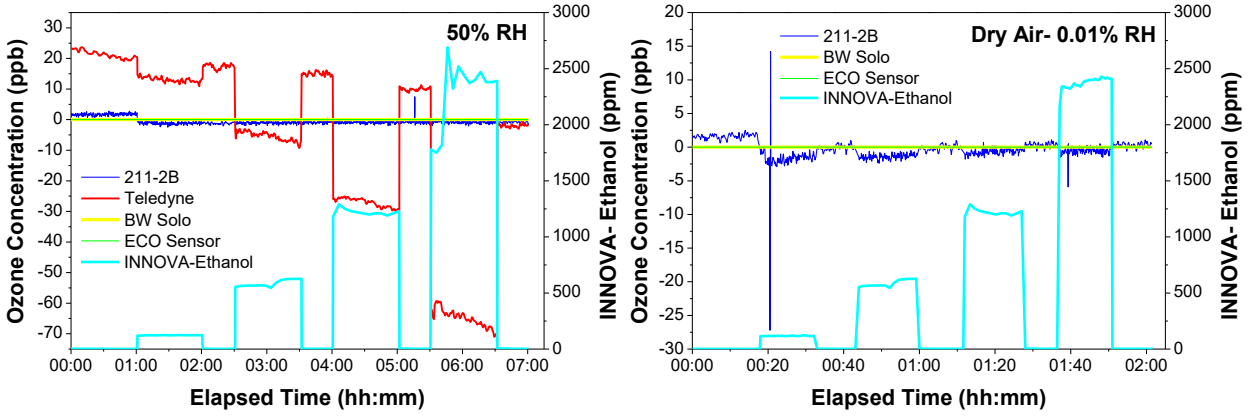

Figure 4. 26- Response of ozone sensors to different concentrations of Ethanol in humid and dry ozone-free air

According to the results, the ECO Sensor and BW solo sensors showed no response to these three VOC compounds, whereas two UV instruments were affected. Figure 4.26 shows that the injection of ethanol resulted in a slight negative interference in the 211-2B sensor measurements so that it measured the ozone concentration 2 to 3 ppb less (Table 4.3). This UV instrument exhibited a similar response to ethanol in both humid and dry air. In the dry air study, upon addition of 100 ppm of ethanol, 211-2B indicated a large rapid increase and decrease and then reached steady values immediately.

Although the response of Teledyne was almost stable in the presence of ethanol (SD= 0.77-2.80 ppb), this compound caused a substantial negative interference to the sensor (Figure 4.26). This sensor experienced the highest and lowest difference with the mean background concentration at 2000 and 100 ppm of ethanol, which was 86.25 and 8.22 ppb. In other words, by increasing the concentration of ethanol, Teledyne further underestimated the ozone concentration and needed more time to reach the initial background value upon the injection was terminated. Unfortunately, due to the sensor malfunctioning, we could not examine its performance in dry air condition.

In humid air, exposure of the 211-2B sensor to acetone did not influence its outputs. In contrast, in the dry air condition, the sensor response was associated with changes, especially with the injection of high acetone concentrations. As shown in Figure 4.27, there was a rapid increase in ozone concentration upon addition of acetone, then decayed immediately. This behavior was also observed by turning off the acetone source but in the form of a rapid negative bias. Besides, as the acetone concentration increased, the sensor reading became more unstable, and the data scatter increased (SD ranged from 0.33 to 6.28 ppb).

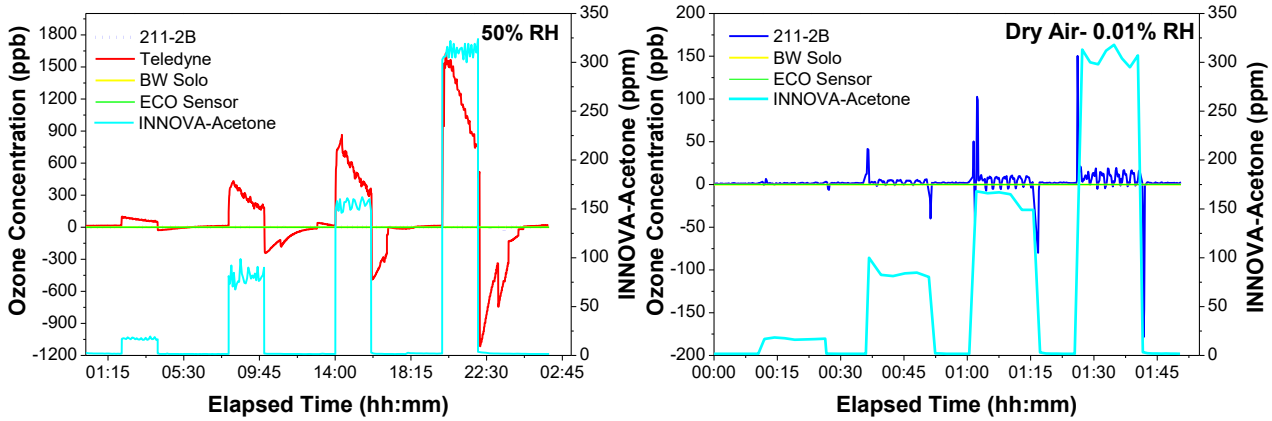

Figure 4. 27- Response of ozone sensors to different concentrations of Acetone in humid and dry ozone-free air

In the humid air experiment, Teledyne experienced a remarkable positive bias in the presence of acetone. This six-channel sensor overestimated the ozone concentration about 47.65 to 953.28 ppb by increasing acetone from 50 ppm to 1000 ppm. Figure 4.27 illustrates that the sensor outputs were not stable during the injection (SD varied from 7.32 to 86.98 ppb) so that its reading dramatically enhanced at the beginning of each step and then gradually decreased. Since this VOC compound had greatly affected the sensor performance, it took more than four hours after stopping the injection for the sensor to recover to 14 ppb (background value).

The 211-2B outputs were affected by cross-interference from toluene (Figure 4.28). According to Table 4.3, the sensor exhibited a similar response to this compound in humid and dry conditions. Toluene caused a positive bias to the 211-2B instrument, overestimating ozone values by 0.5-6 ppb over the 5 to 50 ppm toluene range tested. By adding and removing this compound, 211-2B

indicated a rapid large increase and decrease (Figure 4.28). Dispersion in the sensor measurements was associated with increasing toluene concentration, especially at 25 ppm toluene (humid condition), which had the highest SD (4.83 ppb).

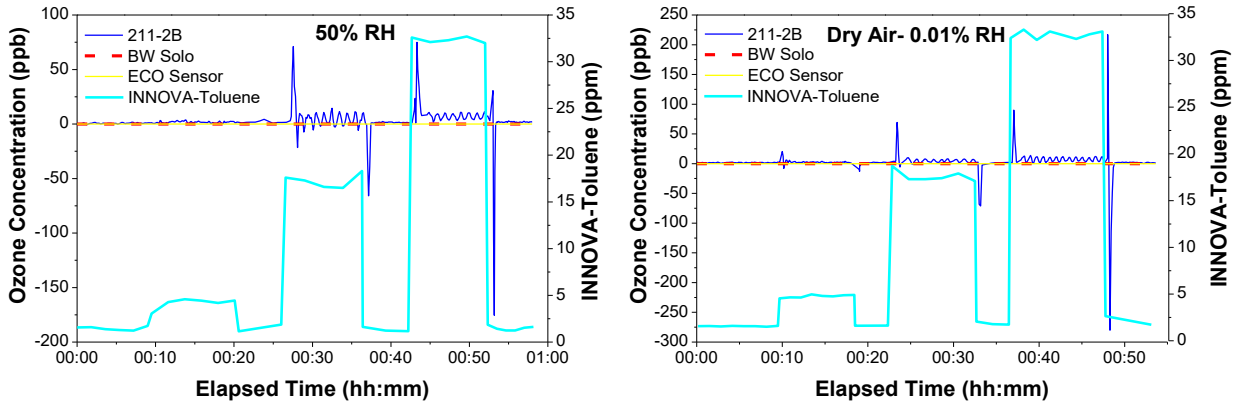

Figure 4. 28- Response of ozone sensors to different concentrations of Toluene in humid and dry ozone-free air

Table 4.3- Ozone sensors measurements in the presence of VOC compounds

BW Solo & ECO Sensor outputs were zero during all injections.			**Ethanol**					
			Background	**100 ppm**	**500 ppm**	**1000 ppm**	**2000 ppm**	**Background**
211-2B Outputs (ppb)	Average	Humid Air	1.7	-1.16	-1.007	-0.86	-0.82	-0.74
		Dry Air	1.60	-1.75	-1.4	-0.67	-0.60	0.33
	SD	Humid Air	0.38	0.40	0.39	0.37	0.39	0.39
		Dry Air	0.36	2.43	0.37	0.44	0.66	0.36
Teledyne Outputs (ppb)	Average	Humid Air	21.306	13.07	-5.41	-27.12	-64.95	-1.98
		Dry Air	-	-	-	-	-	-
	SD	Humid Air	1.25	0.77	1.44	1.46	2.80	0.48
		Dry Air	-	-	-	-	-	-
Acetone								
211-2B Outputs (ppb)	Average		**Background**	**50 ppm**	**250 ppm**	**500 ppm**	**1000 ppm**	**Background**
		Humid Air	1.46	1.54	1.58	1.82	1.03	1.64
		Dry Air	1.05	1.40	2.94	4.65	7.96	1.75
	SD	Humid Air	0.37	0.36	0.40	0.82	0.66	2.25
		Dry Air	0.33	0.84	2.02	4.76	6.28	0.41
Teledyne Outputs (ppb)	Average	Humid Air	14.80	62.46	210.75	525.57	968.09	12.59
		Dry Air	-	-	-	-	-	-
	SD	Humid Air	1.05	7.32	28.97	52.29	86.98	1.91
		Dry Air	-	-	-	-	-	-
Toluene								
211-2B Outputs (ppb)	Average		**Background**	**5 ppm**	**25 ppm**	**50 ppm**	**Background**	
		Humid Air	0.69	1.73	4.03	6.95	1.88	
		Dry Air	1.77	2.35	4.66	7.01	1.81	
	SD	Humid Air	0.46	0.77	4.83	2.44	0.35	
		Dry Air	0.47	0.65	2.46	3.30	0.51	

Generally, the 211 sensor is less susceptible to interfering compounds such as water vapor and VOCs than the Teledyne sensor. In other words, the internal Nafion tube applied in 211-2B minimizes water vapor interference and its gas phase scrubber (NO) is nearly nonreactive with stable chemical species in the gas phase except for ozone. As discussed above, it did not show any response to acetone in the humid air. It may be due to the solubility of the acetone with water, which was removed from the sample air by removing water vapor via the Nafion tube. However, this UV sensor exhibited some positive response (few ppb) in the presence of toluene (in both humid and dry air) and acetone (in dry air) and a slight negative bias by injection of ethanol (in both humid and dry air). The positive bias occurs when the gas phase product produced by the reaction of NO with the interfering compound has an absorption cross section (is the ability of a molecule to absorb a photon of a particular wavelength) smaller than the interfering compound absorption cross section (section 3.9.2). Conversely, a negative response occurs when the absorption cross section of gas phase product is larger. According to the 2B Tech company, none of the test compounds should react with NO, even at high concentrations. Also, the 211-2B monitor will show some positive response (few ppb) at very high concentrations of interfering compounds due to a small dilution that occurs when the NO is added. Since the reaction of these compounds with nitric oxide was not examined, the reason of these changes in the 211-2B response cannot be explained with certainty.

Permeability of interfering compounds in the Nafion tube applied in 211-2B is another factor that should be considered. Nafion is a copolymer that is composed of perfluoro-3, 6-dioza-4-methyl-7-octene-sulfonic acid and polytetrafluoroethylene. In other words, it consists of tetrafluoroethylene backbone with sulfonic acid groups. The presence of sulfonic acid in the Nafion structure makes it selectively permeable to compounds that bind to sulfonic acids such as water, alcohol, and ammonia [40, 120]. The results of various studies represented that some polar compounds, such as alcohols, aldehydes, ketones, and water-soluble esters, permeated the Nafion dryer similar to water vapor [121-123]. Also, the EPA analyzed a Nafion dryer in the presence of some volatile organic compounds (VOC). The results indicated that polar compounds were removed with water vapor so that they could not be identified. Moreover, this study indicated that compounds containing a benzene ring (aromatic compounds) are not removed by Nafion dryer [123, 124]. Based on the EPA report, certain polar VOCs (amines, ketones, alcohols, and some ethers) are lost when humidity is removed by a Nafion dryer [125]. It can be concluded that the 211-2B response did not change at 50% RH by injection of acetone (it is a ketone) due to the solubility of acetone with water and its permeation in the Nafion tube. Toluene is an aromatic compound and because of having a benzene ring, it is not removed by the Nafion tube. That's why the 211-2B outputs in humid and dry air were affected upon injection of toluene. Ethanol belongs to the alcohol group and it can be removed by Nafion tube, but this compound slightly affected the 211-2B response in humid and dry conditions. It means that it was not completely removed from the sample air by the Nafion tube.

While a solid -phase scrubber was used for the Teledyne sensor and the sensor was not equipped with a Nafion tube. It should be said that we could not find any information about the type of

material utilized in the scrubber. In the solid-phase scrubbers, adsorption and desorption of the VOC compounds depend upon the volatility of the VOC, relative humidity, and the scrubber surface area. The conventional solid-phase scrubbers can adsorb water vapor even at low humidity level, affecting the adsorption and desorption of other compounds by the scrubber. When Teledyne was exposed to acetone, a large positive bias was observed. It may relate to the adsorption of acetone by the scrubber, which increased the light intensity during I_0 measurement. Whereas, after ending exposure, this compound was desorbed from the scrubber; thus, the intensity of light (I_0) decreased and resulted in a negative bias. However, an opposite behavior was observed by injection of ethanol. It may be because of the deactivation of scrubber's sites in humid air, allowing ethanol to pass through the scrubber and decrease the light intensity (I_0). Figure 4.26 shows that after each step, the values of the background measured by the sensor were less than the initial value. In fact, due to the continuous exposure of the sensor in humid air, it is possible that humidity changed the reflectivity of the cell surface.

In explaining the effect of VOC compounds on UV monitors, it should be noted that the conjugation between the carbon-carbon double bonds in aromatic compounds makes the absorption spectrum longer and UV cross sections larger. The absorption cross section can also be further enhanced by adding different groups (aldehyde, nitro, hydroxyl, etc.) to the aromatic ring. Moreover, volatility is often reduced by substitutions, in which case these species are more likely to be retained in a solid scrubber. Fortunately, the concentration of substituted aromatic VOCs is low except for in very polluted air [18, 117].

Saturated aliphatic VOCs (no double or triple bonds) like methane, ethane, propane, n-butane, isobutane, etc., cannot interfere with ozone measurements because they do not absorb UV light with the wavelength of 254nm. These compounds have high energy electronic transitions (σ→σ^*) at wavelengths much shorter than 254 nm [117].

Aldehydes and ketones contain a carbonyl group, which n→π^* transitions within this group make additional weak absorbances possible in the vicinity of 254 nm. For example, formaldehyde, which belongs to aldehydes, has an absorption of 10,000 times less than ozone. Although the reaction of ozone with unsaturated VOCs in indoor environments can release aldehydes, the main sources of indoor aldehydes are building materials and appliances. Additionally, the concentrations of aldehydes indoors are 2 to 13 times higher than outdoor [104, 115-117].

Unsaturated VOCs contain at least one double or triple bond in their chain of carbon atoms. They are divided into two categories: Alkenes (including at least one double bond) and Alkynes (including at least one triple bond). Adding a double bond to a molecule makes the wavelengths longer so that the excited electron needs less energy to jump to an anti-bonding orbit (π→π^*). However, the absorption spectrum does not expand to 254 nm unless at least two double bonds are conjugated. For instance, ethylene, propylene and the four isomers of butylene do not affect ozone monitors performance. The other example is isoprene, which has two double bonds, but its absorption is much less than ozone (about 219 times less) [117].

Chapter 5: Conclusions and Recommendations

5.1- Summary

This study experimentally evaluated the performance of three UV ozone sensors, two electrochemical, and one metal oxide sensors under various RHs, ozone concentrations, airflow rates, airflow directions, and selected VOCs concentrations (ethanol, acetone, and toluene) in a full duct and small-scale chamber. To investigate the effect of different airflow orientations, the sensors were placed perpendicular and parallel to the airflow inside the duct. The VOC compounds interferences to ozone monitors were examined in the small chamber in the absence of ozone. The sensor responses were compared with the reference instrument (211-2B) measurements for all experiments. Moreover, the accuracy of ozone sensors was examined to check if their performance complies with the NIOSH accuracy criterion. The conclusions of this study are summarized as follows:

1- The results indicated that exposure to different air flow rates and changing the sensors direction in parallel and perpendicular to the airflow had a negligible effect on the UV sensors response. In contrast, two electrochemical sensors (BW and BW solo) outputs were significantly overestimated with increasing airflow rate. In the perpendicular direction, this increase in measurement was more evident. BW experienced the most data scattering in the perpendicular direction while BW Solo had almost the same scatter in both directions. The increase in the airflow rate led to remarkable growth in the ECO Sensor response, especially in the parallel direction. The highest scatter in the ECO Sensor data was observed at concentrations of 50 ppb (parallel direction) and 80 ppb (perpendicular direction).

Teledyne and POM outputs exhibited good agreement with the reference instrument measurements (R^2> 0.99) at different airflow rates and directions. The slopes of POM regression lines were slightly lower than unity, which can be interpreted as underestimating ozone concentrations by this sensor. A growing linear trend with a coefficient of R^2> 0.96 was observed between BW (in parallel direction) and BW Solo outputs and reference instrument. In the perpendicular direction, BW experienced more data scattering with increasing airflow rate (R^2= 0.79 at 2000 cfm, R^2= 0.88 at 1000 cfm). The intercepts of BW and BW solo regression lines indicate that these sensors overestimated ozone concentrations except for BW measurements at 500 cfm in the parallel orientation, which were almost the same as injected values. The response of ECO Sensor was linearly proportional to the reference measurements (R^2> 0.88). The slope of regression lines had the greatest difference from unity in the parallel direction than the perpendicular one. It means that ozone concentrations were significantly overestimated by this sensor, especially in the parallel direction.

The Teledyne and POM sensors accuracy was in the range of the NIOSH accuracy criterion for all ozone concentrations and airflow rates for both perpendicular and parallel directions. BW only performed well at 500 cfm when it was placed parallel to the flow direction. Its performance deteriorated with increasing airflow rate. BW Solo accuracy did not meet the NIOSH criterion in

any of the experiments. Placing ECO Sensor perpendicular to the flow direction caused the sensor accuracy to be within the standard range at 500 cfm and 50 ppb ozone.

2- It was found that with rapid humidity variations from 30% to about 80% and vice versa, a positive and negative interference was observed in the response of 211-2B, Teledyne, POM and BW, respectively. On the other hand, BW Solo behaved in the opposite manner. Due to the defined time interval (minimum 10 min) for ECO Sensor, it was difficult to follow its changing trend with humidity fluctuations. In the absence of ozone, humidity variations had a slight effect on 211-2B, POM, and ECO Sensor and no influence on the response of BW. While the comparison of the humidity variations test SD values with the low humidity experiment represents that Teledyne and BW Solo responses were significantly affected by humidity changes at zero ppb ozone. It should be noted that BW Solo cannot quantify negative concentrations because of its minimum detection limit, which is zero. With increasing ozone concentration, the response of 211-2B, POM, BW, and ECO Sensor was more affected. Teledyne and BW Solo demonstrated almost the same changes at all concentrations. According to the results, BW underestimated the ozone concentrations in the low humidity experiment. It may be related to the ambient humidity, which was lower than the sensor operation humidity (15%-90%).

The comparison of Teledyne and POM measurements with the reference instrument outputs shows that their performances correlated well with a linear coefficient of R^2> 0.90 in humidity variations and low humidity tests. Two electrochemical sensors (BW and BW Solo) outputs were linearly proportional to the reference instrument in both conditions (R^2> 0.90). The slopes of BW regression equations were lower than unity, especially at low humidity; this difference was higher (52% lower). In contrast, the slopes of BW Solo were significantly greater than unity. The regression equations of ECO Sensor indicate that the outputs of the low humidity experiment were highly linear with R^2=0.90, but the more data scatter in humidity variations test led to the decrease of R^2 to 0.76. Nevertheless, the least difference from unity was related to humidity changes (slope=2.61).

The accuracy of two UV sensors (Teledyne and POM) met the NIOSH criterion in the low humidity and humidity fluctuations experiments. The BW accuracy was within the standard range with humidity changes, but its accuracy did not comply with the NIOSH at low humidity. In none of the experiments, BW Solo and ECO Sensor meet the standard criterion.

3- The effect of different humidity levels on sensors performance was examined in the absence of ozone. Based on the results, Teledyne and POM responses were affected a lot so that Teledyne experienced a positive bias and lots of fluctuations were observed in the POM measurements. While humidity had little or no effect on the response of 211-2B, BW, BW Solo, and ECO Sensor. It should be noted that BW Solo showed zero concentration within the experiment, but it was continuously beeping because of negative concentrations. It means that humidity caused a negative bias to this sensor.

4- Comparing the low humidity experiment results in section 4.2.2.2 with the parallel direction test results in section 4.2.1 at the airflow rate of 500 cfm represents that 211 and POM experienced negligible effects in the presence of water vapor due to being equipped with the Nafion tube. While humidity (50%) caused a positive bias to Teledyne at 80, 200, and 500 ppb, overestimating ozone value by 9 ppb, 20 ppb, and 25 ppb, respectively. A significant positive interference was observed in BW readings at 50% RH so that sensor response increased about 12 ppb, 33 ppb, 43 ppb, 94 ppb, and 225 ppb at concentrations of 50, 80, 100, 200, and 500 ppb. Conversely, humidity caused negative interferences about 16, 37, and 57 ppb by injection of 50, 80, 100 ppb in the response of BW Solo. The impact of humidity on ECO sensor reading was not clear because it estimated ozone concentration at 50 ppb more (around 25 ppb) and less at 80 and 100 ppb (around 125 and 72 ppb, respectively).

5- BW Solo and ECO Sensor did not respond to any of the VOC compounds tested in the absence of ozone. Ethanol caused a negative bias around 2 to 3 ppb to the 211-2B instrument in humid and dry air. A negative interference was also observed in the response of Teledyne by injection of ethanol in the humid air. Increasing ethanol concentration caused more interference. Acetone had no effect on the response of 211-2B in humid air, but the sensor experienced a positive bias in dry air. The sensor reading became more unstable at higher concentrations. Teledyne was significantly affected by acetone injection so that it exhibited a positive bias in the presence of this compound. Teledyne response was not stable during the injection of acetone and gradually decreased. Moreover, after removing acetone, the sensor needed more time to recover to the initial value. Another tested VOC compound was toluene, which led to a slight positive interference in the response of 211-2B in both humid and dry air.

5.2- Recommendations for Users

It is recommended to use tubes made of PTFE and FEP for connection. To prevent or minimize ozone destruction, it is required to select the length of a tube as short as possible. Calibration has to be checked periodically when the instrument experiences variations in response. Temperature and humidity changes or polluted air can affect the performance of sensors; thus, zero calibration is needed after changing the environmental condition to ensure proper sensor performance. It is recommended to apply a humidity sensor to check the humidity level regularly. Moreover, it is necessary to pay attention to the direction of electrochemical and metal oxide sensors toward the airflow. It is recommended to apply these two monitoring technologies in places where the airflow rate and pressure are constant.

Based on Table 5.1, 211-2B sensor is recommended for the accurate measurement of ozone and it showed the best performance among the selected instruments. Also, different airflow rates and directions did not affect its response and interfering compounds slightly changed the sensor outputs. Since 211-2B is large in size, it is not suitable for monitoring areas that are small or hard to reach and need measurement at multiple locations. In this case, POM is the best instrument to use because it is a portable sensor and different environmental parameters slightly affected

its response. BW Solo and ECO Sensor had the worst performance during all experiments and their performance deteriorated over time. Thus, they cannot be applied for accurate measurements.

Table 5.1- Impact of physical and chemical parameters on the response of selected ozone monitors

		211-2B	Teledyne	POM	BW	BW Solo	ECO Sensor
Sensor Type		UV	UV	UV	Electrochemical	Electrochemical	Metal oxide
Performance		Excellent	Good	Good	Not Bad	Unacceptable	Unacceptable
Response to Changes		Fast	Fast	Fast	Fast	Fast	Slow
Airflow Direction Effect		N/A	N/A	No	Yes	Yes	Yes
Airflow rate Effect		No	No	No	Yes	Yes	Yes
Humidity Variations Effect		Slightly	Highly	Slightly	Not too much	Highly	Highly
Ozone Concentration		Similar to injection	Slight difference	Underestimate	Overestimate & Underestimate	Overestimate	Overestimate
VOC Compounds	**Ethanol**	Negative	Negative	-	-	0	0
	Acetone	Positive	Positive	-	-	0	0
	Toluene	Positive	-	-	-	0	0

5.3- Recommendations for Future Work

To examine the electrochemical and metal oxide sensors structural changes at different airflow rates and humidity, further studies are needed to measure sensing electrode voltage and metal oxide resistance during the experiments. Also, the effect of various airflow rates and airflow directions on the sensors response can be repeated at different humidity levels. The sensors response can be examined in the presence of other interfering compounds as well as a mixture of these gases with ozone at different humidity levels.

References

1. Liu, X., et al., *A survey on gas sensing technology.* Sensors, 2012. **12**(7): p. 9635-9665.
2. Lee, D.-D. and D.-S. Lee, *Environmental gas sensors.* IEEE Sensors Journal, 2001. **1**(3): p. 214-224.
3. Ando, M., V. Biju, and Y. Shigeri, *Development of Technologies for Sensing Ozone in Ambient Air.* Analytical Sciences, 2018. **34**(3): p. 263-271.
4. Qu, J., Y. Chai, and S. Yang, *A real-time de-noising algorithm for e-noses in a wireless sensor network.* Sensors, 2009. **9**(2): p. 895-908.
5. Vink, J., H. Verhoeven, and J. Huijsing. *Response speed optimization of thermal gas-flow sensors for medical application*. in *Proceedings of the International Solid-State Sensors and Actuators Conference-TRANSDUCERS'95*. 1995. IEEE.
6. Ke, M.-T., et al., *A MEMS-based benzene gas sensor with a self-heating WO3 sensing layer.* Sensors, 2009. **9**(4): p. 2895-2906.
7. Kwon, J., et al. *A study on NDIR-based CO2 sensor to apply remote air quality monitoring system*. in *2009 Iccas-Sice*. 2009. IEEE.
8. Agency, U.E.P., *Report to Congress on indoor air quality, volume II: assessment and control of indoor air pollution.* Technical Report EPA/400/1-89/001C, 1989.
9. Wallace, L.A., *The total exposure assessment methodology (TEAM) study: Summary and analysis*. Vol. 1. 1987: Office of Research and Development, US Environmental Protection Agency ….
10. Agency, E.P., *Indoor Air Quality*. EPA: United states.
11. OSHA, U., *Indoor Air Quality in Commercial and Institutional Building.* USA: US Department of Labor. Tersedia di: http://www. osha. gov, 2011.
12. Zhang, H. and R. Srinivasan, *A systematic review of air quality sensors, guidelines, and measurement studies for indoor air quality management.* Sustainability, 2020. **12**(21): p. 9045.
13. Takada, T., *Ozone Detection by In2O3 Thin Film Gas Sensor in: T. Seiyama (Ed.), Chemical Sensor Technology, vol. 2*. 1989, Kodansha, Tokyo.
14. EPA, *Ground-level Ozone Basics*. EPA: United States.
15. Ebeling, D., et al., *Electrochemical ozone sensor and instrument with characterization of the electrode and gas flow effects.* Sensors and Actuators B: Chemical, 2009. **137**(1): p. 129-133.
16. Agency, E.P., *National ambient Air quality standards for ozone*. October 26, 2015, EPA.
17. Witherspoon, C., *California Environmental Protection Agency, Air Resources Board.* Regulations to Control Greenhouse Gas Emissions from Motor Vehicles.
18. Turnipseed, A.A., et al., *Use of a heated graphite scrubber as a means of reducing interferences in UV-absorbance measurements of atmospheric ozone.* Atmospheric Measurement Techniques, 2017. **10**(6).
19. EPA, *Health Effects of Ozone in the General Population*. EPA: US.
20. Wang, C., et al., *Metal oxide gas sensors: sensitivity and influencing factors.* Sensors, 2010. **10**(3): p. 2088-2106.
21. Menzel, D.B., *Ozone: an overview of its toxicity in man and animals.* 1984.
22. Lippmann, M., *Health effects of ozone a critical review.* Japca, 1989. **39**(5): p. 672-695.
23. Korotcenkov, G., V. Brinzari, and B. Cho, *In2O3-and SnO2-based thin film ozone sensors: fundamentals.* Journal of Sensors, 2016. **2016**.
24. Morrison, G.C., *In-duct air cleaning devices: Ozone emission rates and test methodology*. 2014: California Air Resources Board, Research Division.
25. Andersen, P.C., C.J. Williford, and J.W. Birks, *Miniature personal ozone monitor based on UV absorbance.* Analytical chemistry, 2010. **82**(19): p. 7924-7928.

26. Pang, X., et al., *Electrochemical ozone sensors: A miniaturised alternative for ozone measurements in laboratory experiments and air-quality monitoring.* Sensors and Actuators B: Chemical, 2017. **240**: p. 829-837.
27. Chou, J., *Hazardous Gas Monitors: A practical guide to selection, operation, and application*. 1 edition ed. October 30 1999: McGraw-Hill professional.
28. Hodgkinson, J., et al., *Gas sensors1. The basic technologies and applications.* Collegium, 2008. **71**.
29. Spicer, C.W., D.W. Joseph, and W.M. Ollison, *A re-examination of ambient air ozone monitor interferences.* Journal of the Air & Waste Management Association, 2010. **60**(11): p. 1353-1364.
30. Long, R., et al., *Performance of the Proposed New Federal Reference Methods for Measuring Ozone Concentrations in Ambient Air. US Environmental Protection Agency. Washington, DC*. 2014, EPA/600/R-14/432 (NTIS PB2015e101240).
31. McELROY, F., D. Mikel, and M. Nees, *Determination of ozone by ultraviolet Analysis, A new method for Volume II, Ambient Air Specific Methods.* Quality Assurance Handbook for Air Pollution Measurement Systems. URL: http://mattson. creighton. edu/Ozone/OzoneEPAMethod. pdf (Accessed 9 October 2011), 1997.
32. EPA, *Laboratory Study to Explore Potential Interferences to Air Quality Monitors*. December 1999, Office of Air Quality Planning and Standards: Research Triangle Park, N.C.
33. Trost, B. and D. Fremgen, *Standard Operating Procedures Ozone (O3) Monitoring in Ambient Air by Ultraviolet Absorption Spectrophotometry*. 2016, The State of Alaska Department of Environmental Conservation (DEC).
34. *Spectrophotometry & spectrofluorimetry*, ed. M.G. Gore. 2000: Oxford university press.
35. Agency, U.E.P., *National ambient air quality standards for ozone; Final rule.* Fed. Regist., 2015. **80**: p. 65292-65468.
36. API, T. *User Manual Model 465L Ozone Monitor*. 2018; Available from: http://www.teledyne-api.com/prod/Downloads/M465L%20Manual%20-%2005509.pdf.
37. 2B Technologies, I. *OPERATION MANUAL Models 106-L and 106-OEM-L*. 2018; G-4:[Available from: https://twobtech.com/docs/manuals/model_106-L_revG-4.pdf.
38. Ollison, W.M., W. Crow, and C.W. Spicer, *Field testing of new-technology ambient air ozone monitors.* Journal of the Air & Waste Management Association, 2013. **63**(7): p. 855-863.
39. Birks, J.W., P.C. Andersen, and C.J. Williford, *Ozone monitor with gas-phase ozone scrubber*. 2013, Google Patents.
40. Wilson, K.L. and J.W. Birks, *Mechanism and elimination of a water vapor interference in the measurement of ozone by UV absorbance.* Environmental science & technology, 2006. **40**(20): p. 6361-6367.
41. Wilson, K.L., *Water Vapor Interference in the UV Absorption Measurement of Atmospheric Ozone*. 2005, University of Colorado.
42. Hudgens, E., et al., *A study of interferences in ozone UV and chemiluminescence monitors*. 1994, Air and Waste Management Association, Pittsburgh, PA (United States).
43. Kleindienst, T., C. McIver, and W. Ollison, *A study of interferences in ambient ozone monitors*. 1997, Air & Waste Management Association, Pittsburgh, PA (United States).
44. Li, Y., S.-R. Lee, and C.-Y. Wu, *UV-absorption-based measurements of ozone and mercury: an investigation on their mutual interferences.* Aerosol and Air Quality Research, 2006. **6**(4): p. 418-429.
45. Fereja, T.H., A. Hymete, and T. Gunasekaran, *A recent review on chemiluminescence reaction, principle and application on pharmaceutical analysis.* Isrn Spectroscopy, 2013. **2013**.
46. Garcia-Campana, A.M., *Chemiluminescence in analytical chemistry*. 2001: CRC Press.

47. Jimenez, A., M. Navas, and G. Galan, *Air analysis: determination of ozone by chemiluminescence.* Applied Spectroscopy Reviews, 1997. **32**(1-2): p. 141-149.
48. Baeyens, W., et al., *Chemiluminescence-based detection: principles and analytical applications in flowing streams and in immunoassays.* Journal of pharmaceutical and biomedical analysis, 1998. **17**(6-7): p. 941-953.
49. Mihalatos, A.M. and A.C. Calokerinos, *Ozone chemiluminescence in environmental analysis.* Analytica chimica acta, 1995. **303**(1): p. 127-135.
50. . Ozone and Other Photochemical Oxidants. 1977: National academy of science, Washangton, D.C.
51. standard, B., *Methods for measurment of air pollution*, in *Determination of the mass concentration of ozone in ambient air: chemiluminescence method*. 1994. p. 16. A.A. 56.
52. Stedman, D., et al., *Analysis of ozone and nitric oxide by a chemiluminescent method in laboratory and atmospheric studies of photochemical smog.* Journal of the Air Pollution Control Association, 1972. **22**(4): p. 260-263.
53. Wei, P., et al., *Impact analysis of temperature and humidity conditions on electrochemical sensor response in ambient air quality monitoring.* Sensors, 2018. **18**(2): p. 59.
54. Guth, U., W. Vonau, and J. Zosel, *Recent developments in electrochemical sensor application and technology—A review.* Measurement Science and Technology, 2009. **20**(4): p. 042002.
55. Korotcenkov, G., *Handbook of gas sensor materials.* Properties, Advantages and Shortcomings for Applications, 2013. **2**.
56. Ishii, Y., et al., *Development of electrolyte-free ozone sensors using boron-doped diamond electrodes.* Analytical chemistry, 2013. **85**(9): p. 4284-4288.
57. Korotcenkov, G. and B. Cho, *Ozone measuring: What can limit application of SnO2-based conductometric gas sensors?* Sensors and Actuators B: Chemical, 2012. **161**(1): p. 28-44.
58. Knake, R. and P.C. Hauser, *Sensitive electrochemical detection of ozone.* Analytica Chimica Acta, 2002. **459**(2): p. 199-207.
59. Stergiou, D.V., P.G. Veltsistas, and M.I. Prodromidis, *An electrochemical study of lignin films degradation: Proof-of-concept for an impedimetric ozone sensor.* Sensors and Actuators B: Chemical, 2008. **129**(2): p. 903-908.
60. Hosoya, Y., et al., *Ozone detection in air using SmFeO3 gas sensor.* Sensors and Actuators B: Chemical, 2005. **108**(1-2): p. 198-201.
61. Saad, K.B., et al., *Growth of lithium silicate crystals inside porous silicon film and their exploitation for ozone detection.* Applied Surface Science, 2008. **254**(13): p. 3955-3958.
62. Awang, Z., *Gas sensors: a review.* Sens. Transducers, 2014. **168**: p. 61-75.
63. Anderson, G.L. and D.M. Hadden, *The gas monitoring handbook*. 1999: Avocet Press Inc.
64. Cretescu, I., D. Lutic, and L.R. Manea, *Electrochemical Sensors for Monitoring of Indoor and Outdoor Air Pollution.* Electrochemical Sensors Technology, 2017: p. 65.
65. Pang, X., et al., *The impacts of water vapour and co-pollutants on the performance of electrochemical gas sensors used for air quality monitoring.* Sensors and Actuators B: Chemical, 2018. **266**: p. 674-684.
66. Rai, A.C., et al., *End-user perspective of low-cost sensors for outdoor air pollution monitoring.* Science of The Total Environment, 2017. **607**: p. 691-705.
67. Peterson, P., et al., *Practical use of metal oxide semiconductor gas sensors for measuring nitrogen dioxide and ozone in urban environments.* Sensors, 2017. **17**(7): p. 1653.
68. Eranna, G., et al., *Oxide materials for development of integrated gas sensors—a comprehensive review.* Critical Reviews in Solid State and Materials Sciences, 2004. **29**(3-4): p. 111-188.

69. Kumar, A., et al., *Application of gas monitoring sensors in underground coal mines and hazardous areas.* International Journal of Computer Technology and Electronics Engineering, 2013. **3**(3): p. 9-23.
70. Gardner, J.W., *Electrical conduction in solid-state gas sensors.* Sensors and Actuators, 1989. **18**(3-4): p. 373-387.
71. Fuchs, A., et al., *Room temperature ozone sensing with KI layers integrated in HSGFET gas sensors.* Sensors and Actuators B: Chemical, 1998. **48**(1-3): p. 296-299.
72. Takada, T., K. Suzuki, and M. Nakane, *Highly sensitive ozone sensor.* Sensors and Actuators B: Chemical, 1993. **13**(1-3): p. 404-407.
73. Doll, T., et al. *Room temperature ozone sensing with conductivity and work function sensors based on indium oxide*. in *Proceedings of International Solid State Sensors and Actuators Conference (Transducers' 97)*. 1997. IEEE.
74. Doll, T., et al., *Conductivity and work function ozone sensors based on indium oxide.* Sensors and Actuators B: Chemical, 1998. **49**(1-2): p. 63-67.
75. Gurlo, A., et al., *Sol-gel prepared In2O3 thin films.* Thin Solid Films, 1997. **307**(1-2): p. 288-293.
76. Gurlo, A., et al., *In2O3 and MoO3–In2O3 thin film semiconductor sensors: interaction with NO2 and O3.* Sensors and Actuators B: Chemical, 1998. **47**(1-3): p. 92-99.
77. Kim, S.-R., et al., *Ozone sensing properties of In2O3-based semiconductor thick films.* Sensors and Actuators B: Chemical, 2000. **66**(1-3): p. 59-62.
78. Galatsis, K., et al., *Comparison of single and binary oxide MoO3, TiO2 and WO3 sol–gel gas sensors.* Sensors and Actuators B: Chemical, 2002. **83**(1-3): p. 276-280.
79. Egashira, M., et al., *Variations in I–V characteristics of oxide semiconductors induced by oxidizing gases.* Sensors and Actuators B: Chemical, 1996. **35**(1-3): p. 62-67.
80. Qu, W. and W. Wlodarski, *A thin-film sensing element for ozone, humidity and temperature.* Sensors and Actuators B: Chemical, 2000. **64**(1-3): p. 42-48.
81. Aguir, K., C. Lemire, and D. Lollman, *Electrical properties of reactively sputtered WO3 thin films as ozone gas sensor.* Sensors and actuators B: Chemical, 2002. **84**(1): p. 1-5.
82. Utembe, S., et al., *An ozone monitoring instrument based on the tungsten trioxide (WO3) semiconductor.* Sensors and Actuators B: Chemical, 2006. **114**(1): p. 507-512.
83. Korotcenkov, G., et al., *The influence of film structure on In2O3 gas response.* Thin Solid Films, 2004. **460**(1-2): p. 315-323.
84. Korotcenkov, G., et al., *In2O3 films deposited by spray pyrolysis as a material for ozone gas sensors.* Sensors and Actuators B: Chemical, 2004. **99**(2-3): p. 297-303.
85. Becker, T., et al., *Ozone detection using low-power-consumption metal–oxide gas sensors.* Sensors and Actuators A: Physical, 1999. **74**(1-3): p. 229-232.
86. Becker, T., et al., *Gas sensing properties of thin-and thick-film tin-oxide materials.* Sensors and Actuators B: Chemical, 2001. **77**(1-2): p. 55-61.
87. Korotcenkov, G., V. Brinzari, and B. Cho, *In2O3-and SnO2-based ozone sensors: Design and characterization.* Critical Reviews in Solid State and Materials Sciences, 2018. **43**(2): p. 83-132.
88. Romppainen, P., et al., *Effect of CH4, SO2 and NO on the CO response of an SnO2-based thick film gas sensor in combustion gases.* Sensors and Actuators, 1985. **8**(4): p. 271-279.
89. Tamaki, J., et al., *Adsorption behavior of CO and interfering gases on SnO2.* Surface science, 1989. **221**(1-2): p. 183-196.
90. Torvela, H., J. Huusko, and V. Lantto, *Reduction of the interference caused by NO and SO2 in the CO response of Pd-catalysed SnO2 combustion gas sensors.* Sensors and Actuators B: Chemical, 1991. **4**(3-4): p. 479-484.
91. Marikutsa, A., M. Rumyantseva, and A. Gaskov, *Selectivity of catalytically modified tin dioxide to CO and NH3 gas mixtures.* Chemosensors, 2015. **3**(4): p. 241-252.

92. Lösch, M., M. Baumbach, and A. Schütze, *Ozone detection in the ppb-range with improved stability and reduced cross sensitivity.* Sensors and Actuators B: Chemical, 2008. **130**(1): p. 367-373.
93. Korotcenkov, G., V. Brinzari, and B. Cho, *Interference effects between hydrogen and ozone in the response of SnO2-based gas sensors.* Sensors and Actuators B: Chemical, 2017. **243**: p. 507-515.
94. Sauter, D., et al., *Development of modular ozone sensor system for application in practical use.* Sensors and Actuators B: Chemical, 2000. **69**(1-2): p. 1-9.
95. Spinelle, L., et al., *Evaluation of metal oxides sensors for the monitoring of O3 in ambient air at Ppb level.* Italian Association of Chemical Engineering, 2016.
96. Berger, F., J.-B. Sanchez, and O. Heintz, *Detection of hydrogen fluoride using SnO2-based gas sensors: Understanding of the reactional mechanism.* Sensors and Actuators B: Chemical, 2009. **143**(1): p. 152-157.
97. Gong, J., et al., *Micromachined nanocrystalline silver doped SnO2 H2S sensor.* Sensors and Actuators B: Chemical, 2006. **114**(1): p. 32-39.
98. Qi, Q., et al., *Electrical response of Sm2O3-doped SnO2 to C2H2 and effect of humidity interference.* Sensors and Actuators B: Chemical, 2008. **134**(1): p. 36-42.
99. Korotcenkov, G., et al., *The nature of processes controlling the kinetics of indium oxide-based thin film gas sensor response.* Sensors and Actuators B: Chemical, 2007. **128**(1): p. 51-63.
100. Korotcenkov, G., et al., *Kinetics of indium oxide-based thin film gas sensor response: the role of "redox" and adsorption/desorption processes in gas sensing effects.* Thin Solid Films, 2007. **515**(7-8): p. 3987-3996.
101. Korotcenkov, G. and B. Cho, *Instability of metal oxide-based conductometric gas sensors and approaches to stability improvement (short survey).* Sensors and Actuators B: Chemical, 2011. **156**(2): p. 527-538.
102. David, M., et al., *Progress in ozone sensors performance: a review.* Jurnal Teknologi, 2015. **73**(6).
103. David, M., et al., *Fundamental Review to Ozone Gas Sensing Using Optical Fibre Sensors.* Telkomnika, 2015. **13**(4): p. 1133.
104. Barro, R., et al., *Analysis of industrial contaminants in indoor air: Part 1. Volatile organic compounds, carbonyl compounds, polycyclic aromatic hydrocarbons and polychlorinated biphenyls.* Journal of Chromatography A, 2009. **1216**(3): p. 540-566.
105. Viegi, G., et al., *Indoor air pollution and airway disease [State of the Art].* The International Journal of Tuberculosis and Lung Disease, 2004. **8**(12): p. 1401-1415.
106. Guo, H., et al., *Risk assessment of exposure to volatile organic compounds in different indoor environments.* Environmental Research, 2004. **94**(1): p. 57-66.
107. Shaw, C.Y., D. Won, and J. Reardon, *Managing Volatile Orgnaic Compounds and Indoor Air Quality in Office Buildings: An Engineering Approach*. 2005: Institute for Research in Construction, National Research Council Canada.
108. Agency, U.S.E.P. *List of Designated Reference and Equivalent Methods*. 2017; Available from: https://www3.epa.gov/ttnamti1/files/ambient/criteria/AMTIC_List_June_2017_update_6-19-2017.pdf.
109. 2B Technologies, I. *Ozone Monitor Scrubberless Dual Beam*. 2018; Available from: https://twobtech.com/docs/manuals/model_211_revG-5.pdf.
110. API, T. *Single/Multi-Channel Industrial Hygiene Ozone Analyzer Model 465L*. Available from: http://www.teledyne-api.com/prod/Downloads/SAL000021D%20-%20465L.pdf.
111. 2B Technologies, I. *Personal Ozone Monitor*. 2020; Available from: https://twobtech.com/docs/manuals/model_POM_revF-5.pdf.
112. ECO Sensors, I. *Ozone Monitor and Controller Model C-30ZX*. Available from: http://www.ecosensors.com/wp-content/uploads/2012/09/C30ZX.pdf.

113. ASHRAE, *Laboratory Test Method for Assessing the Performance of Gas-Phase Air-Cleaning Systems: Air-Cleaning Devices*. 2016.
114. 2B Technologies, I. *Ozone Calibration Source*. 2020; Available from: https://twobtech.com/docs/manuals/model_306_revG-1.pdf.
115. NIOSH, *Components for evaluation of direct-reading monitors for gases and vapors*. 2012, National Institute for Occupational Safety and Health Cincinnati, OH.
116. Isiugo, K., et al., *Assessing the accuracy of commercially available gas sensors for the measurement of ambient ozone and nitrogen dioxide.* Journal of occupational and environmental hygiene, 2018. **15**(11): p. 782-791.
117. Birks, J., *UV-Absorbing Interferences in Ozone Monitors*. 2015, 2B Technologies, Inc. .
118. Lin, T., et al., *Semiconductor metal oxides as chemoresistive sensors for detecting volatile organic compounds.* Sensors, 2019. **19**(2): p. 233.
119. Favard, A., et al. *Humidity Impact Reduction on WO3 Gas Microsensor Response Using New Filters Based on Ionic Liquid*. in *Proceeding of the 3rd International Conference on Advances in Sensors, Actuators, Metering and Sensing (ALLSENSORS 2018)*. 2018.
120. Agency, U.S.E.P., *Recommendations for Nationwide Approval of Nafion™ Dryers Upstream of UV-Absorption Ozone Analyzers*. 2020.
121. Zielinska, B., et al., *Volatile organic compounds up to C20 emitted from motor vehicles; measurement methods.* Atmospheric Environment, 1996. **30**(12): p. 2269-2286.
122. Hsu, J., G. Miller, and V. Moran III, *Analytical method for determination of trace organics in gas samples collected by canister.* Journal of chromatographic science, 1991. **29**(2): p. 83-88.
123. Lee, J.-Y., et al., *Comparison of water pretreatment devices for the measurement of polar odorous compounds.* Applied Sciences, 2019. **9**(19): p. 4045.
124. Agency, U.E.P., *Determination of Volatile Organic Compounds (VOCs) in Ambient Air Using Specially Prepared Canisters with Subsequent Analysis by Gas Chromatography*. 1999, Center for Environmental Research Information Cincinnati^ eOH OH.
125. Epa, U., *Technical assistance document for sampling and analysis of ozone precursors.* United States Environmental Protection Agency, Research Triangle Park, North Carolina http://www. epa. gov/ttn/amtic/files/ambient/pams/newtad. pdf, 1998.

Appendix A: Full-duct Pre-qualification Tests

The following tests were performed as the pre-qualification test:

- Velocity uniformity test
- Contaminant uniformity
- Downstream mixing
- No filter correlation test
- Duct leakage
- Test air RH and temperature
- Ozone concentration uniformity
- 100% efficiency test

❖ Velocity Uniformity Test

According to the ANSI/ASHRAE Standard 145.2; Section 5.2; "Test Duct Velocity Uniformity," the air velocity was measured at nine points of the upstream cross-sectional area duct with the in-duct airflow rates of 500 and 2000 cfm. More than 12 samples were taken with time intervals of 5s during one minute using a velocity detector for each test. The test was repeated three times for each location; then, the average of data was computed at each sampling point. Also, the whole procedure was carried out twice to verify the test repeatability. According to the standard, the coefficient of variation (CV) at each flow rate must be less than 10%. The coefficient of variation (CV) is calculated by dividing the standard deviation of all measured nine-point with the mean average velocity of these points. Therefore, the CV at 500 and 2000 cfm was 7.80%, 6.77% and 9.62%, 7.22%, which are less than 10%.

Location		***2000 cfm(0.9m^3/s)*** -dp-duct-lab air (inchWg): 0.791 -Nozzle: 10" -Average 9 points: 2.687 -SD: 0.258 -CV: 0.096294<10% ASHRAE Std.	***2000 cfm(0.9m^3/s) (repeatability)*** -dp-duct-lab air (inchWG): 0.791 -Nozzle: 10" -Average 9 points: 2.715 -SD: 0.196 -CV: 0.072287<10% ASHRAE Std.
		Velocity	***Velocity***
		Ave.	***Ave.***
Top	20"	2.86	3.11
	12"	2.32	2.74
	4"	2.84	2.75
Middle	20"	2.97	2.64
	12"	2.31	2.40
	4"	2.91	2.53
Bottom	20"	2.75	2.81
	12"	2.42	2.77
	4"	2.78	2.67

Location		***500 cfm (0.2 m^3/s)*** -dp-duct-lab air (inchWg): 0.223 -Nozzle:7" -Average 9 points: 0.702 -SD: 0.054 -CV: 0.07804<10% ASHRAE Std.	***500 cfm (0.2 m^3/s) (repeatability)*** -dp-duct-lab air (inchWG): 0.223 -Nozzle: 7" -Average 9 points: 0.708 -SD: 0.048 -CV: 0.067774<10% ASHRAE Std.
		Velocity	***Velocity***
		Ave.	***Ave.***
Top	20"	0.81	0.77
	12"	0.67	0.71
	4"	0.69	0.75
Middle	20"	0.66	0.64
	12"	0.63	0.63
	4"	0.73	0.71
Bottom	20"	0.71	0.75
	12"	0.66	0.69
	4"	0.74	0.70

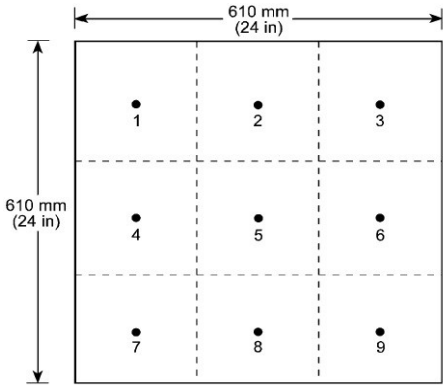

- **Upstream Contaminant Dispersal Uniformity**

This test was performed based on the ANSI/ASHRAE Standard145.2 , section 5.5; "Contaminant Dispersal in the Test Duct;" at the in-duct airflow rates of 500 cfm and 2000 cfm. Cyclohexane was injected into the system for 6 hours when the airflow rate was 500 cfm and at the airflow rate of 2000 cfm, n-octane was introduced into the duct at the injection point. The concentrations of these gases were measured at nine points of the upstream, same as the velocity uniformity test. According to ASHRAE Standard, a sampling time of 1 min is required for each location, while the applied photoacoustic detector (INNOVA AirTech Instrument 1312) had a slow response (longer than 30 s). To this end, the challenge gas concentration at each point was continuously measured by a probe connected to the analyzer for 40 min. This test was conducted in the open-loop case. The calculated coefficient of variation (CV) was 11.18% for 500 cfm and 8.76% for 2000 cfm, which are less than 15% based on the ASHRAE Standard. The mean concentrations of Cyclohexane and n-octane at each measuring point are mentioned in the following table.

Location		***500 cfm (0.2 m^3/s)*** -dp-duct-lab air (inchWg): 0.232 -Nozzle:7” -Average 9 points: 4.44 -SD: 0.496 -CV: 0.111864<15% ASHRAE Std.	***2000 cfm(0.9m^3/s)*** -dp-duct-lab air (inchWG): 0.782 -Nozzle: 10” -Average 9 points: 4.26 -SD: 0.373 -CV: 0.087607<15% ASHRAE Std.
		Cyclohexane Concentration (ppm)	***n-Octane Concentration (ppm)***
		Ave.	***Ave.***
Top	20”	5.42	4.85
	12”	4.98	4.63
	4”	4.29	4.33
Middle	20”	4.64	4.48
	12”	4.39	4.32
	4”	4.25	4.26
Bottom	20”	4.05	3.93
	12”	3.95	3.85
	4”	3.96	3.72

❖ Downstream Mixing of Contaminant

Based on the ANSI/ASHRAE Standard145.2 , section 5.6, “Downstream mixing of contaminant,” we carried out the test by injecting n-octane (for 5 hours) at the airflow rates of 500 cfm and 2000 cfm in the open-loop case. Before beginning the injection, the analyzer connected to the downstream probe should read zero or below the detection limit. Besides, each point sampling was conducted for 15 min continuously after the concentration of injected gas reached equilibrium. Gas concentrations were measured according to the figure at nine downstream points so that eight points were located around the duct and one point in the center. In this test, the CV was calculated 4.60% and 1.53% for 500 cfm and 2000 cfm, respectively. These values are following the standard requirement, less than 10%. The average concentrations of n-octane in each sampling point are mentioned in the following table.

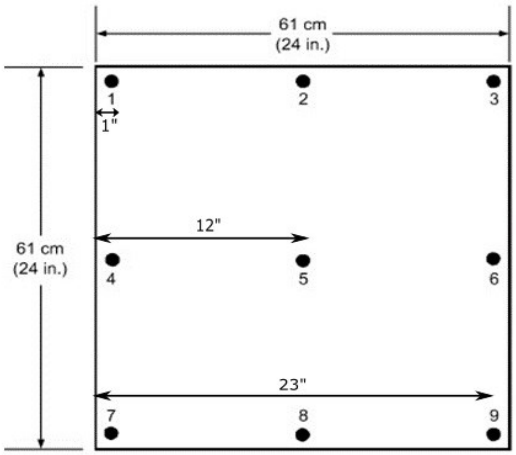

Location		***500 cfm (0.2 m^3/s)*** -dp-duct-lab air (inchWg): 0.2585 -Nozzle:7” -Average 9 points: 4.18 -SD: 0.1926 -CV: 0.046036<10% ASHRAE Std.	***2000 cfm(0.9m^3/s)*** -dp-duct-lab air (inchWG): 0.8249 -Nozzle: 10” -Average 9 points: 3.71 -SD: 0.05725 -CV: 0.015393<10% ASHRAE Std.
		n-Octane Concentration (ppm)	***n-Octane Concentration (ppm)***
		Ave.	***Ave.***
Top	23”	4.19	3.74
	12”	4.21	3.60
	1”	4.26	3.79
Middle	23”	3.72	3.72
	12”	4.20	3.70
	1”	4.11	3.75
Bottom	23”	4.31	3.74
	12”	4.20	3.64
	1”	4.43	3.74

❖ No-Filter Test

This test was performed according to the ANSI/ASHRAE Standard145.2 , section 5.11, “No filter test and overall system check.” It was conducted at the airflow rate of 500 cfm for 400 ppb and three ppm of toluene and the airflow rate of 500, 1000 and 2000 cfm for 75 ppb and 500 ppb of ozone. This test was carried out without removal devices in the open-loop case. An automatic multi-channel sampler (CAI Intelligent Sampling System MK3) and the photoacoustic multi-gas detector were applied to measure the upstream and downstream concentrations. During the toluene testing, the upstream and downstream were connected to channels one and three of the sampler. In this test, four channels were set for the concentration measurement so that channels two and four measured laboratory air. During the ozone testing, three channels (1,3,5) were attached to the upstream and the other three ones (2,4,6) were connected to the downstream of the duct.

The following equation was used to measure removal efficiency.

$$E(t) = \left(\frac{C_{up}(t) - C_{down}(t)}{C_{up}(t)}\right) \times 100\%$$

In this equation, $E(t)$ is the efficiency at time t, C_{up} and C_{down} (ppm) are the upstream and downstream concentrations at time t. The following tables show the results of toluene and ozone testing. Negative efficiency means that the duct did not show any efficiency for toluene and ozone, or it is related to the inaccurate reading of the monitor.

500 cfm (Toluene) **-dp-duct-lab air (inchWg):** 0.225 **-Nozzle:**7″					
Toluene concentration	***Up-stream concentration***		***Down-stream concentration***		***Efficiency (%)***
	Average	***SD***	***Average***	***SD***	
400 ppb	0.381	0.057	0.387	0.059	-1.54
3 ppm	2.843	0.170	2.906	0.150	-2.23

500 cfm (Ozone) **-dp-duct-lab air (inchWg):** 0.2212 (500 ppb) **-dp-duct-lab air (inchWg):** 0.2211 (75 ppb) **-Nozzle:**7″					
Ozone concentration	***Up-stream concentration***		***Down-stream concentration***		***Efficiency (%)***
	Average	***SD***	***Average***	***SD***	
500 ppb	476.754	1.617	478.482	0.973	-0.363
75 ppb	84.976	0.158	84.553	0.153	0.498

1000 cfm (Ozone) **-dp-duct-lab air (inchWg):** 0.8324 (500 ppb) **-dp-duct-lab air (inchWg):** 0.8501 (75 ppb) **-Nozzle:**7″					
Toluene concentration	***Up-stream concentration***		***Down-stream concentration***		***Efficiency (%)***
	Average	***SD***	***Average***	***SD***	
500 ppb	486.212	17.77	498.709	2.483	-3
75 ppb	77.023	0.306	78.440	0.436	-1.83

2000 cfm (Ozone) **-dp-duct-lab air (inchWg):** 0.8090 (500 ppb) **-dp-duct-lab air (inchWg):** 0.8098 (75 ppb) **-Nozzle:**7″					
Toluene concentration	***Up-stream concentration***		***Down-stream concentration***		***Efficiency (%)***
	Average	***SD***	***Average***	***SD***	
500 ppb	514.260	1.364	523.914	0.341	-1.87
75 ppb	84.983	0.5008	86.133	0.5008	-1.353

❖ Test Duct Leakage

This test was performed at the airflow rate of 2000 cfm to evaluate the duct leakage into the workspace. All duct connections were initially sealed using a suitable gasket to minimize any potential leakage into the work area. This test was done in the closed-loop case. After the airflow rate and air temperature reached equilibrium, about 3000ppm CO_2 as a tracer gas was injected into the system. The upstream was connected to a multi-channel sampler by a tube. The sampler was then connected to the photoacoustic multi-gas detector to monitor tracer gas concentrations until it reaches 500 ppm (similar to the concentration of CO_2 in the laboratory air). The decay concentration was calculated by the following equation so that in this equation,

C (ppm) is the CO_2 concentration inside the duct as a function of time, C_0 (ppm) is the initial tracer gas concentration, V is the system volume (m^3), and Q is the airflow rate (m^3/s).

$$C = C_0 \times e^{-\frac{Q}{v}t}$$

The following table and figure represent the result of this test. According to the ASHRAE Standard 145.2, the ratio of leak rate to test airflow rate is less than 1%.

	Test #1	**Test#2**
Q/V	0.0045 (1/min)	0.0053 (1/min)
V	363.65 (ft^3)	363.65(ft^3)
Q (Leakage)	1.67 cfm	1.93 cfm
Q (Flow rate)	2258.49 cfm	2269.35
Q-Leak/Q	0.0739 % <1% ASHRAE Std. 145.2 sec 5.2	0.0851% <1% ASHRAE Std. 145.2 sec 5.2
dp-duct-lab air	1.546 (inchWG)	1.721 (inchWG)

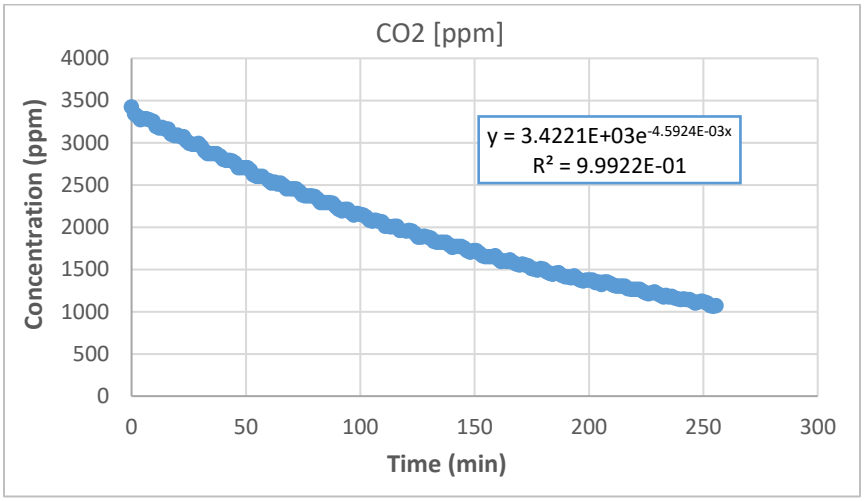

❖ Test Duct Air RH Measurement and Control

Since temperature and humidity variations can affect the performance of system, having a stable condition is essential during a test. The relative humidity and temperature within the duct are controlled by a humidifier (Vapac Humidifiers) and a cooling coil. In this test, the setpoints considered for the relative humidity in duct upstream and downstream included: 0% (humidifier off), 35%, 45%, 55%, 60%, and 65%. The temperature and relative humidity upstream and downstream of the duct were monitored by temperature and RH transmitters (Vaisala HUMICAP series HMT100) installed at the sampling port and before the nozzle and They were connected to a data acquisition system (DAS) (Agilent 34970A Data Acquisition/Switch Unit). The following table and figure indicate the conditions and results of this experiment.

-Carrier gas flow rate: 1000 cfm **-Nozzle:** 7” **-dp-duct-lab air (inchWG):** 0.85 **-Test running duration:** 12:19 PM to 16:37 PM		
-	***RH (%)***	***T (℃)***
Average	49.07	24.64
SD	2.1	0.6

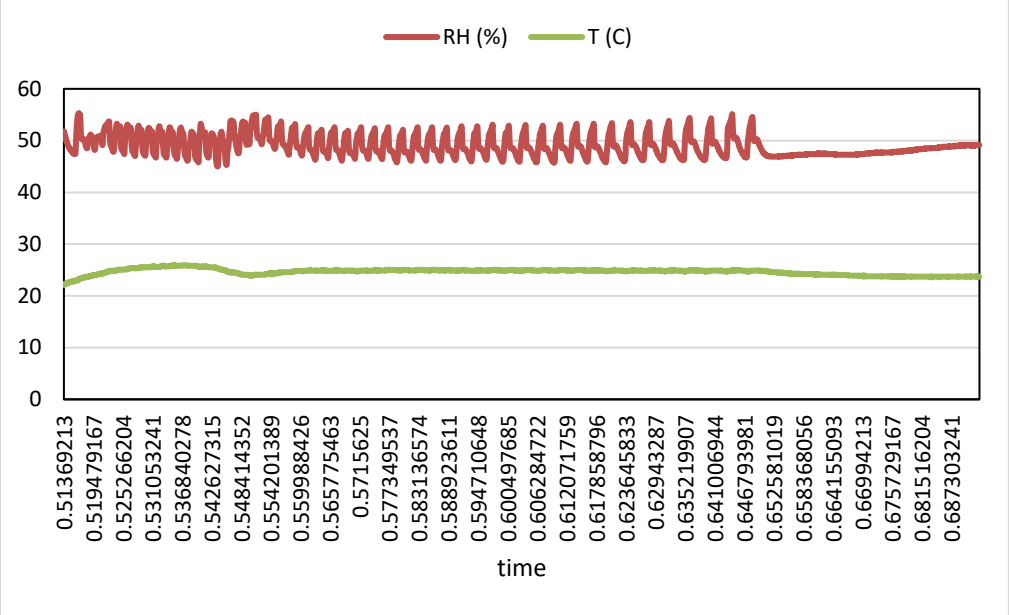

❖ Ozone Concentration Uniformity

In this test, produced ozone by the ozone generator (Ozone Generator BMT 803 N) was introduced into the duct to evaluate concentration uniformity across the full scale. This test was conducted in the open-loop case with three in-duct airflow rates of 500, 1000 and 2000 cfm. The ozone concentration was measured at 9 points of duct upstream, similar to the upstream concentration uniformity test by PTFE probes connected to a multi-channel ozone monitor (Teledyne, Ozone Monitor Model 465L). Since the ozone generator needs pure oxygen, an oxygen cylinder set at 10 psi was attached to a mass flow controller (Matheson 8274 Multiple Channel Mass Flow Controller System) to control the ozone generator inlet flow. According to calculations, the coefficient of variation (CV) was 5.73% for 500 cfm, 6.13% for 1000 cfm and 5.39% for 2000 cfm, which are less than 15%, based on the ASHRAE Standard. The mean concentration of ozone in each measuring point is mentioned in the following table.

In-duct air flow rate	***500 cfm***	***1000 cfm***	***2000 cfm***
Oxygen flow rate(L/min)	0.1	0.2	0.2
Ozone generator level (%)	10%	10%	20%

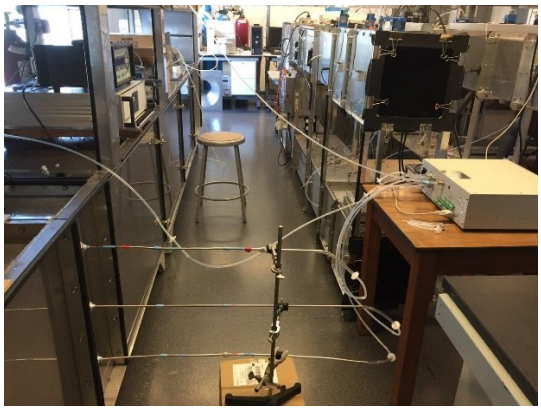

Location		500 cfm -dp-duct-lab air (inchWG): 0.248 -Nazzle: 7” -Average 9 point: 532.22 -SD: 30.52 -RH: 55.70% -CV: 0.0573 <15% ASHRAE Std.	1000 cfm -dp-duct-lab air (inchWG): 0.859 -Nazzle: 7” -Average 9 point: 407.48 -SD: 25.0 -RH: 53.62% -CV: 0.0613 <15% ASHRAE Std.	2000 cfm -dp-duct-lab air (inchWG): 0.802 -Nazzle: 10” -Average 9 point: 262.56 -SD: 14.17 -RH: 62.51% -CV: 0.0539 <15% ASHRAE Std.
		Ozone Concentration (ppb)	Ozone Concentration (ppb)	Ozone Concentration (ppb)
		Ave.	Ave.	Ave.
Top	20”	539.88	445.65	275.43
	12”	521.85	419.10	269.08
	4”	490.81	404.30	250.31
Middle	20”	558.23	430.99	277.06
	12”	530.68	401.97	263.29
	4”	499.18	384.29	245.94
Bottom	20”	587.28	422.13	279.87
	12”	550.60	395.16	260.98
	4”	511.42	363.68	241.11

❖ 100% Efficiency Test

This test was performed based on the ANSI/ASHRAE Standard145.2, section 5.10, “100% Efficiency filter test and purge time determination” at the in-duct airflow rate of 500 cfm for 400 ppb toluene and 75 ppb ozone. For toluene testing, the upstream was connected to a multi-channel sampler (channel 1) by a tube. Then the sampler was connected to the photoacoustic detector to monitor toluene concentration. Channels 2, 3, and 4 of the sampler measured concentrations of before injection (after clean-up bed), downstream, and before injection, respectively. Granular activated carbon (GAC) was used in the pre-cleanup bed to treat airflow before injecting toluene.

Also, enough GAC beds and 50% GAC and 50% permanganate (KMNO4) beds were applied in the upstream to remove compounds that are not removed by the GAC pre-cleanup bed. The measured concentrations after the pre-cleanup bed were considered as background readings. Since the photoacoustic detector gives total hydrocarbon readings but calibrated with toluene,

background readings are not zero. To this end, background reading should be subtracted from upstream and downstream concentrations. As shown in the following table, this test efficiency is 116.87%, which is higher than 99%, as mentioned in the ASHRAE Standard.

-Contaminant: Toluene **-dp-duct-lab air (inchWG):** 0.217			**-Carrier gas flow rate:** 500 cfm **-Toluene concentration:** 400 ppb		
Ave. Background (ppm)	Ave. Up-stream (ppm)	Ave. Down-stream (ppm)	Subtract Background readings		Efficiency (%)
			Upstream (ppm)	Down-stream (ppm)	
1.910	2.395	1.829	0.484	-0.081	116.878

This test was also performed in the presence of ozone. A multi-channel ozone monitor (Teledyne, Ozone Monitor Model 465L) was used to measure ozone concentrations before injection (channels 3&6), in upstream (channels 1&4) and downstream (channels 2&5). Besides, two other ozone monitors (2B Tech, Model 202 and 211) were connected to the upstream and downstream to double-check the ozone concentration in these sections. In this test, enough activated carbon beds were placed in the upstream to remove compounds that are not removed by the GAC pre-cleanup bed. Based on the results, the calculated efficiency is 100.337, which complies with ASHRAE Standard (>99%).

-Contaminant: Ozone **-dp-duct-lab air (inchWG):** 0.223			**-Carrier gas flow rate:** 500 cfm **-Toluene concentration:** 75 ppb		
Ave. Background (ppm)	Ave. Up-stream (ppm)	Ave. Down-stream (ppm)	Subtract Background readings		Efficiency (%)
			Upstream (ppm)	Down-stream (ppm)	
13.189	80.230	12.962	67.04148	-0.22637	100.337

Tube Testing

One of the things that should be taken into account when using ozone monitors, is the type of tube used for connection so that if we do not choose the right one, ozone inside it can be decomposed. In this situation, the exact concentration of ozone in the desired environment is not properly measured by the ozone monitor. To this end, we examined the response of the six-channel ozone monitor (Teledyne, Model 465L) by connecting several types of tubes, including PTFE, FEP, Viton, Tygon PVC, Tygon SE200, Silicon, Stainless steel (S.S) 316, and stainless steel 304. To minimize ozone decomposition inside the tubes, those with the shortest possible length were used.

This test was conducted in dry air and at 50% humidity at the airflow rate of 1000 cfm by injecting 100 ppb, 200 ppb, 500 ppb, and 1ppm ozone. The downstream of duct using a cross fitting was divided into three parts so that every part using a wye (Y) connector was attached to the two types of tubes. Moreover, the 2B Tech ozone monitor (Model 211) as the reference device, was

also connected to the downstream to double-check the ozone concentration. The following tables indicate the results of this test.

1000 cfm **-dp-duct-lab air (inchWg):** 0.873 **-Nozzle: 7”**									**RH-Up:** 9.61% **RH-Down:** 9.57%						
Concentration		Dry Condition							RH 50%						
		Channel No. & tube type							Channel No. & tube type						
		#1	#2	#3	#4	#5	#6	2B Tech	#1	#2	#3	#4	#5	#6	2B Tech
		PTFE	***FEP***	***Viton***	***Tygon PVC***	***Tygon SE200***	***Upstream of Tube (PTFE)***	***PTFE***	***PTFE***	***Tygon PVC***	***Viton***	***FEP***	***Tygon SE200***	***Upstream of Tube (PTFE)***	***PTFE***
100 ppb	Average	107.51	106.82	81.42	57.007	107.43	108.22	105.55	126.15	89.068	102.19	126.61	125.65	125.68	111.738
	SD	0.719	0.740	1.45	0.467	0.536	0.602	0.818	2.733	2.341	1.563	2.218	2.735	1.57	1.44
	Error (%)	0.659	1.292	24.76	47.32	0.732	-	2.471	-0.37	29.13	18.69	-0.743	0.026	-	11.09
200 ppb	Average	204.09	201.33	168.40	101.6	204.9	204.52	202.13	215.78	147.31	183.44	217.80	216.70	216.66	206.94
	SD	0.987	0.867	0.962	0.447	1.030	0.840	0.918	1.584	1.096	2.287	1.741	1.85	1.840	0.951
	Error (%)	0.211	1.558	17.65	50.323	-0.183	-	1.169	0.406	32.009	15.33	-0.524	-0.015	-	4.489
500 ppb	Average	496.97	498.26	439.17	242	500.88	501.28	509.49	509.22	340.31	450.33	512.47	510.022	510.30	508
	SD	2.007	1.291	1.584	0.828	1.320	0.976	1.360	1.870	2.204	7.246	3.101	3.790	2.430	2.2740
	Error (%)	0.859	0.602	12.38	51.72	0.079	-	-1.637	0.21	33.31	11.752	-0.425	0.056	-	0.450
1 ppm	Average	977.41	971.11	898.45	477.55	981.44	987.72	1000.37	988.96	659.95	908.43	994.582	993.473	991.17	997.96
	SD	1.635	2.806	1.671	1.292	1.845	0.966	2.354	2.942	2.401	5.667	9.526	3.66	3.7130	3.27
	Error (%)	1.043	1.681	9.037	51.65	0.635	-	-1.281	0.22	33.417	8.3482	-0.343	-0.23	-	-0.68

1000 cfm **-dp-duct-lab air (inchWg):** 0.864 **-Nozzle:**7”									**RH-Up:** 7.03 % **RH-Down:** 6.97%						
Concentration		Dry Condition							RH 50%						
		Channel No. & tube type							Channel No. & tube type						
		#1	#2	#3	#4	#5	#6	2B Tech	#1	#2	#3	#4	#5	#6	2B Tech
		PTFE	***S.S 316***	***Viton***	***S.S 304***	***Silicon***	***Upstream of Tube (PTFE)***	***PTFE***	***PTFE***	***S.S 316***	***FEP***	***S.S 304***	***Silicon***	***Upstream of Tube (PTFE)***	***PTFE***
100 ppb	Average	103.73	7.09	94.67	49.77	26.15	104.24	110.87	117.49	24.91	116.83	21.34	32.89	117.47	111.44
	SD	2.06	1.47	2.40	8.260	1.54	1.748	1.754	2.96	6.945	2.66	4.67	2.07	1.906	1.302
	Error (%)	0.49	93.19	9.18	52.25	74.90	-	-6.35	-0.0096	78.78	0.55	81.83	72.003	-	5.13
200 ppb	Average	197.14	69.20	181.64	138.49	58.49	197.60	205.38	208.90	88.62	208.02	73.023	59.6	209.11	202.98
	SD	3.247	16.90	3.909	9.008	5.65	3.164	1.82	2.71	11.36	2.825	8.45	2.33	2.314	2.89
	Error (%)	0.23	64.97	8.074	29.91	70.39	-	-3.93	0.099	57.621	0.523	65.079	71.499	-	7.36
500 ppb	Average	499.22	329.92	469.96	425.92	198.42	504.30	518.10	501.89	326.52	499.62	283.42	180.96	500.97	495.45
	SD	3.56	17.78	5.16	11.05	20.76	3.480	2.78	1.69	9.61	1.54	11.59	1.40	0.64	4.00
	Error (%)	1.005	34.57	6.80	15.54	60.65	-	-2.73	-0.18	34.82	0.269	43.42	63.87	-	1.10
1 ppm	Average	976.80	814.63	934.64	915.04	605.738	987.66	1010.62	1007.16	806.05	1003.60	773.46	446.95	1005.41	1004.98
	SD	4.69	18.33	6.25	10.12	37.07	3.90	3.82	1.54	3.65	1.042	8.048	3.220	2.330	3.091
	Error (%)	1.09	17.51	5.368	7.35	38.66	-	-2.32	-0.17	19.82	0.180	23.07	55.54	-	0.0430

Based on the results, PTFE, FEP, and Tygon SE200 tubes showed the best results in the presence of ozone. In contrast, Tygon PVC, Viton, and Silicon tubes decomposed ozone both in dry air and at 50% humidity. Besides, stainless steel 316 and 304 did not show good results during the tests.

They were conditioned over time so that their difference with the injected value became less and less but not as good as PTFE and FEP tubing.

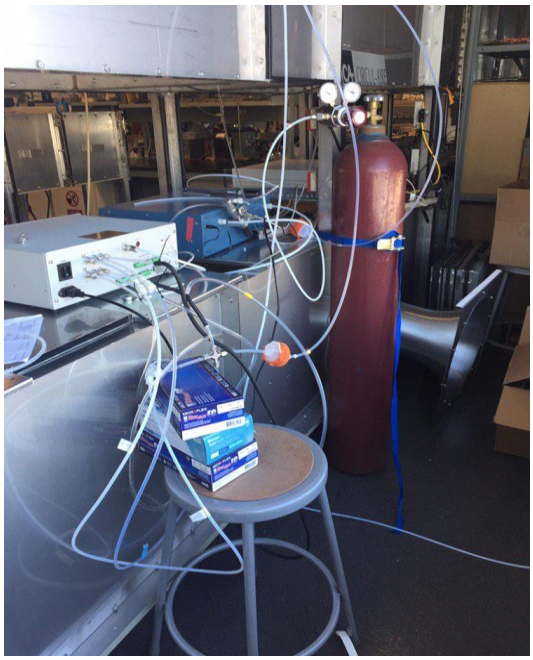

Appendix B: Photoacoustic Detector Calibration Curves

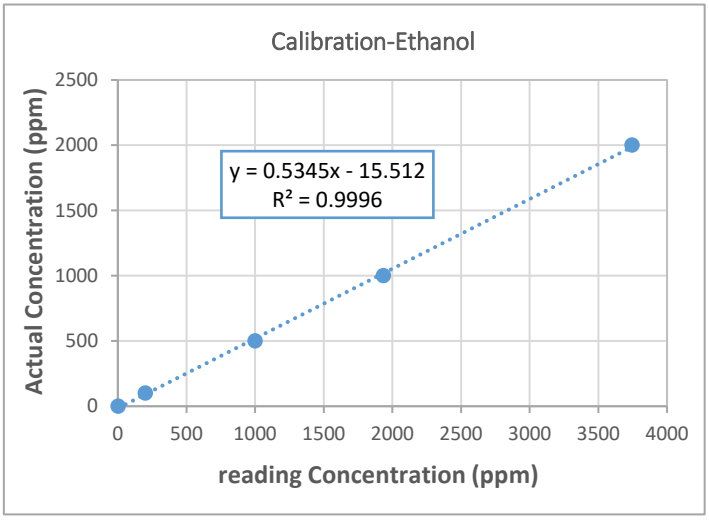

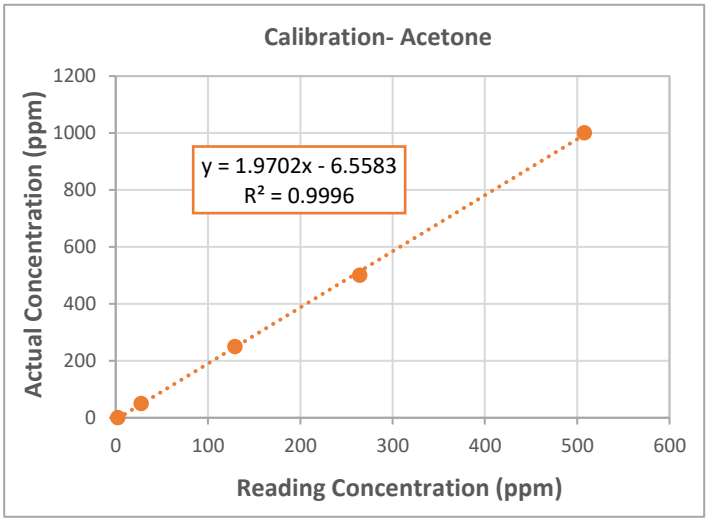

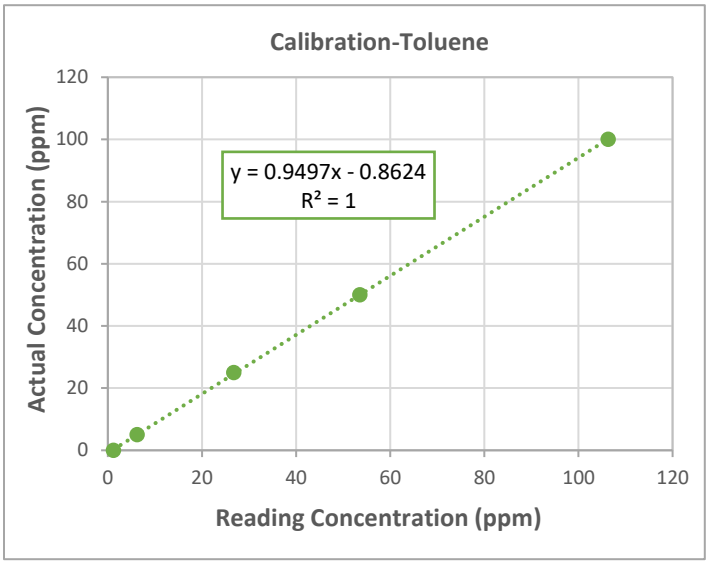

Appendix C: Calculation of 95% CI using MATLAB

```
% Import the calculated error variables (Excel file) into MATLAB
>> nBoot= 3000;
>> [bci, bmeans] = bootci (nBoot, {@mean, data}, 'alpha', .05, 'type', 'per');
>> bmu= mean (bmeans);
>> figure (1)
>> subplot (2,3,1)
>> hist (bmeans, 50);
>> hold on
>> xline (bmu, 'r-', sprintf ('mean error=% .2f', bmu), 'LineWidth', 3, 'FontSize', 8);
>> xline (bci (1), 'b- ', sprintf ('% .1f', bci (1)), 'LineWidth', 2, 'FontSize', 8);
>> xline (bci (2), 'b- ', sprintf ('% .1f', bci (2)), 'LineWidth', 2, 'FontSize', 8);
```

Appendix D: Summary of Ozone Sensors Measurements in Different Directions and Airflow Rates

	211-2B			POM			BW			Teledyne			BW Solo			ECO Sensor		
Ozone Concentration	***2000 cfm***	***1000 cfm***	***500 cfm***	***2000 cfm***	***1000 cfm***	***500 cfm***	***2000 cfm***	***1000 cfm***	***500 cfm***	***2000 cfm***	***1000 cfm***	***500 cfm***	***2000 cfm***	***1000 cfm***	***500 cfm***	***2000 cfm***	***1000 cfm***	***500 cfm***
Background	3.16	2.65	3.77	1.06	0.36	1.34	11.25	0	0	17.93	23.78	27.28	0	7.40	32.55	2.75	0.014	0.1
50ppb	54.90	54.45	53.13	45.45	45.30	46.18	142.18	108.35	77.47	47.52	50.45	48.74	260.82	255.49	198.56	152.85	121.7	54.36
80ppb	84.23	83.28	83.58	71.003	71.78	72.90	212.55	163.85	120.33	80.06	78.62	79.21	438.15	384.74	304.64	250.08	264.97	161.71
100ppb	105.68	102.40	104.47	90.008	87.86	92.34	257.65	195.60	150.05	96.2	97.91	99.68	527.05	480.70	383.70	350.78	352.82	271.93
200ppb	205.14	203.83	202.88	179.07	176.93	182.37	471.97	372.52	283.04	209.47	215.22	213.31	-	-	-	-	-	-
500ppb	501.17	503.69	507.91	442.41	444.19	464.53	999.12	870.44	668.35	501.74	509.36	515.36	-	-	-	-	-	-
1ppm	1007.12	1004.59	1003.96	891.002	893.33	915.10	1000	1000	999.56	1002.93	1003.27	1003.71	-	-	-	-	-	-
Background	-	3.379	3.32	-	1.12	1.003	-	0	0	-	17.62	18.34	49.06	56.14	0	20.32	6.585	0.0142

Results of Perpendicular direction

	211-2B			POM			BW			BW Solo			ECO Sensor		
Ozone Concentration	***2000cfm***	***1000 cfm***	***500 cfm***	***2000 cfm***	***1000 cfm***	***500 cfm***	***2000 cfm***	***1000 cfm***	***500 cfm***	***2000 cfm***	***1000 cfm***	***500 cfm***	***2000 cfm***	***1000 cfm***	***500 cfm***
Background	7.90	6.78	4.30	4.75	3.06	1.41	10	0	0	4.005	0	0.49	10.71	0.085	0.1
50ppb	51.12	51.49	50.28	44.761	45.41	43.19	94.79	75.45	50.97	226.71	184.33	140.80	205.35	146.86	146.96
80ppb	81.54	81.67	81.96	71.45	72.77	72.55	140.08	114.63	83.94	383.36	330.99	260.77	363.45	329.04	280.34
100ppb	101.25	99.38	100.27	89.29	88.74	89.58	164.06	139.08	103.17	489.76	436.23	325.22	438.12	397.96	369.71
200ppb	201.71	202.58	202.12	182.83	183.31	181.71	285.41	271.95	203.04	-	-	-	-	-	-
500ppb	498.48	502.49	502.64	456.63	451.18	457.47	673.58	644.06	480.10	-	-	-	-	-	-
1ppm	1000.99	1011.34	1001.95	916.98	908.009	908.11	1000	1000	954.52	-	-	-	-	-	-
Background	7.48	7.07	5.89	4.11	5.01	2.41	49.24	33.52	17.142	0	0	0	31.65	25.15	23.66

Results of parallel direction

Table D.1- Average concentrations of ozone sensors in different airflow rates and directions

	211-2B			POM			BW			Teledyne			BW Solo			ECO Sensor		
Ozone Concentration	***2000 cfm***	***1000 cfm***	***500 cfm***	***2000 cfm***	***1000 cfm***	***500 cfm***	***2000 cfm***	***1000 cfm***	***500 cfm***	***2000 cfm***	***1000 cfm***	***500 cfm***	***2000 cfm***	***1000 cfm***	***500 cfm***	***2000 cfm***	***1000 cfm***	***500 cfm***
Background	0.34	0.41	0.41	1.19	1.41	0.60	15.52	0	0	0.83	0.70	1.01	0	12.96	14.52	1.35	0.03	0.1
50ppb	1.18	1.007	1.27	1.08	0.80	1.15	11.23	10.88	8.49	1.47	0.73	1.17	8.21	10.75	10.70	6.86	13.85	2.37
80ppb	0.92	0.83	1.15	1.26	0.93	1.98	15.66	14.88	14.13	2.98	0.74	1.04	11.29	13.98	14.27	22.79	21.18	20.29
100ppb	1.30	1.16	1.83	1.02	1.33	2.12	17.05	20.44	15.86	3.07	1.50	1.37	11.80	12.92	15.40	10.44	8.27	15.26
200ppb	3.93	2.46	2.24	3.46	3.0	3.44	36.34	37.12	29	2.88	2.48	2.19	-	-	-	-	-	-
500ppb	3.97	5.51	5.20	3.70	6.10	9.67	5.06	80.49	75.70	2.95	6.21	7.01	-	-	-	-	-	-
1ppm	9.70	8.55	11.71	6.87	14.04	20.99	0	0	6.27	7.50	10.80	12.97	-	-	-	-	-	-
Background	-	0.42	0.37	-	1.72	1.14	-	0	0	-	0.54	0.75	19.10	13.37	0	3.85	4.81	0.037

Results of perpendicular direction

	211-2B			POM			BW			BW Solo			ECO Sensor		
Ozone Concentration	***2000 cfm***	***1000 cfm***	***500 cfm***	***2000 cfm***	***1000 cfm***	***500 cfm***	***2000 cfm***	***1000 cfm***	***500 cfm***	***2000 cfm***	***1000 cfm***	***500 cfm***	***2000 cfm***	***1000 cfm***	***500 cfm***
Background	0.46	0.41	0.41	0.85	0.74	1.35	15.49	0	0	12.83	0	4.03	2.08	0.12	0.07
50ppb	0.59	0.69	0.87	1.34	1.30	1.38	5.83	5.10	5.44	11.93	16.52	11.32	12.44	25.21	20.74
80ppb	0.60	0.77	0.94	0.75	1.36	1.17	6.38	5.38	5.14	12.97	15.28	11.68	7.59	12.46	7.85
100ppb	0.65	0.89	1.88	0.89	1.40	1.85	6.10	6.72	5.31	13.41	17.77	13.55	0.75	5.057	16.44
200ppb	2.16	1.90	2.50	2.23	3	2.32	10.30	10.25	10.02	-	-	-	-	-	-
500ppb	3.27	4.32	5.01	3.34	4.34	5.20	32.59	28.11	22.66	-	-	-	-	-	-
1ppm	6.89	8.39	6.72	6.39	8.18	8.46	0	0	36.59	-	-	-	-	-	-
Background	0.47	0.39	0.40	0.95	0.90	0.82	12.31	14.39	16.03	0	0	0	0.35	1.83	0.57

Results of parallel direction

Table D.2- Estimated standard deviations of ozone sensors in different airflow rates and directions

Appendix E: 95% CI and Precision of Ozone Sensors in Different Airflow Rates, Directions, and Humidity Variations Experiments

			POM			BW			BW Solo			ECO Sensor		
Direction	**Ozone Concentration**		***2000 cfm***	***1000 cfm***	***500 cfm***	***2000 cfm***	***1000 cfm***	***500 cfm***	***2000 cfm***	***1000 cfm***	***500 cfm***	***2000 cfm***	***1000 cfm***	***500 cfm***
Perpendicular	**50 ppb**	**Mean error**	-17.99	-14.51	-13.04	159.62	99.32	45.95	414.50	380.30	268.54	202.82	128.25	2.76
		95% CI (%)	-18.4- -17.6	-15.2- -13.8	-13.6- -12.5	156.5-162.8	96.4-102.1	43.7-48.3	413-416	378.4-382.2	265.7-271.4	196.9-209.5	114.7-141.9	-0.9-6.3
	80 ppb	**Mean error**	-16.35	-13.81	-12.74	152.14	96.75	44.04	436.35	367.79	270.55	203.39	222.34	95.82
		95% CI	-16.6- -16.1	-14- -13.6	-13.1- -12.4	149.2-155	94.3-99.5	41.6-46.6	435.2-437.5	366.3-369.3	268.7-272.4	187-218.3	209.1-237.9	80.7-110
	100 ppb	**Mean error**	-15	-16.77	-11.37	143.61	91.10	43.73	424.20	370.90	273.42	248.83	240.33	164.02
		95% CI	-15.2- -14.8	-17.6- -16	-11.7- -11	141.2-146.1	88.2-94	41.4-45.9	423.1-425.3	369.6-372.2	271.8-275	243.6-253.6	229.1-2448	155.6-171.9
	200 ppb	**Mean error**	-11.67	-13.07	-10.01	130.06	82.79	39.51	-	-	-	-	-	-
		95% CI	-12- -11.4	-13.4- -12.8	-10.3- -9.7	127.5-132.6	80.4-85.3	37.4-41.6	-	-	-	-	-	-
	500 ppb	**Mean error**	-11.46	-11.80	-8.55	99.79	72.82	31.60	-	-	-	-	-	-
		95% CI	-11.7- -11.3	-12- -11.6	-8.9- -8.2	99.5-100	70.4-75.2	29.5-33.8	-	-	-	-	-	-
	1 ppm	**Mean error**	-11.58	-10.92	-8.77	-0.91	-0.45	-0.39	-	-	-	-	-	-
		95% CI	-11.8- -11.4	-11.1- -10.7	-9.1- -8.4	-1- -0.8	-0.6- -0.3	-0.6- -0.2	-	-	-	-	-	-
Parallel	**50 ppb**	**Mean error**	-12.44	-11.80	-14.09	85.46	46.53	1.38	346.37	263.51	169.95	304.17	189.71	181.56
		95% CI	-12.8- -12.1	-12.2- -11.4	-14.4- -13.8	84-86.9	45.1-47.9	0.7-2.1	3442-348.6	261.6-265.5	168.6-1713	289.7-316.1	161.8-220.7	155.1-202
	80 ppb	**Mean error**	-12.38	-10.90	-11.48	71.77	40.35	2.43	373.88	306.89	217.18	347.13	304.46	241.04
		95% CI	-12.5- -12.3	-11.1- -10.7	-11.7- -11.3	70.8-72.7	39.5-41.1	1.6-3.2	371.6-374.6	305.7-308	216.3-218.1	341.5-352.4	294.9-313	235.6-246.7
	100 ppb	**Mean error**	-11.81	-10.70	-10.66	62.04	399.93	2.89	384.15	333.60	223.57	333.26	295.54	267.77
		95% CI	-11.9- -11.7	-10.9- -10.5	-10.9- -10.4	61.3-62.8	39.1-40.8	2.2-3.6	383-385.3	332.5-334.7	222.7-224.4	332.7-333.7	292.5-298.5	258.1-277.2
	200 ppb	**Mean error**	-9.36	-9.49	-10.10	41.49	34.24	0.46	-	-	-	-	-	-
		95% CI	-9.5- -9.2	-9.7- -9.3	-10.3- -9.9	40.8-42.1	33.5-35	-0.2-1.1	-	-	-	-	-	-
	500 ppb	**Mean error**	-8.40	-10.20	-8.99	35.13	28.18	-4.48	-	-	-	-	-	-
		95% CI	-8.5- -8.3	-10.3- -10.1	-9.1- -8.8	34.2-36	27.5-28.9	-5.1- -3.8	-	-	-	-	-	-
	1 ppm	**Mean error**	-8.39	-10.22	-9.37	-0.10	-1.12	-4.74	-	-	-	-	-	-
		95% CI	-8.5- -8.3	-10.3- -10.1	-9.5- -9.3	-0.1- -0.1	-1.1- -1.1	-5.2- -4.2	-	-	-	-	-	-

		50 ppb		80 ppb		100 ppb		200 ppb		500 ppb		1 ppm	
		Mean error	**95% CI (%)**	**Mean error**	**95% CI (%)**	**Mean error**	**95% CI (%)**	**Mean error**	**95% CI (%)**	**Mean error**	**95% CI (%)**	**Mean error**	**95% CI (%)**
Teledyne	**500 cfm**	-5.80	-6.3- -5.2	-3.86	-4.4- -3.4	-3.54	-4.2- -2.7	5.41	5-5.9	1.27	0.8-1.7	0.02	-0.4-0.4
	1000 cfm	-6.03	-6.5- -5.5	-5.61	-6- -5.2	-3.92	-4.4- -3.5	5.73	5.3-6.2	1.64	1.2-2	-0.31	-0.7-0.1
	2000 cfm	-13.67	-14.3- -12.9	-5.23	-6.2- -4.2	-8.95	-9.6- -8.2	**2.28**	1.8-2.7	0.36	0.1-0.6	-0.34	-0.6- -0.1

Table E.1- 95% CI of ozone sensors in different airflow rates and directions (perpendicular and parallel) tests

	211-2B			POM			BW			Teledyne			BW Solo			ECO Sensor		
Ozone Concentration	***2000 cfm***	***1000 cfm***	***500 cfm***	***2000 cfm***	***1000 cfm***	***500 cfm***	***2000 cfm***	***1000 cfm***	***500 cfm***	***2000 cfm***	***1000 cfm***	***500 cfm***	***2000 cfm***	***1000 cfm***	***500 cfm***	***2000 cfm***	***1000 cfm***	***500 cfm***
Background	10.96	15.61	10.88	112.6	390.7	44.9	138.01	0	0	4.64	2.94	3.73	0	175.09	44.61	49.01	264.57	100
50ppb	2.15	1.85	2.40	2.37	1.78	2.50	7.9	10.04	10.96	2.01	1.01	1.68	3.14	4.20	5.38	4.48	11.38	4.35
80ppb	1.09	1.0	1.38	1.77	1.3	2.72	7.36	9.08	11.74	2.9	0.75	1.07	2.57	3.63	4.68	9.11	7.99	12.54
100ppb	1.23	1.13	1.75	1.13	1.51	2.3	6.61	10.45	10.57	3.45	1.29	1.16	2.24	2.68	4.01	2.97	2.34	5.61
200ppb	1.91	1.21	1.1	1.93	1.7	1.88	7.7	9.96	10.24	1.37	1.15	1.02	-	-	-	-	-	-
500ppb	0.79	1.09	1.02	0.83	1.37	2.08	0.50	9.24	11.32	0.58	1.21	1.36	-	-	-	-	-	-
1ppm	0.96	0.85	1.16	0.77	1.57	2.29	0	0	0.62	0.74	1.07	1.29	-	-	-	-	-	-

Results of perpendicular direction

	211-2B			POM			BW			BW Solo			ECO Sensor		
Ozone Concentration	***2000 cfm***	***1000 cfm***	***500 cfm***	***2000 cfm***	***1000 cfm***	***500 cfm***	***2000 cfm***	***1000 cfm***	***500 cfm***	***2000 cfm***	***1000 cfm***	***500 cfm***	***2000 cfm***	***1000 cfm***	***500 cfm***
Background	5.83	6.06	9.62	17.89	24.34	95.57	154.91	0	0	320.41	0	818.37	19.41	141.74	70.71
50ppb	1.17	1.34	1.74	2.99	2.88	3.21	6.15	6.75	10.68	5.26	8.96	8.04	6.05	17.16	14.11
80ppb	0.73	0.95	1.14	1.05	1.87	1.61	4.56	4.7	6.12	3.38	4.61	4.47	2.08	3.78	2.8
100ppb	0.64	0.9	1.88	1.0	1.58	2.07	3.72	4.83	5.15	2.73	4.07	4.16	0.17	1.27	4.44
200ppb	1.07	0.94	1.23	1.22	1.64	1.28	3.61	3.76	4.93	-	-	-	-	-	-
500ppb	0.65	0.86	0.99	0.73	0.96	1.13	4.83	4.36	4.72	-	-	-	-	-	-
1ppm	0.68	0.82	0.67	0.69	0.9	0.93	0	0	3.83	-	-	-	-	-	-

Results of parallel direction

Table E.2- Ozone sensors precision values in different airflow rates and directions

			Teledyne	POM	BW	BW Solo	ECO Sensor
Humid Air (30%-80%)	**50 ppb**	Mean error	-3.07	-11.98	-8.86	237.16	-13.89
		95% CI (%)	-13.3-7.2	-12.6- -11.3	-10.2- -7.6	233.1-241.3	-35.7-5.3
	80 ppb	Mean error	-0.83	-10.76	-6.71	263.89	62.35
		95% CI	-6.9-5.1	-11.1- -10.4	-7.9- -5.6	261.7-266.1	44.2-81.9
	100 ppb	Mean error	0.53	-10.55	-6.43	267.42	155.91
		95% CI	-4.1-5.2	-10.9- -10.2	-7.6- -5.3	265.8-269.1	130.5-179.2
	200 ppb	Mean error	-1.84	-8.30	-9.22	-	-
		95% CI	-4.4-0.7	-8.8- -7.8	-10.2- -8.2	-	-
	500 ppb	Mean error	-2.03	-7.53	-15.52	-	-
		95% CI	-3.3- -0.8	-8- -71	-16.4- -14.6	-	-
Dry Air (7.5±0.3% and 15±2% RH	**50 ppb**	Mean error	-7.45	-10.59	-25.97	218.74	147.99
		95% CI	-8.7- -6.2	-11.2- -10	-27- -24.9	217.5-220	123.3-174.8
	80 ppb	Mean error	-11.75	-9.57	-37.14	270.88	405.39
		95% CI	-12.2- -11.3	-9.7- -9.4	-37.3- -36.9	270-271.7	382.9- 428.5
	100 ppb	Mean error	-0.34	-9.33	-40.06	278.17	335.75
		95% CI	-0.6- -0.1	-9.6- -9.1	-40.1- -39.9	277-279	335.7- 335.8
	200 ppb	Mean error	-3.55	-7.49	-45.14	-	-
		95% CI	-3.7- -3.4	-7.7- -7.3	-45.3- -45	-	-
	500 ppb	Mean error	-3.62	-5.44	-48.91	-	-
		95% CI	-3.8- -3.5	-5.7- -5.2	-49.1- -48.7	-	-

Table E.3- 95% CI of ozone sensors in humidity variations experiments